Fisheries and Oceans Canada | Pêches et Océans Canada
Ecosystems and Oceans Science | Sciences des écosystèmes et des océans

Canadian Science Advisory Secretariat (CSAS)

Research Document 2022/007

Maritimes Region

Quantifying changes in the Distribution of Atlantic Cod and Yellowtail Flounder on Georges Bank

David M. Keith[1], Jessica A. Sameoto[1], Freya M. Keyser[1], and Irene Andrushchenko[2]

[1]Bedford Institute of Oceanography
Fisheries and Oceans Canada
1 Challenger Dr.
Dartmouth Nova Scotia, B2Y 4A2

[2]St. Andrews Biological Station
Fisheries and Oceans Canada
125 Marine Science Dr.
St. Andrews New Brunswick, E5B 0E4

October 2023

Canada

Foreword

This series documents the scientific basis for the evaluation of aquatic resources and ecosystems in Canada. As such, it addresses the issues of the day in the time frames required and the documents it contains are not intended as definitive statements on the subjects addressed but rather as progress reports on ongoing investigations.

Published by:

Fisheries and Oceans Canada
Canadian Science Advisory Secretariat
200 Kent Street
Ottawa ON K1A 0E6

http://www.dfo-mpo.gc.ca/csas-sccs/
csas-sccs@dfo-mpo.gc.ca

ISSN 1919-5044
ISBN 978-0-660-41314-3 Cat. No. Fs70-5/2022-007E-PDF

Correct citation for this publication:

Keith, D.M., Sameoto, J.A., Keyser, F.M., and Andrushchenko, I. 2023. Quantifying changes in the Distribution of Atlantic Cod and Yellowtail Flounder on Georges Bank. DFO Can. Sci. Advis. Sec. Res. Doc. 2022/007. iv + 82 p.

Aussi disponible en français :

Keith, D.M., Sameoto, J.A., Keyser, F.M., et Andrushchenko, I. 2023. Quantifier les changements dans la répartition de la morue franche et de la limande à queue jaune sur le banc de Georges. Secr. can. des avis sci. du MPO. Doc. de rech 2022/007. iv + 85 p.

TABLE OF CONTENTS

ABSTRACT

Georges Bank (GB) has historically been one of the world's most productive fishing grounds. Several formerly abundant groundfish stocks have experienced declines that have resulted in the cessation of directed fisheries. Subsequently, management agencies in both Canada and the United States (U.S.) have implemented various restrictions in an effort to rebuild these stocks; these restrictions include the implementation of closures. Yellowtail Flounder (*Limanda ferruginea*) and Atlantic Cod (*Gadus morhua*) are two groundfish stocks that have substantially declined and the rationale for closures on GB has included the need to protect these stocks. In the U.S., these closures are larger and focus more broadly on rebuilding these and other stocks on GB, while in Canada the closures are smaller and directed towards the protection of these two stocks during spawning. This document presents temporally variable species distribution models for these two stocks using a suite of static environmental covariates and presence-absence information from groundfish trawl surveys in Canada and the U.S. These models indicate that there have been both seasonal and long-term shifts in the distribution of both stocks. Significant predictors of the distribution of both stocks throughout the year were the average Sea Surface Temperature (SST; average from 1997-2008) and depth (Dep), while sediment type (Sed) was also a significant predictor for Yellowtail Flounder. The seasonal distribution of the core area of Atlantic Cod is similar in the late winter and spring, while in the fall the distribution shifts to the edge of the bank. For Yellowtail Flounder, the core area is found in a similar location throughout the year. The distribution of Atlantic Cod differed approximately every five years, while the Yellowtail Flounder distribution differed every three years. These shifts in distribution are not random, with the centre of gravity of the core areas for both stocks shifting to the northeast throughout the study period. Much of this shift is due to the loss of core area from southern and western portions of GB. The shifts in the distributions have resulted in an increase in the proportion of both stocks in Canadian waters throughout the year. During Atlantic Cod spawning there has been a substantial decline in the core area inside the two large closures in the U.S. In recent years, Yellowtail Flounder have predominately straddled the Canada-U.S. border; during spawning, the proportion of core area observed in Closed Area II (U.S.) has steadily increased to almost half of the total core area on GB. In Canada, the closures to protect Atlantic Cod and Yellowtail Flounder during spawning both predominately include core area, but due to their limited size these closures make up only a small proportion of the core area on the Canadian portion of GB. Finally, during spawning, the models for both stocks were successful at capturing the spatial dynamics up to three years into the future. The framework methodology applied here provides novel insights into both seasonal and inter-annual variability in the spatial distributions of these stocks and provides a quantitative evaluation of closures relative to these distributions. Incorporation of the information from approaches such as this into the science advice process, can facilitate improved decision-making for fishery management.

1. INTRODUCTION

Georges Bank (GB) has been home to some of the most productive fisheries in the world as well as a wealth of other natural resources (Backus and Bourne 1987). In the 1960s and 1970s numerous countries had large unsustainable fisheries in the region, but with the expansion of territorial seas to 200 miles offshore in 1977, control of resource exploitation (e.g., fisheries) on GB fell under the jurisdiction of the United States (U.S.) and Canada (Halliday and Pinhorn 1996; Anderson 1998). The final demarcation of the Canadian and U.S. territorial waters on GB was implemented with an International Court of Justice (ICJ) decision in 1984. Within three years of this decision both countries had independent groundfish surveys, with each survey covering the entirety of GB at different times of the year.

Historically, GB supported substantial groundfish fisheries including Atlantic Cod (*Gadus morhua*), Haddock (*Melanogrammus aeglefinus*), Yellowtail Flounder (*Limanda ferruginea*) and numerous other species (Anderson 1998). As observed throughout the northwest Atlantic, the biomass of Atlantic Cod on GB declined significantly in the early 1990s and there has been little evidence for recovery of this stock since this collapse (Andrushchenko et al. 2018). Between the 1970s and the 1990s, the biomass of Yellowtail Flounder on GB was low, but evidence for a rapid recovery of this stock in the early 2000s resulted in directed fisheries for several years. However, this recovery was short lived and the biomass of this stock has been near historical lows for the last decade (Legault and McCurdy 2018). While the biomass of Atlantic Cod and Yellowtail Flounder remains low, both Haddock and Sea Scallop (*Placopecten magellanicus*), the latter being one of the most lucrative fisheries on GB over the last two decades, have experienced unprecedented productivity during this time (Stokesbury 2002; Hart et al. 2013; DFO 2019a; Finley et al. 2019).

Fisheries management bodies in both Canada and the U.S. have implemented measures to protect the Atlantic Cod and Yellowtail Flounder stocks on GB. While these measures vary between the countries, there is a collaborative process to develop a shared quota for these two stocks (TRAC 2020); a quota which has declined substantially for both stocks over the last decade (Andrushchenko et al. 2018; Legault and McCurdy 2018). In addition to regulations that attempt to directly limit fishing mortality, both countries have implemented spatial closures (Figure 1). In the U.S., two large closed areas were implemented (Closed Area I [CA I] and II [CA II]) with the intent of aiding in the recovery of groundfish and invertebrate stocks on GB. These closures were established in 1994 and have been modified over time to occasionally allow some fishing activity (Murawski et al. 2000; Link et al. 2005). On the Canadian portion of GB, the groundfish fishery has historically been closed from March 1st to May 31st to protect spawning groundfish. In 1994 the closure was expanded to include the months of January and February in an effort to rebuild the Atlantic Haddock stock. This closure was subsequently shortened in 2005 to exclude January, resulting in a closure of the groundfish fishery from February through to the end of May. The Canadian Offshore Scallop Fishery (COSF) also faces restrictions on fishing during the peak groundfish spawning periods with time-area closures limiting the area in which this fishery can operate during February and March (Atlantic Cod, DFO 2019b) and June (Yellowtail Flounder, DFO 2014). The U.S. closures have been linked to the recovery of several stocks on GB (Murawski et al. 2000; Link et al. 2005), although the reasons for the recent decline of Yellowtail Flounder and the ongoing lack of recovery of Atlantic Cod on the bank since the implementation of these closures remains uncertain (Andrushchenko et al. 2018; Legault and McCurdy 2018). In Canada, there had been no comprehensive review of the closures until a recent review by Keith et al. (2020) that found little evidence that the COSF time-area closures

were achieving their management objectives. This analysis also highlighted the need for a better understanding of the spatio-temporal distributions of both of these stocks in relation to the location and timing of these closures.

Several metrics have been developed to track changes in species distribution at a broad scale. These metrics include the Gini index, concentration metrics (e.g., D90%), area occupied, along with various other density metrics (Myers and Cadigan 1995; Hutchings 1996; Reuchlin-Hugenholtz et al. 2015). These metrics have been used to identify shifts in the distributional characteristics at the stock scale and to understand how these shifts may indicate changes in the dynamics of these stocks (Myers and Cadigan 1995; Reuchlin-Hugenholtz et al. 2015). While they are appropriate tools for understanding changes in distribution in a coarse sense, these metrics are not able to quantify changes that may occur at scales smaller than the aggregation unit (e.g., many of these indices aggregate data within strata that are 1000s of km^2 in size). They also give no indication of the spatial location of the stock. Thus, when trying to understand fine-scale spatial dynamics, as would be necessary to understand the overlap between the distribution of a stock and some underlying feature (e.g., a closure), these metrics have little stand-alone utility and additional tools are needed.

Species Distribution Models (SDMs) were one of the earliest modelling frameworks developed to better understand spatial distributions and the processes that influence where a species is likely to be observed (Grinnell 1904; Box 1981; Booth et al. 2014). These models use environmental data and species ecological information to map the Occurrence Probability (OP; or some measure of abundance) of a species across some land(sea)-scape; quantitative SDMs originated with attempts to predict terrestrial plant distributions (Box 1981). In the marine realm, the use of SDMs has increased rapidly in recent years; SDMs have been used in the development of Marine Protect Areas (MPAs), MPA networks, to better understand the distribution of Species at Risk (SAR), and to predict the impact of climate change (Cheung et al. 2008; Robinson et al. 2011; Sundblad et al. 2011; Domisch et al. 2019; McHenry et al. 2019). Historically, SDMs often did not explicitly consider temporal changes in the relationship between the environment and the response of the species; these SDMs therefore provide a snapshot in time based on available data (Elith and Leathwick 2009). However, more sophisticated SDM frameworks have been developed in which the underlying relationships can vary in time and space while explicitly accounting for spatial patterns, which results in more dynamic models that can provide improved predictions (Merow et al. 2011; Thorson et al. 2016; Martínez-Minaya et al. 2018). The development of these new spatio-temporal SDM models have been made possible by a number of recent statistical and computational advances, such as the implementation of the Laplace Approximation (LA), Automatic Differentiation (AD), Stochastic Partial Differential Equations (SPDE), and Gaussian Markov Random Fields (GMRF) in commonly used programming languages (Kristensen et al. 2016; Rue et al. 2017; Thorson 2019). This has enabled the complex spatio-temporal analytical problems required for these advanced SDM models to be solved in a fraction of the time required by traditional methods.

While data collection in fisheries science, both biological and environmental, is often spatial and temporal in nature, computational and statistical limitations have resulted in science products that do not fully utilize the spatio-temporal information contained in these data. Traditional SDM applications often do not include a temporal component (Elith and Leathwick 2009), while traditional fisheries stock assessment methods aggregate information spatially and treat stocks as spatially homogeneous entities (Hilborn and Walters 1992). The aforementioned computational advances, coupled with more accessible statistical methods, have resulted in new methodologies that are capable of harnessing both the spatial and temporal information

contained within fisheries data and could be used to develop science advice that can facilitate dynamic management solutions.

1.1. OBJECTIVES

A recently developed statistical tool (Integrated Nested Laplace Approximation (INLA), Lindgren and Rue 2015; Rue et al. 2017; Bakka et al. 2018) was used to apply a framework methodology that developed spatio-temporal SDMs for two depleted groundfish stocks on GB (Atlantic Cod and Yellowtail Flounder). The objectives were to: 1) use a suite of static environmental layers to determine whether the stock distributions changed over time and, if so, determine how rapidly changes in the distributions could be detected, 2) determine whether the stock distributions change seasonally using data from annual surveys in the *Winter*, *Spring*, and *Fall*, 3) investigate how well existing closures on GB align with these stocks, 4) quantify how well the proposed models can predict the spawning distribution of these stocks 1, 2, and 3 years into the future, and 5) discuss these results in the context of closed areas on GB.

2. METHODS

2.1. STUDY AREA

Georges Bank, located in the northwest Atlantic straddling the U.S.-Canada maritime border, is a 3-150m deep plateau that covers approximately 40,000 km^2 and is characterized by high primary productivity, and historically high fish abundance (Townsend and Pettigrew 1997). It is an eroding bank with no sediment recharge and covered with coarse gravel and sand that provides habitat for many species (Valentine and Lough 1991). Since the establishment of the ICJ decision in 1984, the Canadian and U.S. portions of GB have been largely managed separately by the two countries, though some collaborative management exists (Figure 1).

2.2. DATA

Survey data were obtained from the Fisheries and Oceans Canada (DFO) “Winter” Research Vessel (RV) survey from 1987-2019 and the National Marine Fisheries Service (NMFS) “Spring” and “Fall” groundfish surveys from 1972-2019. The Winter survey on GB typically occurs in February and March, the Spring survey typically occurs in April and May, while the Fall survey generally takes place between September and November. For all surveys, only tows deemed *valid* were used in this analysis. This resulted in 2,590 tows from the Winter survey, 2,393 tows from the Spring survey, and 2,506 tows from the Fall survey.

2.3. ENVIRONMENTAL COVARIATES

A suite of 21 spatial environmental and oceanographic datasets were obtained for this analysis (Table 1). To eliminate redundant variables, Variance Inflation Factors (VIFs) were calculated for all variables and any variables with VIF scores > 3 were removed. This procedure was repeated until no variables remained with a VIF score > 3 (Zuur et al. 2010). A Principal Component Analysis (PCA) was undertaken using the data from the associated station locations for each survey with variables excluded from the PCA if they showed no evidence for correlation with other variables or if they had very non-linear correlation patterns (Table 1). The top four PCA components, accounting for at least 80% of the variability in the data for a given survey, were

retained and included as covariates for the models in addition to the retained environmental covariates (Figure 2).

2.4. SPATIAL STATISTICAL ANALYSIS

2.4.1. Gini Index

The Gini index measures how evenly biomass is distributed through space. The index can range from 0 to 1, where low values indicate that the stock is spread evenly across the region, while high values indicate that the biomass for the stock is distributed unevenly (clumped). To calculate this index the tows need to be aggregated into pre-defined areas; for simplicity the strata from the surveys were used as the grouping areas for this analysis. The strata biomass (SB_r) which was calculated by stratum (*r*) in each year for a particular stock as;

$$SB_r = \frac{\sum_{i=1}^{n} B_i}{n} \times A_r \tag{1}$$

Where (B_i) is the biomass of tow *i* within stratum *r*, A_r is the area of the stratum, and *n* is the number of tows within the stratum. The total biomass for all strata (TSB) was calculated as;

$$TSB = \sum_{r=1}^{n} SB_r \tag{2}$$

Finally, the proportion of the total biomass for each stratum PSB_r was calculated as;

$$PSB_r = \frac{SB_r}{TSB} \tag{3}$$

The PSB_r were then ordered from smallest to largest. The proportion of the total area on GB represented by each stratum was given by PA_r. The Gini index ($G_{s,t}$) was then calculated for each stock (*s*) and year (*t*) using;

$$G_{s,t} = 1 - 2\int_0^1 L_x dx \tag{4}$$

Where L_x is the Lorenz curve, this describes the relationship between the cumulative PSB_r and the cumulative PA_r. The Gini index is the area between the 1:1 line (which represents a situation in which the biomass is evenly distributed through space) and 2 times the Lorenz curve.

2.4.2. Species Distribution Models

A Bayesian hierarchical methodology was implemented using the INLA approach available within the R Statistical Programming software R-INLA (Lindgren and Rue 2015; Bakka et al. 2018; R Core Team 2020). In recent years, R-INLA has seen a rapid increase in use for modeling species distributions in both the terrestrial and marine realms (e.g., Cosandey-Godin et al. 2015; Leach et al. 2016; Boudreau et al. 2017). This methodology solves stochastic partial differential equations on a spatial triangulated mesh; the mesh is typically based on the available data (Rue et al. 2017). The mesh used in this study included 6,610 vertices and was extended beyond the boundaries of the data to avoid edge effects (Figure 3). Default priors were used for the analysis, except for the range and standard deviation hyperparameters used to generate the random fields, which were Penalized Complexity (PC) priors (Zuur et al. 2017; Fuglstad et al. 2019). The range PC prior had a median of 50 km with a probability of 0.05 that the range was smaller than 50

km. The standard deviation of the PC prior had a median of 0.5 with a probability of 0.05 that the marginal standard deviation was larger than 0.5.

For the INLA models, survey data up to 2016 were used ('Winter' survey from 1987-2016, 'Spring' and 'Fall' surveys from 1972-2016). Survey data from 2017-2019 were excluded from the main analysis and used only as a testing dataset for the closure case study. For all analyses, the response variable was the probability of the survey detecting an individual from the stock of interest (Occurrence Probability, OP_{it}, where *i* is an observation in time period *t*) and a *Bernoulli* GLM was utilized within R-INLA. Cells with an estimated OP $\geq$ 0.75 were considered the *core area*. An interactive dashboard has been developed that can be used to explore the effect of defining different OPs as *core area*.

$$OP_{it} \sim Bernoulli(\pi_{it})$$

$$E(OP_{it}) = \pi_{it} \qquad and \qquad var(OP_{it}) = \pi_{it} \times (1 - \pi_{it}) \tag{5}$$

$$logit(\pi_{it}) = \alpha + f(Cov_i) + u_{it}$$

$$u_{it} \sim GMRF(0, \Sigma)$$

Each variable retained after the VIF analysis, along with the four PCA components, was added to the model individually. All continuous covariates were modelled using the INLA random walk $'rw2'$ smoother, which allows for non-linear relationships between the response and each covariate (Zuur et al. 2017; Zuur and Leno 2018). The continuous covariates were centred at their mean value and scaled by their standard deviation. Covariates that were highly skewed (e.g., depth) were log transformed before being standardized. Due to low sample size of several of the levels the Sediment type [Sed; data obtained from McMullen et al. (2014)], these infrequent categories were amalgamated into one factor level that was represented by an *Other* term, resulting in three levels for the Sediment covariate (*Other*, *Sand*, and *Gravel-Sand*). Across the three surveys, approximately 93% of the survey tows were on the *Sand* or *Gravel-Sand* bottoms and 7% were in the amalgamated *Other* category.

Four spatial random field (u_{it}) models with differing temporal components were compared for each stock and each survey, these were a) a static random field (t = 1), b) independent random fields every 10 years, c) independent random fields every 5 years, and d) and independent random fields every 3 years. The independent random fields (options b through d) were set retroactively from the most recent year, resulting in a shorter duration random field at the beginning of the time series whenever the field time period was not a multiple of the whole time series length (e.g., the 10 year random fields for the Spring models were 2007-2016, 1997-2006, 1987-1996, 1977-1986, and 1972-1976). Models with the same covariate structure but different random fields were compared using Watanabe–Akaike Information Criterion (WAIC), Conditional Predictive Ordinate (CPO), and Deviance Information Criterion (DIC); the results for each of these metrics were similar and only the WAIC results are discussed further. In all cases, the static random field was an inferior model when compared to models with multiple random fields, and the results discussed here are largely limited to the comparison of the 10/5/3 year random fields. For brevity, we refer to the results from each random field as an *era* (e.g., the *core area* estimated when using the 2012-2016 random field is the *core area* during the 2012-2016 *era*).

2.4.3. Model Selection Overview

Stage 1 model selection for the different covariate models was undertaken using the static random field by adding individual covariates. For this first analysis, covariates were retained if low WAIC scores were obtained. CPO and DIC results were similar to WAIC, so only WAIC is discussed further; complete model selection results are available in the Model Output and Model Diagnostics sections of the interactive dashboard. For Atlantic Cod, this analysis identified depth (Dep) and the average sea surface temperature between 1997 and 2008 (SST) as having low WAIC scores in two of the three surveys (data obtained from Greenlaw et al. 2010). For Yellowtail Flounder, Dep was identified as an informative covariate in all three surveys. In addition, Sed and the average chlorophyll concentration between 1997 and 2008 (CHL) were retained based on their low WAIC scores in the Fall survey. Given the low number of informative covariates, Dep, SST, and CHL were all retained for both species in Stage 2 of model selection. In Stage 2 of model selection, these variables were added pairwise (e.g., models included SST + Dep, Dep + CHL, and SST + CHL) for both stocks and again compared using WAIC using the 10-year random fields. In Stage 3 of covariate model selection, models with three covariates were tested based on the Stage 2 results. For Atlantic Cod, a three term model that included additive terms for SST, Dep, and CHL was the most complex model tested. For Yellowtail Flounder, the most complex model included SST, Dep, and Sed. In Stage 3, additional covariates were retained if the WAIC for that model resulted in an improvement of the WAIC of more than 2, as compared to the lowest WAIC for the more parsimonious model.

Model selection on the temporal random fields was done while holding the environmental covariate terms the same. Initial model selection for the random fields (10 and 5-year fields) was done using the Dep + SST model for both species in all seasons given the general support for the Dep + SST model identified in Stage 2 of covariate model selection. For both species, this indicated that the 10-year field was inferior to the more flexible 5-year random fields. For Atlantic Cod, the 3 and 5-year random fields were compared using the Dep + SST (which was the covariate model with the lowest WAIC). For Yellowtail, the final step of the random field model selection used the Dep + SST + Sed model (which was the covariate model with the lowest WAIC) for the 3-year and 5-year random field comparison. Note that for Yellowtail Flounder the Dep + SST + Sed covariate model was not run with the 10 year random field and the Dep + SST covariate model was not run using the 3-year random fields in all three seasons, thus there were no results to show for these *potential* models.

2.5. MODEL PREDICTION

A predictive grid with cells having an area of approximately 9.1 km^2 was developed (Figure 4). The models chosen to predict OP on the predictive grid were the additive SST + Dep models with the 5 year random fields for both stocks and the three surveys. Each cell was intersected with average SST and Dep fields, and the OP was estimated for each grid cell in each *era* for Atlantic Cod and Yellowtail Flounder in the Winter, Spring, and Fall. The results using the predictive grid were used to calculate the *core area* for each *era*.

This predictive grid was used to calculate the centre of gravity (COG) of the core area for each era. The COG was calculated in the UTM coordinate system (UTM Zone 19N) using the easting (X) and northing (Y) for each cell identified as *core area* (i) in each *era* (t) and weighted by the

OP at each of these locations where *n* is the number of observations.

$$x_t^{cog} = \frac{\sum_{i=1}^{n}(X_{i,t} \times OP_{i,t})}{\sum_{i=1}^{n} OP_{i,t}} \tag{6}$$

$$y_t^{cog} = \frac{\sum_{i=1}^{n}(Y_{i,t} \times OP_{i,t})}{\sum_{i=1}^{n} OP_{i,t}} \tag{7}$$

The standard deviation around the mean COG in the X and Y direction was calculated as:

$$\sigma_{cog,t}^{y} = \sqrt{\frac{\sum_{i=1}^{n} OP_{i,t}}{[(\sum_{i=1}^{n} OP_{i,t})^2 - \sum_{i=1}^{n} OP_{i,t}^2] \times \sum_{i=1}^{n}(OP_{i,t} \times (Y_{i,t} - y_t^{cog})^2)}} \tag{8}$$

2.6. MODEL VALIDATION

Five-fold cross validation was used to test the predictive performance of a selection of the 5-year random field models: intercept only, SST (Atlantic Cod), Dep (Yellowtail Flounder), and Dep + SST. The Atlantic Cod model validation was performed using the Winter survey; the Yellowtail Flounder validation used the Spring survey. The data were randomly divided into five subsets and trained using four of the subsets; the fifth dataset was treated as a testing dataset to determine how well the model was able to predict out-of-sample data. Model performance was measured by comparing the model residuals from the training data to the prediction error from the testing data. The metrics used for this comparison were Root Mean Squared Error (RMSE), Mean Average Error (MAE), and the Standard Deviation (SD).

2.7. CASE STUDY: QUANTIFYING THE IMPACT OF DISTRIBUTIONAL SHIFTS ON GEORGES BANK CLOSURES

Model results were used to track changes in the distributions of Atlantic Cod and Yellowtail Flounder on GB.

There are five distinct closures within the domain of the U.S. and Canadian groundfish surveys on Georges Bank (Figure 1) that are relevant to this analysis. There are two large closures on the U.S. side of GB, two smaller time-area closures in Canadian waters that affect only the COSF, and a full closure of the Canadian portion of GB to the Canadian Groundfish Otter-trawl Fishery that begins in early February and runs until the end of May. This groundfish closure results in the complete exclusion of this fishery from the Canadian portion of GB. Consequently, we do not discuss the groundfish closure in detail here since the results of any analyses would be the same as the analyses for the Canadian portion of GB.

In the U.S., CA I and CA II were implemented in 1994 in an effort to rebuild stocks in the region (Link et al. 2005). CA I was originally approximately 3,950 km^2 and extended outside the primary GB domain used in this study; this analysis was therefore limited to the subset of CA I region that is inside this study's GB survey domain (1,938 km^2). The management of the CA I closure has changed over time and it is currently part of a larger seasonal closure covering a large area within the Gulf of Maine. CA II is adjacent to the ICJ line and covers 6,807 km^2 with the majority of this area (6,683 km^2) within the GB survey domain used in this study. Since 1999, portions of both of these closed areas have allowed U.S. scallop fishery access (Link et al. 2005; O'Keefe and DeCelles 2013).

To quantify the ability of these models to predict the location of the stocks in future years, data from the 2017-2019 surveys were used as a testing dataset to predict the OP in 2017, 2018, and 2019. In addition to the final model, an *Intercept Model* that used only the temporally varying random field for prediction (i.e., the model excluded all environmental covariates) was compared to the predictions from the final models. Both the model residual and the 2017-2019 predictive error were calculated for each year using RMSE, MAE, and the SD. Given the similarity of the results, only the RMSE is presented (full results are available in the interactive interactive dashboard).

On the Canadian side of GB, the objectives of the COSF time-area closures are to reduce discards during spawning from the COSF for either Atlantic Cod or Yellowtail Flounder. The closure in February and March was designed to protect spawning Atlantic Cod and was first implemented in its current form in 2006. The other closure was implemented in 2007, occurs in June, and was designed to protect spawning Yellowtail Flounder. The location and size of each closure can vary from year to year, although the location of the Yellowtail Flounder closure has not changed since 2014 (DFO 2014, 2019b). To assess the spatio-temporal overlap between these closures and the stock distributions, the historical trends of OP for Atlantic Cod and Yellowtail Flounder were assessed in Canadian waters (Figure 1) and compared to trends in the Canadian Atlantic Cod and Yellowtail Flounder closures between 2007-2016.

Atlantic Cod spawn between November and May on GB, with a spawning peak in February and March (O'Brien et al. 1993). The Winter survey occurs during this period and was used for the Atlantic Cod spawning analyses. Yellowtail Flounder spawning occurs mostly in the spring between April and August, with peak spawning in May and June (O'Brien et al. 1993). The Spring survey occurs during this period and was used for the Yellowtail Flounder analyses.

3. RESULTS AND DISCUSSION

3.1. GINI INDEX

The Gini index provides a synoptic view of changes in the distribution of both stocks throughout the year. During the Winter and Spring, the Gini index increased from the start of both time series until the mid-late 2000's and stabilized thereafter. This is indicative of a long-term decrease in the evenness of the distribution of both stocks throughout the time-series, followed by a period of stabilization over the last 10-15 years (Figure 5). During the Fall, the index has been increasing over time for both stocks, although the rate of increase slowed for Yellowtail Flounder in the mid-2000s (Figure 5). These general trends can also be observed in Figure 6, in which the curves tend to move further from the 1:1 line in more recent years for both species in all three seasons.

3.2. SDM MODEL SELECTION

Stage 1 of model selection resulted in a significant reduction in the number of covariates. For Atlantic Cod, Sea Surface Temperature (SST) was identified as a significant covariate in the Winter and Spring. In addition, depth (Dep) and stratification were also significant predictors, but only in the Spring. In the Fall, no covariates had a WAIC that were a significant improvement from the intercept only model (Figure 7). Further model selection indicated that an additive Dep + SST model was the preferred model in all 3 seasons for Atlantic Cod (Figures 8 and 9). When

exploring the effect of temporal variability on the random fields, the models using the 5-year random field had the lowest WAIC in all seasons (Figure 10).

For Yellowtail Flounder, stage 1 of model selection indicated that the inclusion of Dep significantly improved the models in all three seasons (surveys), while Sediment type (Sed) and Chlorophyll concentration (Chl) in the Fall had a similar impact on the model WAIC as Dep. As a result, SST, Dep, Chl, and Sed were used to explore the development of more complex covariate models. For Yellowtail Flounder, the best models in stage 2 of model selection included two covariates with a combination of Dep, SST, and Sed (Figure 8). Further model selection indicated that the preferred model for Yellowtail Flounder in all three seasons was an additive model including Dep, SST, and Sed (Figure 9). When exploring the effect of temporal variability on the random fields, the 3-year field had the lowest WAIC in the Winter and Spring, while the 5-year field had the lowest WAIC in the Fall (Figure 10). Additional model selection results are available in the Model Output and Model Diagnostics sections of the interactive dashboard.

3.3. ENVIRONMENTAL VARIABLES

The spatial fields for the three environmental variables retained by model selection are shown in Figure 11. The average SST between 1997 and 2008 had the largest effect on the OP of Atlantic Cod; they were more likely to be found in regions of the bank with a lower SST (Figure 12). For all three surveys, the OP of Atlantic Cod declined rapidly in regions of the bank where the SST was above approximately 10°C (Figure 12). Although the Dep relationship was also retained in the final Atlantic Cod model, the effect of Dep on OP was substantially smaller than the SST effect. During the Winter and Spring the OP peaked between 70-82 m and declined slowly in shallower and deeper waters (Figure 12). There was no clear relationship with Dep in the Winter.

For Yellowtail Flounder, Dep had the largest effect on OP, with Yellowtail Flounder most likely to be observed between depths of 66-75 m in each of the three surveys, and the Dep effect on OP was highest during the Spring (Figure 13). The average SST between 1997 and 2008 was also included in the final model for all three seasons, with Yellowtail Flounder OP generally declining as SST increased. The effect of SST was least pronounced in the Fall. The sediment type also had a significant influence on the OP for Yellowtail Flounder, with Sand and Gravel-Sand having higher OPs than the Other sediment category. This difference is most notable during the Winter, but model selection slightly favoured the inclusion of Sed in the Spring and Fall as well, although the effect size was reduced in these seasons (Figures 9 and 13).

3.4. RANDOM FIELDS

The 5-year random fields for Atlantic Cod in the Winter and Spring are seasonally consistent through time, with lower effect sizes observed in both seasons starting in 1992 and the largest declines in the effect size observed in the southern and western portions of GB (Figures 14-15). In the Fall the higher effect sizes were generally observed towards the north and in Canadian waters, with larger declines in the random field effect size towards the west over the study period (Figure 16).

The Yellowtail Flounder 3-year random field patterns were similar between the seasons although the random field effect sizes were somewhat smaller during the Fall (Figures 17-19). The effect size of the random fields were lower in all seasons throughout the latter half of the 1980s and the early 1990s. The highest effect size of the random fields were observed in the 1970s and in the 2000s. Since the mid-1970s, an area straddling the Canadian-U.S. border has been consistently

identified as an area where the Yellowtail Flounder effect size of the random field is elevated (Figures 17-19).

The standard deviation (SD) of the random fields for Atlantic Cod were also similar between seasons, with the lowest SD generally observed in the north and east and highest SD in the south. The SD was somewhat higher in the Fall throughout the central portion of GB (Figures 20-22). For Yellowtail Flounder, the SD was higher towards the south of the bank, with localized regions having elevated SD scattered throughout the bank in the Winter, Spring and Fall (Figures 23-25).

3.5. MODEL PREDICTIONS

The modelled OP for Atlantic Cod in the Winter and Spring was elevated on all but the most southern portion of GB in the 1970s and 1980s. In the early 1990s, there was an abrupt decline in the OP throughout much of the U.S. portion of GB, while OP remained elevated in Canadian waters and in the area straddling the ICJ line (Figures 26-27). In the Fall, the core areas were isolated to the north of GB. An area on the northwest of GB had some core area until the early 1980s, but the OP in this area declined steadily after this time and has had a low OP in the Fall for over 20 years. The highest OP areas remaining during the Fall are along the northern edge of the bank and mostly in Canadian waters (Figure 28).

The modelled OP patterns for Yellowtail Flounder on GB are similar in Winter, Spring, and Fall, with the core area consistently observed in the region straddling the ICJ line in each season and throughout the study period (Figures 29-31). A second region along the western border of the bank also has an elevated OP and appears to be connected via a narrow band of varying width to the core area straddling the ICJ line. The core area of Yellowtail Flounder declined in the late 1980s and early 1990s and remained relatively stable until 2016 (Figure 31).

The SD of the Atlantic Cod prediction field in the Winter and Spring tended to be elevated in the central portion of the bank, and lowest in the south and along the edges of the prediction domain. In the Fall, the Atlantic Cod prediction field SD was lowest in the south, with the low SD area expanding to central regions later in the study period (Figures 32-34). For Yellowtail Flounder, the SD was consistently low in the part of the region, with a core area that straddled the ICJ line in the Winter, Spring, and Fall (Figures 35-37). Areas surrounding this region displayed an increase in the SD, while a region in the north and along the southern flank of GB had relatively low SDs; these regions also had relatively low OPs (Figures 29-31 and 35-37).

3.6. INTER-ANNUAL AND SEASONAL VARIABILITY

For both stocks, the core areas shifted towards the north and east throughout the study period; a trend most noticeable when focusing on the core area (OP $\geq$ 0.75) regions (Figure 38). For Atlantic Cod, the shift in distribution of the core area regions occurred relatively rapidly in the 1990s, and the Centre of Gravity (COG) has been relatively stable since that period (Figure 38). In the 1970s and 1980s, core area was observed across the bank. Since the mid-1990s, however, there is a clear shift in distribution with core area concentrated along the north-east of the bank, mainly in Canadian waters (Figures 26-28). In addition, in the Fall, Atlantic Cod tended to be distributed along the northern edge of GB and likely encompasses the northern slope of the bank, where there is limited survey coverage, as well. The size of the core area has followed a similar temporal pattern as the distribution, with a rapid decline in the core area for Atlantic Cod occurring in the 1990s in the Winter and Spring (Figure 39). In the Fall, the decline in the size of the core area was observed approximately a decade earlier than in the Winter or Spring, and the

core area has been much smaller in the Fall (Figure 39). Given the location of the stock along the edge of the bank during the Fall, it is likely that a substantial portion of the stock is located along the slope where survey coverage is limited (Figure 1).

The shift in Yellowtail Flounder core area has, in large part, resulted from a reduction in the core area along the southern flanks of GB. The core area has been consolidated in a central region of GB that straddles the ICJ line separating Canada and the U.S. (Figure 38). The COG of Yellowtail Flounder has been relatively stable both seasonally and between eras since the 1990s despite large changes in the size of the core area during this time. The size and location of the core area during the Spring and Fall have been very similar since the 1980s. In both seasons, there were large increases in core area in the 1990s followed by a variable, yet generally increasing, size of core area more recently (Figure 39). In the Winter, an area of similar location and size is observed, but the size of the core area in the Winter has been in decline since a period of increase in the 1990s (Figure 39).

For both stocks, the changes in the size of the core area were larger in the U.S. than in Canadian waters (Figure 40). In the U.S., the declines in the size of core area of Atlantic Cod occurred rapidly in the early 1990s in the Winter and Spring. In the Fall, the loss of core area occurred approximately a decade earlier, although the size of the core area in the U.S. during the Fall was always substantially lower than in the Winter or Spring. In Canadian waters, there has been minimal change in the size of the core area in any of the seasons through time, although the size of the core area in the Fall has tended to be smaller than observed in the Winter or Spring (Figure 40). The size of the core area of Yellowtail Flounder in the U.S. declined steadily throughout the 1970s and 1980s, followed by an increase in the 1990s and early 2000s (Figure 40). In the last decade, the size of the core area in the U.S. appeared to stabilize. In Canada, the size of core area for Yellowtail Flounder throughout the 1970s and 1980s was variable and relatively low, but increased in the mid-1990s and has been relatively stable since then (Figure 40).

3.7. MODEL HYPERPARAMETERS

For Atlantic Cod, the estimate of the Dep variance hyperparameter was highest in Winter and declined throughout the Spring and Fall, reflecting the decline in the influence of this covariate in the Fall (Figure 41). For Yellowtail Flounder, the Dep variance hyperparameter was higher than observed for Atlantic Cod throughout the year and reflected the relative stability in the effect size of this covariate throughout the year (Figure 41). The SST variance hyperparameter for Atlantic Cod was relatively stable throughout the year and reflects the consistent influence of the SST covariate on the distribution of Cod. For Yellowtail Flounder, the SST variance hyperparameter was relatively low throughout the year, and aligns with the consistent small effect of the SST covariate on the distribution of Yellowtail Flounder (Figure 42). The uncertainty of these estimates precludes the observation of statistical differences between the seasons.

The decorrelation range for Atlantic Cod was above 100 km throughout the year and was generally higher than that observed for Yellowtail Flounder (Figure 43). The range was highest for Atlantic Cod in the Spring (218km [95% CI:131-346]), while the range during the Winter spawning period was the lowest (154km [95% CI:99-227]). In the Fall, the estimate declined from the Spring; the range in this period may be influenced by a portion of the stock being located outside of the survey domain and the stock being more concentrated in one area (Figure 43). For Yellowtail Flounder, the lowest range was estimated in the Winter at 86km (95% CI:63-109), with the Spring and Fall range estimates being higher and somewhat more variable than the

Winter range estimate. The range estimates of Yellowtail Flounder throughout the year were smaller and less variable than that observed with Atlantic Cod (Figure 43). The uncertainty of these estimates precludes the observation of statistical differences between the seasons.

The standard deviation of the random field was lower for Atlantic Cod in the Winter and Spring than during the Fall (Figure 44). The significant increase in the standard deviation in the Fall was related to the increased influence of the random field (i.e., the relatively small effect of the environmental covariates) during this season for Atlantic Cod. The standard deviation of the random field is highest for Yellowtail Flounder in the Winter, and the seasonal differences for Yellowtail Flounder are smaller than those observed with Atlantic Cod (Figure 44). The standard deviation of the Yellowtail Flounder field is higher than that of Atlantic Cod in the Winter and Spring, but lower in the Fall (Figure 44).

The posteriors of these hyperparameters for both stocks in the Winter, Spring, and Fall are provided in Figures 45-50.

3.8. VALIDATION

The five-fold cross validation indicated that each of the models used for five-fold cross validation (intercept only, SST [Atlantic Cod], Dep [Yellowtail Flounder], and Dep + SST) were able to predict the distribution for both stocks without an increase in bias or a loss of accuracy (Figure 51). The mean error of the residuals for the validation training set predictions were similar to the error from the predicted test data, and while the mean error of the test data was generally more variable, the estimates were centred on 0 and, thus, there was no evidence of bias in these predictions (Figure 51). The RMSE from the test and training data showed similar patterns for both stocks and most of the models, although for Yellowtail Flounder the RMSE for both the training and the test data from the intercept only model was slightly lower than either of the models with covariates indicating that the inclusion of the environmental covariates may result in a small loss of out-of-sample prediction (Figure 51).

The flexibility of the random fields alone (intercept models) indicated that from a predictive standpoint the random fields were often able to predict the OP without a substantial loss of predictive ability when compared to the more complex models including the static environmental data (e.g., Figure 51). This occurred because the random fields are flexible enough to capture the variability inherent in the data in each era, while the environmental covariate relationships were constrained to be invariant throughout the entire time series. Recent research suggests that using a static random field in conjunction with a spatio-temporal random field may provide comparable, and in some cases better, estimates than models that rely on environmental covariates (Yin et al. 2022)[1].

3.9. IMPLICATIONS

The core area for Atlantic Cod collapsed rapidly in the early 1990s in unison with the collapse of Atlantic Cod (and other groundfish) stocks throughout the Northwest Atlantic (Bundy et al. 2009). Since the collapse, the size of the core area has remained relatively consistent but has continued to slowly shift to the northeast, especially in the Fall.

In addition, the Fall distribution of Atlantic Cod is likely now located on the northeastern slope of the bank outside of the domain of this study and also in an area that is not fully included

[1]Yin Y., Sameoto J.A., Keith D.M., and Mills Flemming J. Improving Estimation of Length-Weight Relationships Using Spatiotemporal Models. Manuscript submitted for publication.

in the stock assessment for the stock. This northeastern shift of the stock over the course of this study suggests that a higher proportion of the stock may now be migrating outside of the area used in the stock assessment than observed in the past. Each of the survey indices had been used as inputs to the Atlantic Cod stock assessment model for eastern GB Atlantic Cod (Andrushchenko et al. 2018). However, this assessment model suffered from such significant retrospective patterns that the model was recently rejected; the results of this study are in agreement with the suggestion that the observed shift in the distribution of Atlantic Cod could have been a contributing factor to the model retrospective problems (Andrushchenko et al. 2018). In addition, because the management of this stock is shared between Canada and the U.S., the observed shift in the core distribution to Canadian waters suggests that shared management policies, such as quota sharing agreements between the two jurisdictions, may require regular review (e.g., TMGC 2002).

Yellowtail Flounder was unlikely to be found on bottom types that did not include sand and was more frequently found at depths between 66-75 meters which is consistent with the known life history for this species (Johnson et al. 1999). In historically lower SST regions of the bank most of the remaining habitat on GB that meet these criteria straddle the ICJ line on GB. In addition, there was a consistent increased likelihood of encountering Yellowtail Flounder in this area that was not explained by the environmental covariates. This suggests this region has some unexplained ecological or environmental significance to Yellowtail Flounder.

The shift in the distribution of Yellowtail Flounder away from more southern and western parts of GB, combined with the declines in biomass of Yellowtail Flounder throughout the U.S. supports the view that the environmental change observed throughout U.S. waters has been a factor in the recent decline of Yellowtail Flounder both on GB and throughout the region (NFSC 2012; Pershing et al. 2015; Legault and McCurdy 2018; NOAA 2020). Given the loss of Yellowtail Flounder from the warmer portions of the bank observed in this study, it is possible that the remaining core area straddling the ICJ line represents the most northern suitable habitat on GB for this species. If temperatures continue to increase, as projected with climate change, the suitability of this habitat may also decline; this would increase the risk of extirpation of Yellowtail Flounder from GB, irrespective of any fisheries management action (Allyn et al. 2020).

The influence of the average SST layer as an environmental covariate in the models was somewhat surprising given this layer was derived from monthly SST composites from the Advanced Very High Resolution Radiometer (AVHRR) satellite from 1997 to 2008 (Greenlaw et al. 2010) and, thus, represents an aggregate, static layer from only a temporal subset of the time period covered by the groundfish survey data. However, the importance of this SST layer may be due to it capturing general widespread oceanographic features across the bank domain. Furthermore, the observed variability of the effect between seasons is likely a reflection of the connection between surface waters and the benthos, given that the degree of vertical mixing and stratification varies with season and spatially across the bank (Kavanaugh et al. 2017). It is acknowledged that the interpretation of the static SST layer used in these analyses as a thermal effect is likely somewhat unrealistic as it assumes that the relative temperature patterns and the species reaction to these patterns have remained static over the study period. Therefore, more advanced models using either dynamic SST or modelled bottom temperature layer could lead to further insights into how changes in the thermal environment have influenced the distribution of both stocks (Pershing et al. 2015; Greenan et al. 2019).

3.10. CASE STUDY: QUANTIFYING THE IMPACT OF DISTRIBUTIONAL SHIFTS ON GEORGES BANK CLOSURES

3.10.1. Closures

In the U.S., the size of the core area in the portion of CA I included in this analysis declined for both stocks in all three seasons, with the core area approaching 0 for both stocks starting around the year 2000 (Figures 52 and 53). In CA II, the decline in core area for Atlantic Cod was similar to that observed in CA I, although during the spring a substantial amount of core area has been observed over the last two decades (Figures 52 and 53). For Yellowtail Flounder, the size of the core area in CA II declined rapidly during the 1970s and 1980s, but has since rebounded with the total core area similar to that observed during the early 1970s (Figures 52 and 53). Since CA II was implemented in the early 1990s, the core area in this closed area has increased substantially, although in the most recent era the size of the core area had declined in all three seasons (Figure 53).

In Canada, the time-area closures were compared to the core area for each groundfish species in Canadian waters. The size of the core area for Atlantic Cod within Canadian waters has fluctuated over time, with the highest estimates of core area in the 1980s in the Winter and Spring, while in the Fall the size of the core area peaked in the 1970s (Figures 54 and 55). In the most recent era, the size of the core area was the lowest observed since the 1990s (Figures 54 and 55). The overall proportion of the core area on GB located within Canadian waters has increased in all three seasons; this is a result of the decline in core area throughout much of the U.S. portion of GB (Figure 55). The Atlantic Cod closure has included between 209 and 299 km^2 of core area since 2007, and over 81% of the closure has historically been core area for Atlantic Cod (Figure 57). Despite this, the small size of these closures resulted in them accounting for less than 8% of the core area within Canadian waters (Figure 57).

The size of the core area of Yellowtail Flounder within Canadian waters increased rapidly in the mid-1990s in all three seasons, with some of highest area observed in the time series over the last two decades, although the size of the core area in the most recent era in the Winter and Spring were relatively low (Figures 54 and 56). In the 1970s and early 1980s Canadian waters generally had < 25% of the core area for Yellowtail Flounder on GB, but since then this proportion has generally increased (Figure 55). The core area within the Yellowtail Flounder closures has ranged between 128 and 300 km^2. Similar to the Atlantic Cod closures, less than 8% of the total core area within Canadian waters is accounted for by the Yellowtail Flounder closures (Figure 57).

3.10.2. Predicting Aggregations in Future Years

The 3 and 5-year random field models resulted in a slight loss of accuracy when predicting the distributions of each stock one, two, and three years into the future (Figure 58), but the predictions were well below the RMSE associated with a model with no predictive ability (dashed line; Figure 58). In the Winter and Spring, the 2018 predictions tended to have a higher RMSE than the other two years. This is in agreement with observations of the survey biomass indices being near historic lows for both stocks in 2018 (Andrushchenko et al. 2018; Legault and McCurdy 2018). For Atlantic Cod, the predictive error from these models were generally at the high end of the range of the RMSE when data were available and indicated that these models provided reasonable prediction of the location of both species up to three years into the future

(Figure 58). For Yellowtail Flounder, the RMSE was highest in the Winter and lowest in the Fall, with the Fall prediction RMSEs similar in magnitude to the model residuals.

3.10.3. Implications

In the U.S., portions of GB closures were put in place in 1994 to assist with the rebuilding of stocks in the region; these closures have been considered instrumental in the rebuilding of several stocks in the late 1990s (Murawski et al. 2000; Link et al. 2005). Despite the successes of these closed areas for other stocks, the biomass of Atlantic Cod on GB has remained low since the early 1990s (Andrushchenko et al. 2018). The substantial loss of core area for Atlantic Cod observed within CA I and CA II was generally observed throughout the U.S. portion of GB. Unfortunately, both CA I and CA II appear to be used substantially less by Atlantic Cod than in the past.

There was a slight increase in the core area for Yellowtail Flounder in CA I around the inception of this closure (1994), which followed a steady decline in the 1970s and 1980s. Following the slight increase, the core area for Yellowtail Flounder in CA I has generally declined. While CA I historically had represented less than 21% of core area for Yellowtail Flounder, in recent decades this has dropped to near 0. Given the restrictions on fishing activity inside CA I during much of this period, it is likely that this shift in the distribution is due to shifting environmental conditions on GB (Allyn et al. 2020).

Closed Area II (CA II), which is adjacent to the ICJ line, had experienced a large rapid decline in the size of the core area for Yellowtail Flounder in the years leading up to the implementation of this closure (1994). This was followed by a large rapid increase in core area for Yellowtail Flounder near the time that CA II was put in place. In recent years, CA II has contained a substantial proportion of the core area for Yellowtail Flounder on GB, and it appears to represent the last large scale habitat suitable for Yellowtail Flounder on the U.S. side of GB. The rapid expansion of the core Yellowtail Flounder habitat in the early 2000s was centered on CA II and in Canadian waters; this occurred at the same time as the rapid increase in Yellowtail Flounder biomass on GB (Legault and McCurdy 2018). The core area for Yellowtail Flounder remained relatively stable starting in the early 2000s and was similar in size to what was observed in the 1970s before CA II was put in place. While these results suggest a positive association between this closure and Yellowtail Flounder stock status, the abrupt Yellowtail Flounder stock decline in the early 2010s (Legault and McCurdy 2018), that occurred despite relatively low fishing effort in CA II, suggests that shifting environmental conditions on GB may now be affecting the stock within CA II (Pershing et al. 2015).

In Canada, previous research on the COSF time-area closures indicates that discard rates from the COSF were elevated when these closures were active (Keith et al. 2020). More generally, this study found little evidence of an effect of these closures on discards from the COSF despite a substantial reduction in discards of these two stocks since the closures were first implemented. The results of the current study confirm the suggestion in Keith et al. (2020) that the closures likely only protect a small proportion of the core-area within the COSF domain; as a result, the discards from the COSF when the closures were active remained elevated for both species. However, Keith et al. (2020) also identified an order of magnitude decline in discards since the closures were first implemented; this reduction was attributed to the significant decline in effort from the COSF, other undocumented voluntary measures the COSF has implemented to reduce discards (e.g., gear modifications, DFO 2008; Walsh 2008), and the ongoing decline in the abundance for both of these stocks.

Currently, the location of the COSF time-area closures are determined, in part, using Science Advice that relies on both fishery dependent and independent data. The results of this study indicate that this methodology has generally been successful in placing the closures within core areas of Atlantic Cod and Yellowtail Flounder (DFO 2014, 2019b). However, the results of this study also indicate that the success of the existing methodology is due in large part to the high proportion of core area within Canadian waters (especially for Yellowtail Flounder). The methodology outlined in the current study provides an alternative quantitative framework that can identify the core area for each stock while quantifying how frequently changes in the distributions can be identified by the existing survey data. In addition, the models for both stocks were able to predict the location where each stock was most likely to be observed up to three years into the future. These predictions could be used when survey information is unavailable for a year, when Science Advice is required before survey information was available, or if multi-year Science Advice is required.

4. FUTURE CONSIDERATIONS

One of the main limitations of the environmental analysis used herein was the static nature of the environmental data. While this was less problematic for covariates that changed slowly over time at broad scales (e.g., depth), the interpretation of environmental covariates that varied at time scales shorter than the time series used in this study should be done cautiously. For these covariates, any relationships identified (e.g., SST) were likely reflective of the stock's distribution following the general pattern of a covariate, rather than evidence for a mechanistic link between the stock's distribution and the covariate. In this regard, we cannot say that SST was the mechanism causing variability in the distribution of either stock, only that there was a correlation observed between the average SST from 1997-2008 and the distribution of these stocks on GB. Static environmental data are also problematic because there is no means to determine if relationships between variables were changing over time (e.g., it is not possible to detect change in these relationships due to climate change). Fortunately, datasets are increasingly becoming available on the spatio-temporal scales necessary to fully explore the relationships between environmental covariates and stock distributions. Finally, many of the covariates evaluated in this study were measured at the surface, whereas groundfish are most affected by the benthic environment. Therefore, the environmental layers near the surface are most likely proxies for other mechanisms. The degree of coupling and correlation between surface and benthic conditions likely varies both spatially across the bank and with season, in particular with seasonal patterns in stratification. However, recent work to correlate benthic temperatures with remotely sensed data has shown promise (Kavanaugh et al. 2017).

The Winter survey (DFO) did not start until 1987, which was approximately the start of a period of substantial shifts for both Atlantic Cod and Yellowtail Flounder. As such, we have limited knowledge of the patterns observed in the Winter before this time. However, from 1987 onward the patterns observed in the Winter and Spring were quite similar for both of these stocks; therefore, it is likely the Spring survey is a good proxy for what was observed during the Winter for both stocks.

The models used in this study were based on presence-absence data. Although abundance data are collected as part of the surveys, they were excluded from the modelling approach used here. This removes potentially informative data regarding the location of these stocks. The DFO and NMFS trawl surveys were designed to provide abundance estimates at the scale of the survey strata, while the SDMs developed here were attempting to elucidate patterns

at much finer scales. The ability of spatio-temporal models to properly account for spatial abundance information at the scale of kilometres from a survey that is designed to provide synoptic estimates at a scale of 10s-100s of kilometres is an active area of research (Punt 2019; Cadrin 2020). A comparison of the results of this study with more advanced models, e.g., Delta models (Thorson et al. 2015) or more flexible random fields (Anderson and Ward 2019), would be informative, but this was beyond the scope of the present study.

The definition of core area used here in the predictions is subjective and other definitions of core area could be developed. Here, we defined core area as the area in which the model predicted that the OP was at least 0.75. Different defensible interpretations of what defines a core area could lead to results which differ somewhat from the results presented here. However, the general trends observed in this study are not unduly influenced by the choice of what the authors consider reasonable values of OP to define the core area (i.e., the conclusions from this study would not change substantially using any OP between 0.5 and 0.9 to define the core area). The interactive dashboard enables the exploration of the results of this study using different OP values to define the core area.

The temporal random fields used in this analysis are a small subset of possible temporally variable random fields. Models using a random field that changes annually either independently of the previous year, or, more likely, correlated annual random fields would be worth further exploration. In addition, using random fields of other durations (e.g., a 4-year field) could also be explored, although an exhaustive exploration of the possible temporal random fields would be computationally and logistically challenging. While the Atlantic Cod model results suggest that distributional shifts using these data are only observed every 5 years, for Yellowtail Flounder shorter duration random fields may be preferred to the 3-year random field models. Finally, the changes observed in the temporal random fields are limited by the survey observations and the scale of the environmental covariates used. Increased survey coverage and finer scale environmental covariates would likely identify changes in the distribution of these species at finer temporal scales than is possible with the available data.

Five-fold model validation using the R-INLA methodology remains computationally demanding and a full comparison of all the models was impractical. Therefore, only a subset of the models were compared using model validation. The most complex models used for model validation used a 5-year random field and the SST and Dep covariates that were identified in Stage 2 of model selection as the favoured models for both stocks. While further model selection identified a more complex final model for Yellowtail Flounder, these models were not included in the model validation due to computational and logistical constraints. However, the more complex Yellowtail Flounder models would be unlikely to have a significant impact on the results observed from the model validation.

5. CONCLUSION

This study developed a framework methodology that can be used to provide insight into how the spatial distribution of Atlantic Cod and Yellowtail Flounder have changed both seasonally and inter-annually since the 1970s. Further, although a substantial suite of environmental variables were examined, only a few were found to influence these distributions, and overall, the covariates investigated have had little impact on the observed distributional patterns of either stock. The only static environmental data that had a consistent significant effect on the stock distributions were the average sea-surface temperature (1997-2008), depth, and bottom type

(Yellowtail Flounder only). The inter-annual shifts in the stock distributions indicate the increasing importance of Canadian waters for both stocks on GB. This is likely due to the long-term environmental shifts observed in the region. Given the habitat constraints faced by both stocks and the continuation of directed environmental change, increased reliance of habitat in Canadian waters is likely to continue irrespective of any fisheries management action.

The distributional shifts demonstrated in this study also highlight the difficulties encountered by static closed areas in achieving stock specific conservation objectives in light of environmental change. For both stocks, the degree of overlap between the closed areas and the core stock area has changed over time. For the portion of CAI included in this study, our results suggest that this area likely no longer contains substantial core habitat for Atlantic Cod or Yellowtail Flounder at any time of the year. In Canadian waters, the proportion of both stocks' core area has increased over time. Unfortunately, the COSF time-area closures protect only a small proportion of the core area in Canadian waters, and this helps explain the elevated discard rates from the COSF for both stocks when the time-area closures were active (Keith et al. 2020).

The utilization of the spatio-temporal information contained in these models provides novel insights that can be used to improve science advice (e.g., accounting for shifting distributions in stock assessment, choosing the location and size of protected areas, etc.), which can improve decision-making related to the management of these stocks.

6. ACKNOWLEDGEMENTS

Thanks to Yanjun Wang, Dheeraj Busawon, Monica Finley, Phil Politis, and Nancy Shackell for help with data, questions, and the development and exploration of various parts of this project. Thanks to the CSASdown team for the development of the tools used to craft this manuscript. Thanks to Tricia Pearo Drew, Jamie Raper, and Brittany Wilson for general support. Finally, thanks to Dan Ricard and Joanna Mills Flemming for their helpful reviews. This project was made possible by funding from DFOs Strategic Program for Ecosystem-based Research and Advice (SPERA).

7. REFERENCES CITED

Allyn, A.J., Alexander, M.A., Franklin, B.S., Massiot-Granier, F., Pershing, A.J., Scott, J.D., and Mills, K.E. 2020. Comparing and synthesizing quantitative distribution models and qualitative vulnerability assessments to project marine species distributions under climate change. PLOS ONE 15(4): e0231595.

Anderson, E.D. 1998. The history of fisheries management and scientific advice – the ICNAF/NAFO history from the end of World War II to the present. J. Northw. Atl. Fish. Sci 23: 75–94.

Anderson, S.C., and Ward, E.J. 2019. Black swans in space: Modeling spatiotemporal processes with extremes. Ecology 100(1): e02403.

Andrushchenko, I., Legault, C., Martin, R., Brooks, E., and Wang, Y. 2018. Transboundary Resources Assessment Committee: Assessment of Eastern Georges Bank Atlantic Cod for 2018. TRAC Ref. Doc. 2018/01.

Backus, R.H., and Bourne, D.W. 1987. Georges Bank. MIT, Cambridge, Mass.

Bakka, H., Rue, H., Fuglstad, G.-A., Riebler, A., Bolin, D., Krainski, E., Simpson, D., and Lindgren, F. 2018. Spatial modelling with R-INLA: A review. Wiley Interdisciplinary Reviews: Computational Statistics 10(6): e1443.

Booth, T.H., Nix, H.A., Busby, J.R., and Hutchinson, M.F. 2014. Bioclim: The first species distribution modelling package, its early applications and relevance to most current MaxEnt studies. Diversity and Distributions 20(1): 1–9.

Boudreau, S.A., Shackell, N.L., Carson, S., and den Heyer, C.E. 2017. Connectivity, persistence, and loss of high abundance areas of a recovering marine fish population in the Northwest Atlantic Ocean. Ecology and Evolution 7(22): 9739–9749.

Box, E.O. 1981. Predicting Physiognomic Vegetation Types with Climate Variables. Vegetatio 45(2): 127–139. Springer.

Bundy, A., Heymans, J.J., Morissette, L., and Savenkoff, C. 2009. Seals, cod and forage fish: A comparative exploration of variations in the theme of stock collapse and ecosystem change in four Northwest Atlantic ecosystems. Progress in Oceanography 81(1): 188–206.

Cadrin, S.X. 2020. Defining spatial structure for fishery stock assessment. Fisheries Research 221: 105397.

Cheung, W.W.L., Close, C., Lam, V., Watson, R., and Pauly, D. 2008. Application of macroecological theory to predict effects of climate change on global fisheries potential. Marine Ecology Progress Series 365: 187–197.

Cosandey-Godin, A., Krainski, E.T., Worm, B., and Flemming, J.M. 2015. Applying Bayesian spatiotemporal models to fisheries bycatch in the Canadian Arctic. Can. J. Fish. Aquat. Sci. 72(2): 186–197.

DFO. 2008. Review of scallop gear modification report. DFO Can. Sci. Advis. Sec. Sci. Resp. 2008/14.

DFO. 2014. Scallop fishery area/time closure to reduce Yellowtail Flounder by-catch on Georges Bank in 2014. DFO Can. Sci. Advis. Sec. Sci. Resp. 2014/034.

DFO. 2019b. Scallop fishery area/time closure to protect Atlantic Cod (*Gadus morhua*) spawning aggregations in NAFO Division 5Z (Georges Bank). DFO Can. Sci. Advis. Sec. Sci. Resp.

DFO. 2019a. Stock status update of Georges Bank 'a' scallops (*Placopecten magellanicus*) in Scallop Fishing Area 27. DFO Can. Sci. Advis. Sec. Sci. Resp. 2019/036.

Domisch, S., Friedrichs, M., Hein, T., Borgwardt, F., Wetzig, A., Jähnig, S.C., and Langhans, S.D. 2019. Spatially explicit species distribution models: A missed opportunity in conservation planning? Diversity and Distributions 25(5): 758–769.

Elith, J., and Leathwick, J.R. 2009. Species Distribution Models: Ecological Explanation and Prediction Across Space and Time. Annu. Rev. Ecol. Evol. Syst. 40(1): 677–697.

Finley, M., Brooks, E.N., McCurdy, Q., Barrett, M.A., and Wang, Y. 2019. Transboundary Resources Assessment Committee: Assessment of Haddock on Eastern Georges Bank for 2019. TRAC.

Fuglstad, G.-A., Simpson, D., Lindgren, F., and Rue, H. 2019. Constructing Priors that Penalize the Complexity of Gaussian Random Fields. Journal of the American Statistical Association 114(525): 445–452.

Greenan, B.J.W., Shackell, N.L., Ferguson, K., Greyson, P., Cogswell, A., Brickman, D., Wang, Z., Cook, A., Brennan, C.E., and Saba, V.S. 2019. Climate Change Vulnerability of American Lobster Fishing Communities in Atlantic Canada. Front. Mar. Sci. 6: 579.

Greenlaw, M.E., Sameoto, J.A., Lawton, P., Wolff, N.H., Incze, L.S., Pitcher, C.R., Smith, S.J., and Drozdowski, A. 2010. A geodatabase of historical and contemporary oceanographic datasets for investigating the role of the physical environment in shaping patterns of seabed biodiversity in the Gulf of Maine. Can. Tech. Rep. Fish. Aquat. Sci. 2895: iv + 35 p.

Grinnell, J. 1904. The Origin and Distribution of the Chestnut-Backed Chickadee. Auk 21(3): 364–382. Oxford Academic.

Halliday, R.G., and Pinhorn, A.T. 1996. North Atlantic Fishery Management Systems: A Comparison of Management Methods and Resource Trends. Journal of Northwest Atlantic Fishery Science 20: 1–135.

Hart, D.R., Jacobson, L.D., and Tang, J. 2013. To split or not to split: Assessment of Georges Bank sea scallops in the presence of marine protected areas. Fisheries Research 144: 74–83.

Hilborn, R., and Walters, C.J. 1992. Quantitative fisheries stock assessment: Choice, dynamics and uncertainty. Chapman and Hall, New York.

Hutchings, J.A. 1996. Spatial and temporal variation in the density of northern cod and a review of hypotheses for the stock's collapse. Can. J. Fish. Aquat. Sci. 53(5): 943–962. NRC Research Press.

Johnson, D.L., Morse, W.W., Berrien, P.L., and Vitaliano, J.J. 1999. Essential Fish Habitat Source Document: Yellowtail Flounder, Limanda ferruginea, Life History and Habitat Characteristics. NOAA Technical Memorandum NMFS-NE-140.

Kavanaugh, M.T., Rheuban, J.E., Luis, K.M.A., and Doney, S.C. 2017. Thirty-Three Years of Ocean Benthic Warming Along the U.S. Northeast Continental Shelf and Slope: Patterns, Drivers, and Ecological Consequences. Journal of Geophysical Research: Oceans 122(12): 9399–9414.

Keith, D.M., Sameoto, J.A., Keyser, F.M., and Ward-Paige, C.A. 2020. Evaluating socio-economic and conservation impacts of management: A case study of time-area closures on Georges Bank. PLOS ONE 15(10): e0240322.

Kristensen, K., Nielsen, A., Berg, C.W., Skaug, H., and Bell, B.M. 2016. TMB: Automatic Differentiation and Laplace Approximation. Journal of Statistical Software 70(1): 1–21.

Leach, K., Montgomery, W.I., and Reid, N. 2016. Modelling the influence of biotic factors on species distribution patterns. Ecological Modelling 337: 96–106.

Legault, C.M., and McCurdy, Q.M. 2018. Stock assessment of Georges Bank Yellowtail Flounder for 2018. TRAC. Ref. Doc.

Lindgren, F., and Rue, H. 2015. Bayesian Spatial Modelling with R-INLA. Journal of Statistical Software 63(1, 1): 1–25.

Link, J., Almeida, F.P., Valentine, P., Auster, P., Reid, R.N., and Vitaliano, J. 2005. The Effects of Area Closures on Georges Bank. *In* Benthic Habitats and the Effects of Fishing (American Fisheries Society, Symposium 41,Bethesda, Maryland, 12–14 November, 2002). (Eds P.W.Barnes and J.P. Thomas). pp. 345–368.

Martínez-Minaya, J., Cameletti, M., Conesa, D., and Pennino, M.G. 2018. Species distribution modeling: A statistical review with focus in spatio-temporal issues. Stoch Environ Res Risk Assess 32(11): 3227–3244.

McHenry, J., Welch, H., Lester, S.E., and Saba, V. 2019. Projecting marine species range shifts from only temperature can mask climate vulnerability. Global Change Biology 25(12): 4208–4221.

McMullen, K.Y., Paskevich, V.F., and Poppe, L.J. 2014. 2014, GIS data catalog, in Poppe, L.J., McMullen, K.Y., Williams, S.J., And Paskevich, V.F., Eds., 2014, USGS east-coast sediment analysis: Procedures, database, and GIS data (ver. 3.0, November 2014).

Merow, C., LaFleur, N., Silander Jr., J.A., Wilson, A.M., and Rubega, M. 2011. Developing Dynamic Mechanistic Species Distribution Models: Predicting Bird-Mediated Spread of Invasive Plants across Northeastern North America. The American Naturalist 178(1): 30–43. The University of Chicago Press.

Murawski, S.A., Brown, R., Lai, H.-L., Rago, P.J., and Hendrickson, L. 2000. Large-scale closed areas as a fishery-management tool in temperate marine systems: The Georges Bank experience. Bull. US FIsh Comm 66: 775–798.

Myers, R.A., and Cadigan, N.G. 1995. Was an increase in natural mortality responsible for the collapse off northern cod? Can. J. Fish. Aquat. Sci. 52(6): 1274–1285.

NFSC. 2012. 54th Northeast Regional Stock Assessment Workshop (54th SAW), assessment summary report.

NOAA. 2020. NOAA Yellowtail Flounder Overview. Accessed Septemer 1, 2020. NOAA Yellowtail Flounder Overview.

O'Brien, L., Burnett, J., and Mayo, R. 1993. Maturation of Nineteen Species of Finfish off the northeast coast of the United States, 1985-1990. NOAA Technical Report NMFS 113.

O'Keefe, C.E., and DeCelles, G.R. 2013. Forming a Partnership to Avoid Bycatch. Fisheries 38(10): 434–444.

Pershing, A.J., Alexander, M.A., Hernandez, C.M., Kerr, L.A., Bris, A.L., Mills, K.E., Nye, J.A., Record, N.R., Scannell, H.A., Scott, J.D., Sherwood, G.D., and Thomas, A.C. 2015. Slow adaptation in the face of rapid warming leads to collapse of the Gulf of Maine cod fishery. Science 350(6262): 809–812.

Punt, A.E. 2019. Spatial stock assessment methods: A viewpoint on current issues and assumptions. Fisheries Research 213: 132–143.

R Core Team. 2020. R: A language and environment for statistical computing. R Foundation for Statistical Computing, Vienna, Austria.

Reuchlin-Hugenholtz, E., Shackell, N.L., and Hutchings, J.A. 2015. The Potential for Spatial Distribution Indices to Signal Thresholds in Marine Fish Biomass. PLOS ONE 10(3): e0120500.

Robinson, L.M., Elith, J., Hobday, A.J., Pearson, R.G., Kendall, B.E., Possingham, H.P., and Richardson, A.J. 2011. Pushing the limits in marine species distribution modelling: Lessons from the land present challenges and opportunities. Global Ecology and Biogeography 20(6): 789–802.

Rue, H., Riebler, A., Sørbye, S.H., Illian, J.B., Simpson, D.P., and Lindgren, F.K. 2017. Bayesian Computing with INLA: A Review. Annual Review of Statistics and Its Application 4: 395–421.

Stokesbury, K.D.E. 2002. Estimation of Sea Scallop Abundance in Closed Areas of Georges Bank, USA. Transactions of the American Fisheries Society 131(6): 1081–1092.

Sundblad, G., Bergström, U., and Sandström, A. 2011. Ecological coherence of marine protected area networks: A spatial assessment using species distribution models. Journal of Applied Ecology 48(1): 112–120.

Thorson, J.T. 2019. Guidance for decisions using the Vector Autoregressive Spatio-Temporal (VAST) package in stock, ecosystem, habitat and climate assessments. Fisheries Research 210: 143–161.

Thorson, J.T., Ianelli, J.N., Larsen, E.A., Ries, L., Scheuerell, M.D., Szuwalski, C., and Zipkin, E.F. 2016. Joint dynamic species distribution models: A tool for community ordination and spatio-temporal monitoring. Global Ecology and Biogeography 25(9): 1144–1158.

Thorson, J.T., Shelton, A.O., Ward, E.J., and Skaug, H.J. 2015. Geostatistical delta-generalized linear mixed models improve precision for estimated abundance indices for West Coast groundfishes. ICES J Mar Sci 72(5): 1297–1310.

TMGC. 2002. Development of a sharing allocation proposal for transboundary resources of Atlantic Cod, Haddock and Yellowtail Flounder on Georges Bank. Fisheries and Oceans Canada. Fisheries Management Regional Report 2002/01: 1–59.

Townsend, D.W., and Pettigrew, N.R. 1997. Nitrogen limitation of secondary production on Georges Bank. J Plankton Res 19(2): 221–235.

TRAC. 2020. Transboundary Resource Assessment Committee. Accessed Sept 1, 2020.

Valentine, P., and Lough, R.G. 1991. The Sea Floor Environment and the Fishery of Eastern Georges Bank - The Influence of Geological and Oceanographic Environmental Factors on the Abundance and Distribution of Fisheries Resources of the Northeast United States Continental Shelf. Open- File Rep: 91–439.

Walsh, S.J. 2008. A Review of Current Studies on Scallop Rake Modifications to Reduce Groundfish Bycatch in the Canadian Offshore Scallop Fishery on Georges Bank. DFO Can. Sci. Advis. Sec. Res. Doc. 2008/050. x + 77 p.

Zuur, A.F., Ieno, E.N., and Elphick, C.S. 2010. A protocol for data exploration to avoid common statistical problems: Data exploration. Methods in Ecology and Evolution 1(1): 3–14.

Zuur, A.F., and Leno, E.N. 2018. Beginner's guide to spatial, temporal, and spatial-temporal ecological data analysis with R-INLA. Highland Statistics Ltd, Newburgh, United Kingdom.

Zuur, A.F., Leno, E.N., and Saveliev, A.A. 2017. Beginner's guide to spatial, temporal, and spatial-temporal ecological data analysis with R-INLA. Highland Statistics Ltd, Newburgh, United Kingdom.

8. TABLES

*Table 1. Environmental variables used in the analysis. Variables in **bold** were retained after Variance Inflation Factor (VIF) analyses and were included in the linear models. Variables in **italics** were used for the Principal Component Analysis (PCA).*

Data	Variable	Source	Resolution(m)	Units
USGS Yearly median Bottom Shear Stress	Year.median	$USGS(SFS-SMD)^3$	3,500	Pa
Stratification (1996-2007)	***Strat***	$CoML^1$	***2,500***	***none***
Seasonal Range of SST (1997-2008)	**SST.rg**	$CoML^1$	**972**	$°C$
Average SST (1997-2009)	***SST***	$CoML^1$	***972***	$°C$
Benthic Silicate	***Sil***	$CoML^1$	***6,000***	M
Sediment Grain size (CONMAP)	**Sed**	$USGS(CONMAP)^2$	**-**	**none**
Sand	**Sand**	$CoML^1$	**6,000**	$\%$
Seasonal Range of Benthic Salinity (1996-2007)	***Sal.rg***	$CoML^1$	***6,000***	psu
Benthic Salinity (1996-2007)	***Sal.avg***	$CoML^1$	***6,000***	psu
Benthic Phosphate (1996-2007)	***Phos.avg***	$CoML^1$	***6,000***	μM
Benthic Nitrate (1996-2007)	*Nit.avg*	$CoML^1$	*40,000*	M
Mud	***Mud***	$CoML^1$	***6,000***	$\%$
Average K490	K490.avg	$CoML^1$	8,000	none
USGS Median of Bottom Shear Stress	***Gmaine***	$USGS(SFS-SMD)^3$	***3,500***	Pa
Benthic Complexity	**Complexity**	$CoML^1$	**397**	°
Slope	**Slope**	$CoML^1$	**397**	°
Depth	***Dep***	$CoML^1$	***397***	m
Aspect	**Aspect**	$CoML^1$	**397**	°
Seasonal Range of Sea Surface Chlorophyll	Chl.rg	$CoML^1$	1,119	$mg \times m^{-3}$
Average Sea Surface Chlorophyll	***Chl***	$CoML^1$	***855***	$mg \times m^{-3}$
Benthic Current Stress with Wind and Tidal Influences	Botstr.wt	$CoML^1$	952	$N \times m^{-2}$
Benthic Current Stress with only tidal influence	Botstr.t	$CoML^1$	3,800	$N \times m^{-2}$

[1] CoML obtained from here.
[2] USGS(CONMAP) obtained from here.
[3] USGS(SFS-SMD) obtained from here.

9. FIGURES

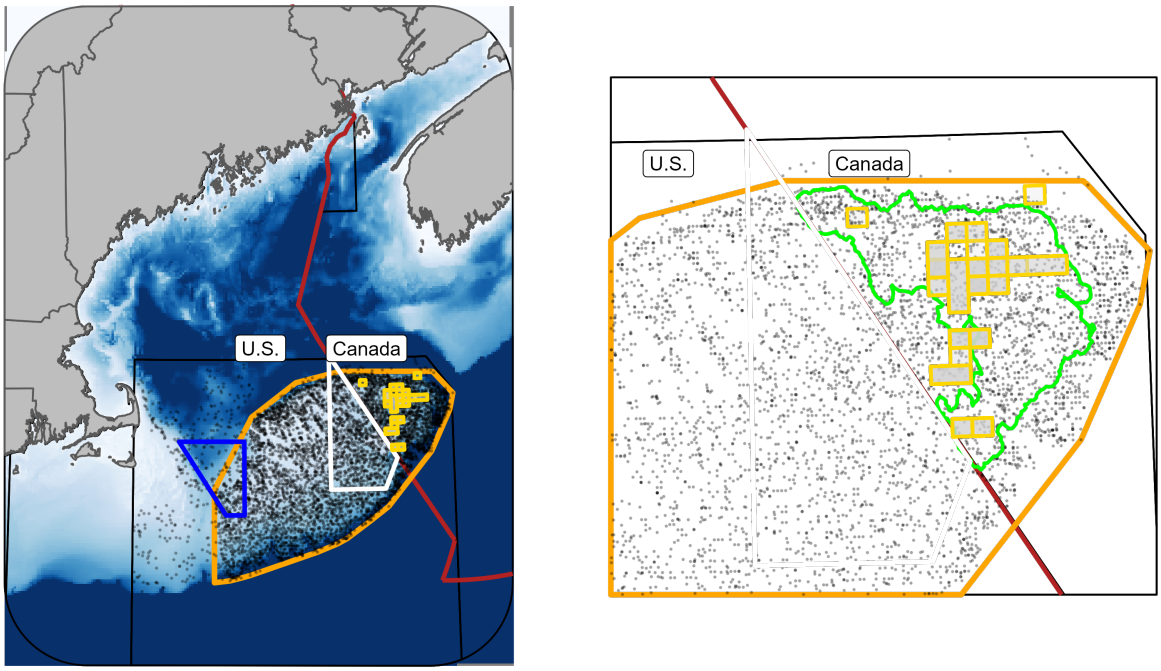

Figure 1. Georges Bank (GB) study area. Points represent the sample locations for the Winter (1987-2019, n = 2,590), Spring (1972-2019, n = 2,393), and Fall (1972-2019, n = 2,506). The orange outline represents the region of GB included in these analyses (42,000 km^2). In the U.S. the blue polygon is Closed Area I (CA I) and the white polygon is Closed Area II (CA II). In Canada the small gold bordered cells (each cell covers an area of approximately 42.7 km^2) represent areas which have been included in either the Atlantic Cod or Yellowtail Flounder closures at least once. Some of the cells have been part of both closures and not all cells are closed each year; darker fill indicates cells which have been closed more frequently. The red line indicates the Canadian Exclusive Economic Zone (EEZ).

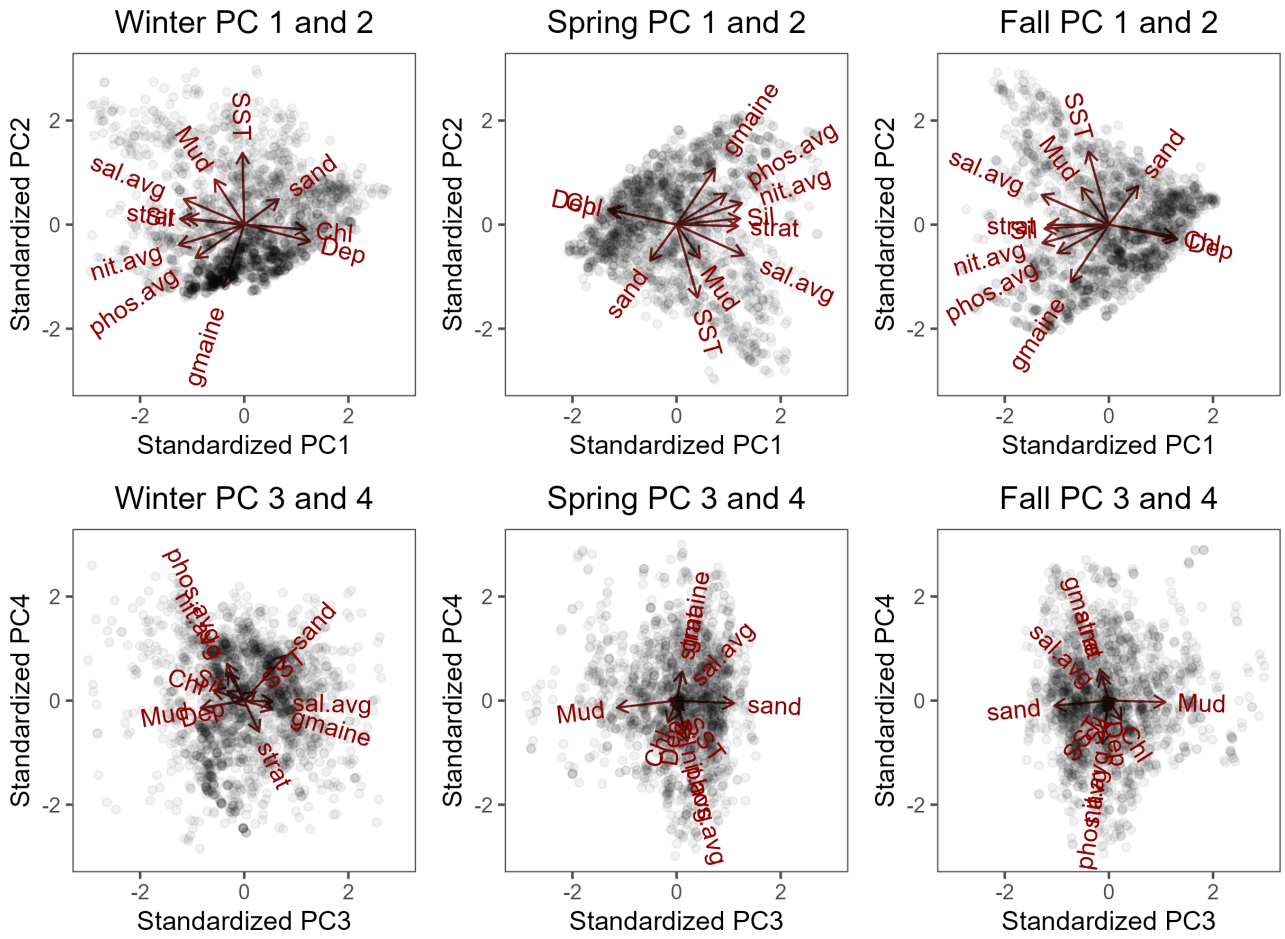

Figure 2. Principal Component Analysis (PCA) results for the Winter, Spring, and Fall seasons using the retained environmental data and the 4 retained Principal Components (PCs). The results for PC 1 and 2 for each season are on the top and the PC 3 and 4 results are on the bottom. Left column are the results for Winter, middle column for Spring, and right column is for the Fall. Points represent the score for each survey observation. The loadings for each covariate in the analysis are shown by the length of their respective lines. PC scores greater than ± 3 units not shown.

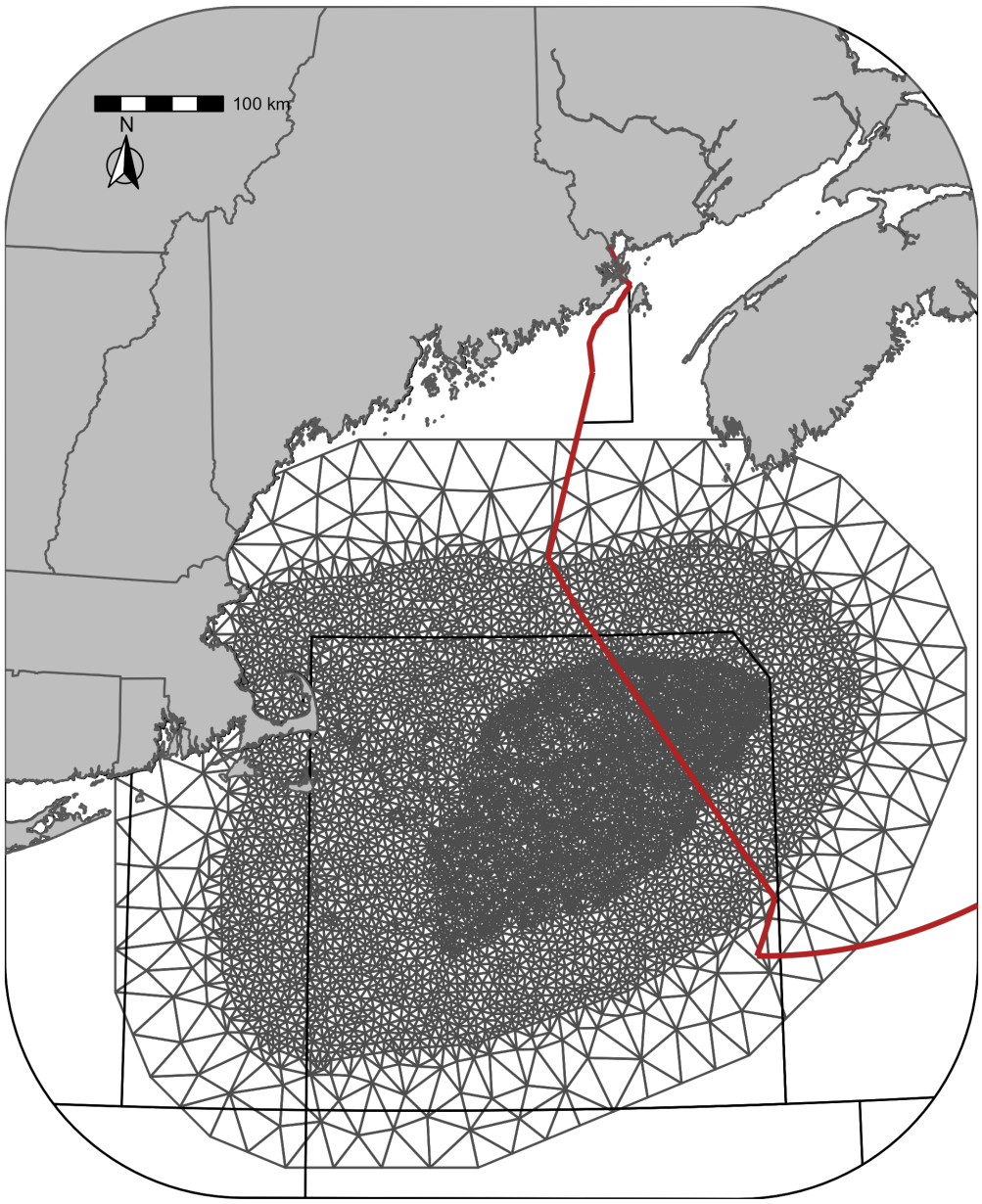

Figure 3. Delaunay triangular mesh used for the spatial fields mesh. The mesh contains 6,610 vertices.

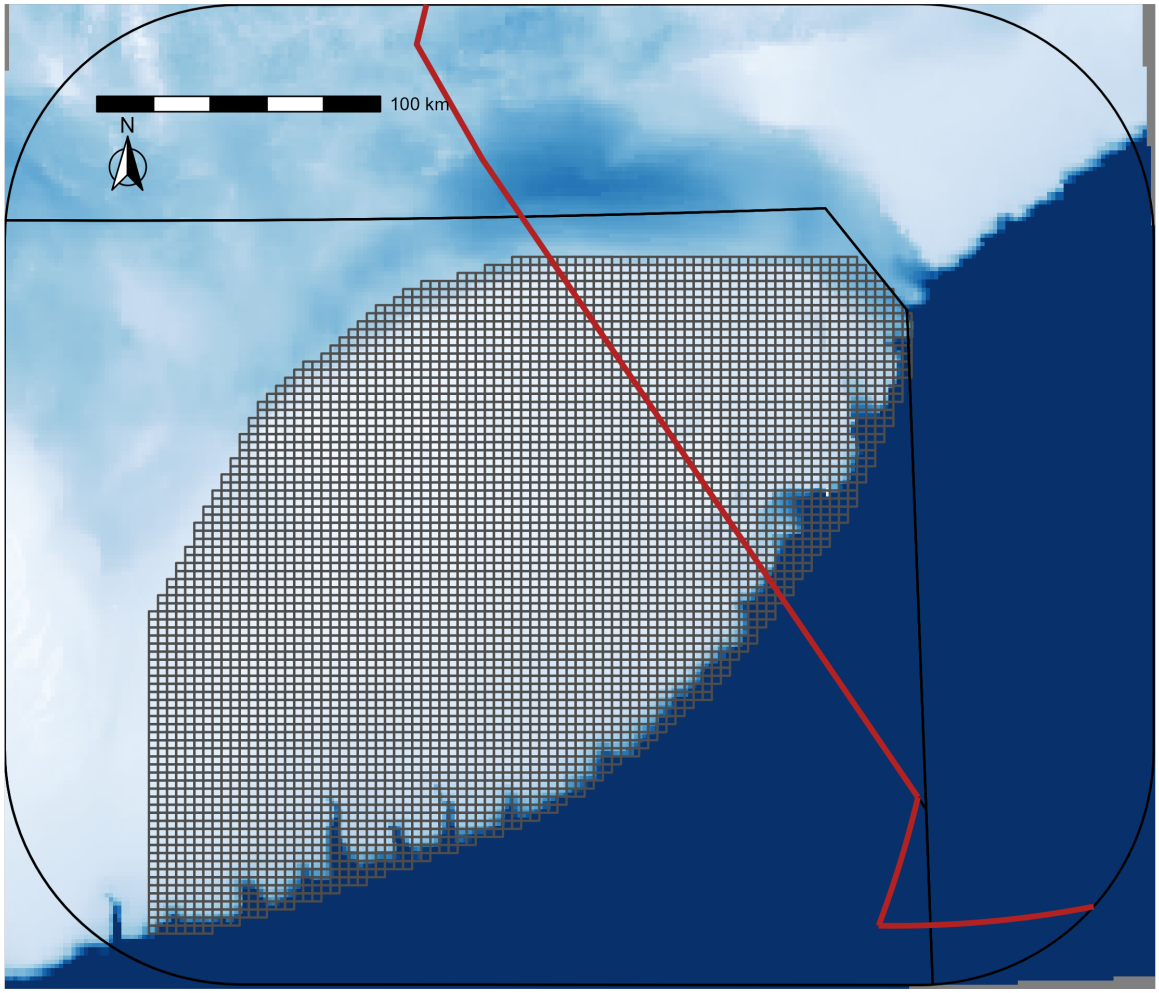

Figure 4. Prediction grid used for prediction of Occurrence Probability (OP).

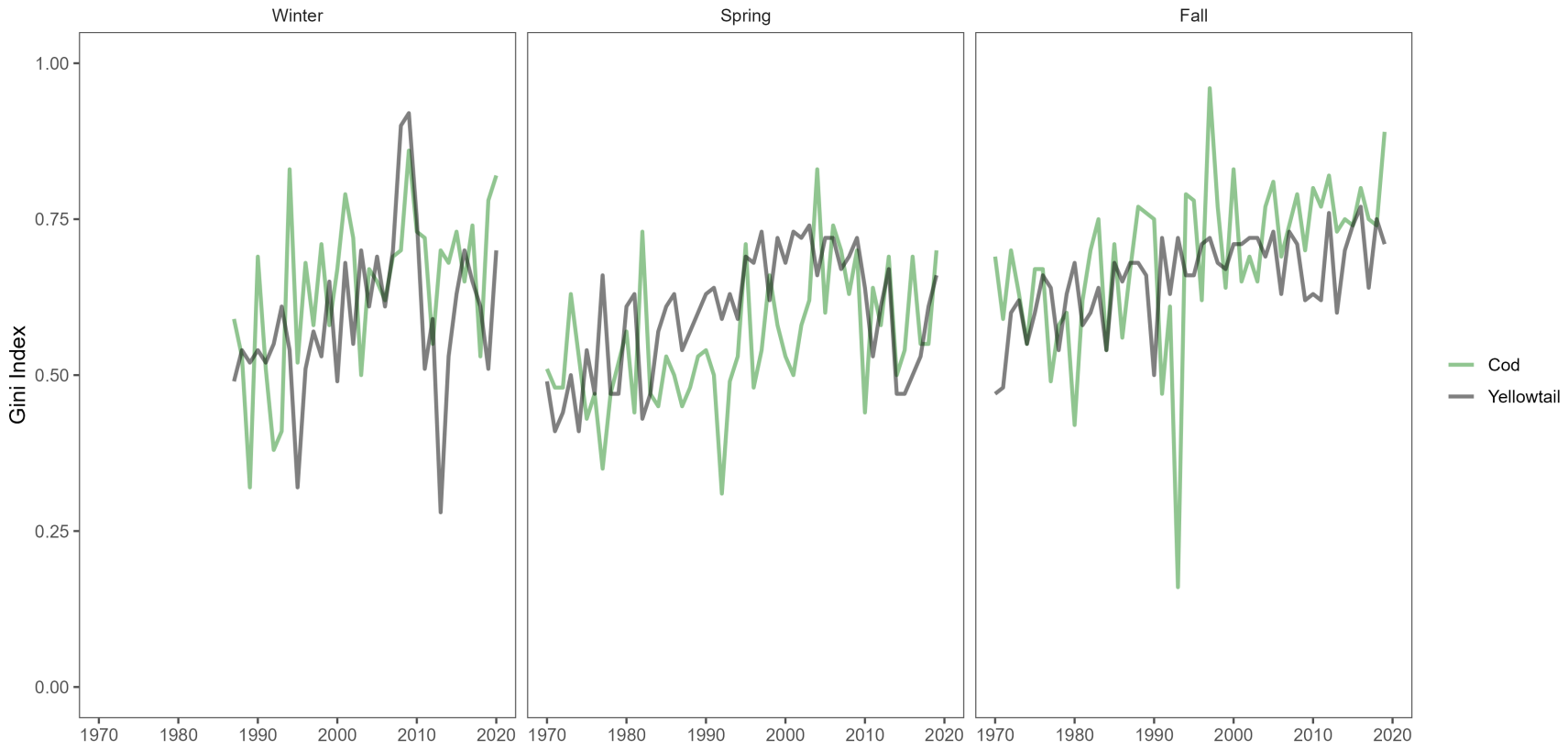

Figure 5. Gini Index time series in the Winter, Spring, and Fall. The green line represents Atlantic Cod and the black line represents Yellowtail Flounder.

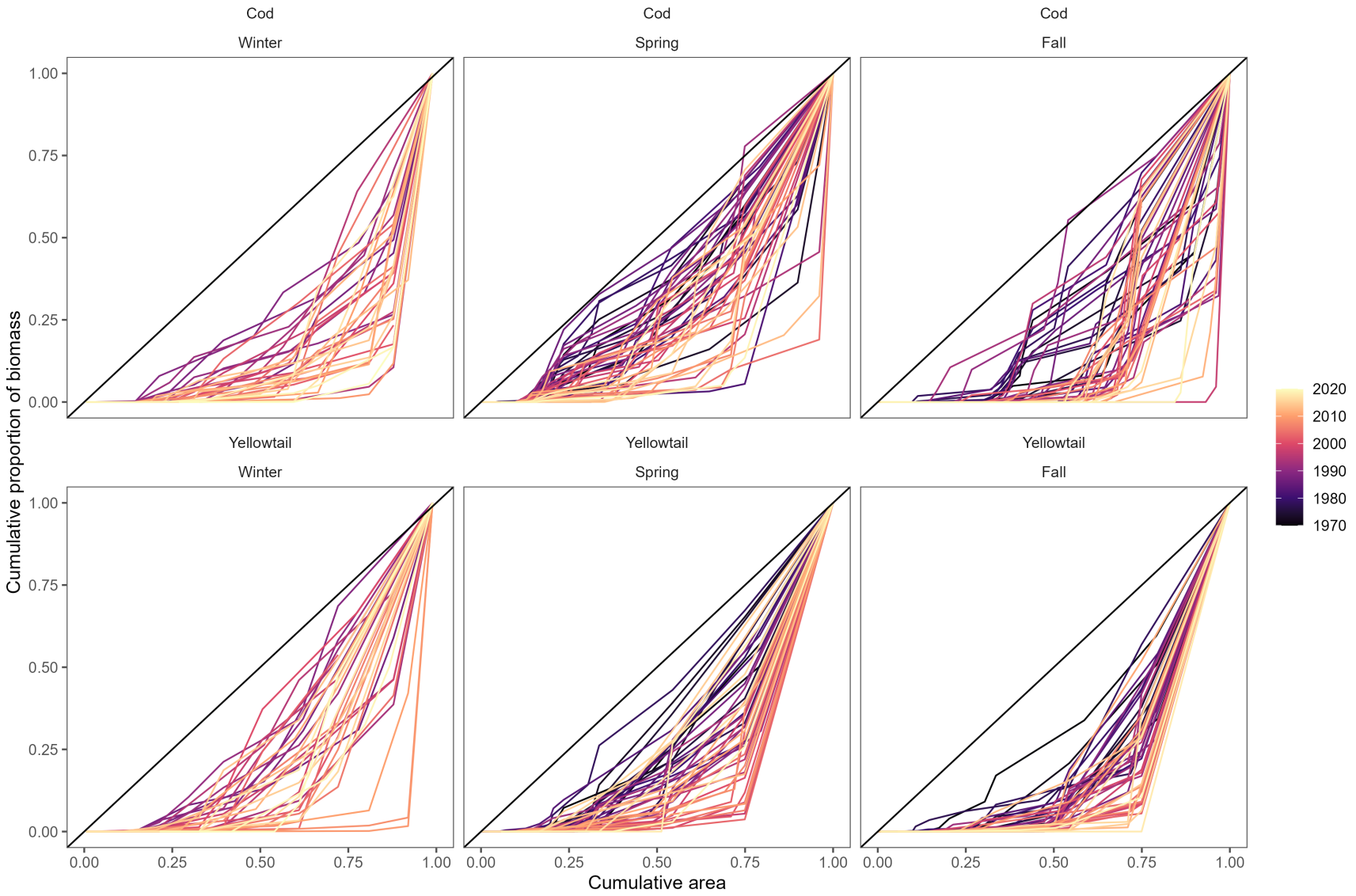

Figure 6. The relationship between the cumulative proportion of biomass and cumulative proportion of the total survey area. Atlantic Cod relationship shown on the top row and Yellowtail Flounder on the bottom row. The left column contains the results for the Winter, the center contains the Spring results, and Fall results are shown in the column on the right.

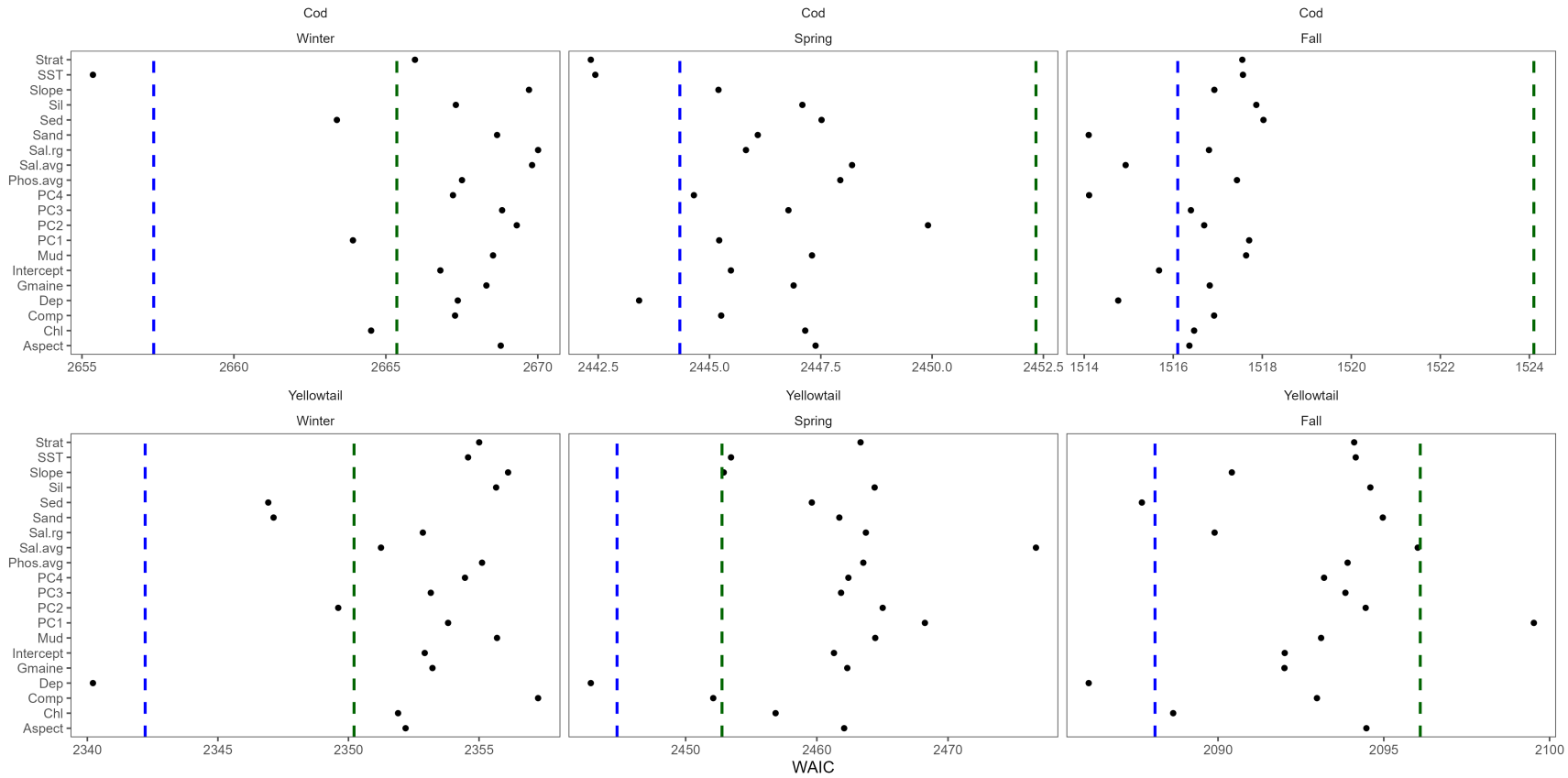

Figure 7. Stage 1 of forward model selection using each of the environmental covariates individually. This model selection was done using a static random field. Blue dashed line represents 2 WAIC units larger than the lowest WAIC model, the green dashed line is 10 WAIC units larger than the lowest model WAIC. The covariate descriptions can be found in Table 1.

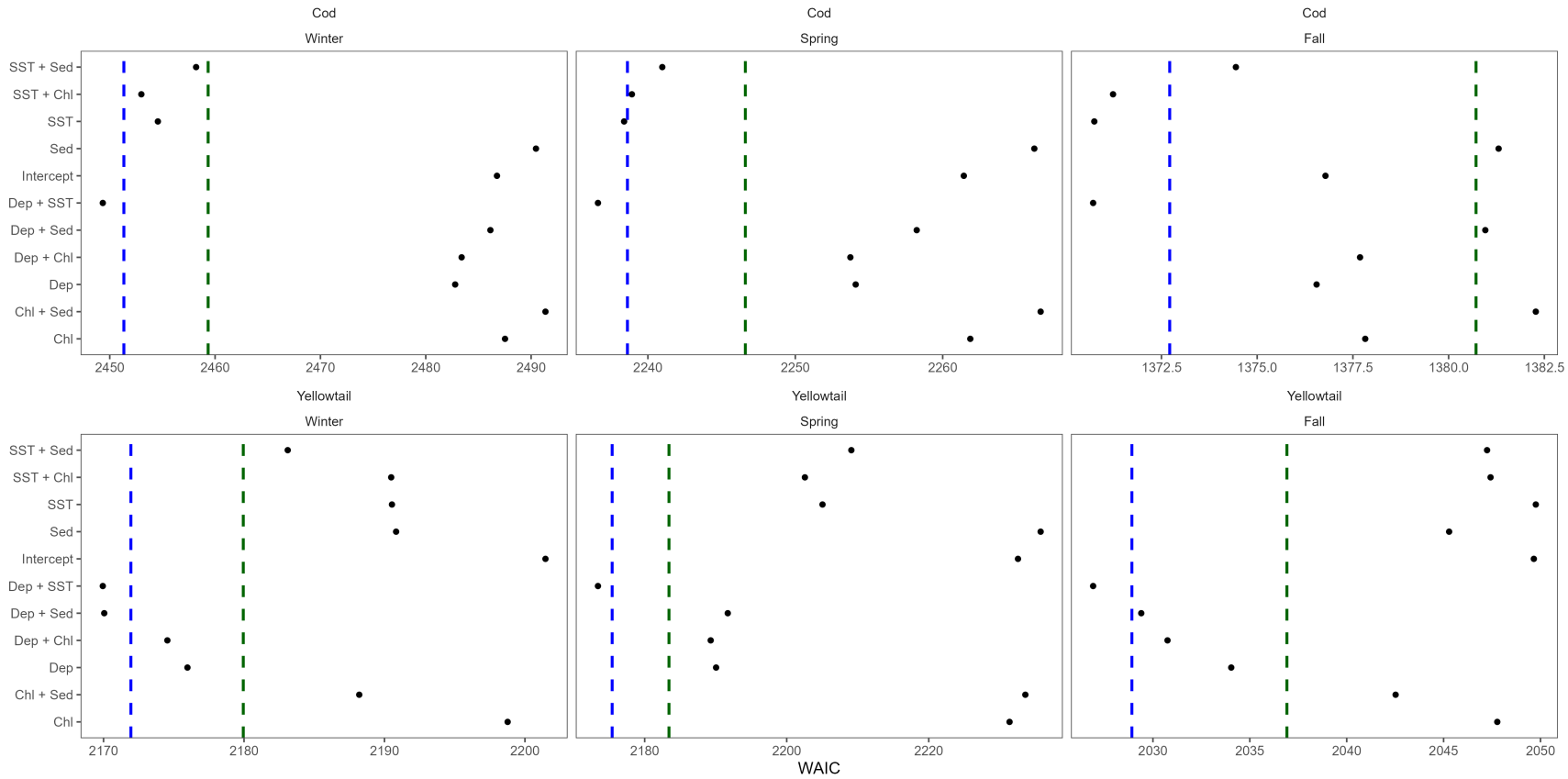

Figure 8. Stage 2 of model selection including additive models with 2 covariates based on the covariates identified in the initial model selection stage. These models were compared using the 10-year random field models. Blue dashed line represents 2 WAIC units larger than the lowest WAIC model, the green dashed line is 10 WAIC units larger than the lowest model WAIC.

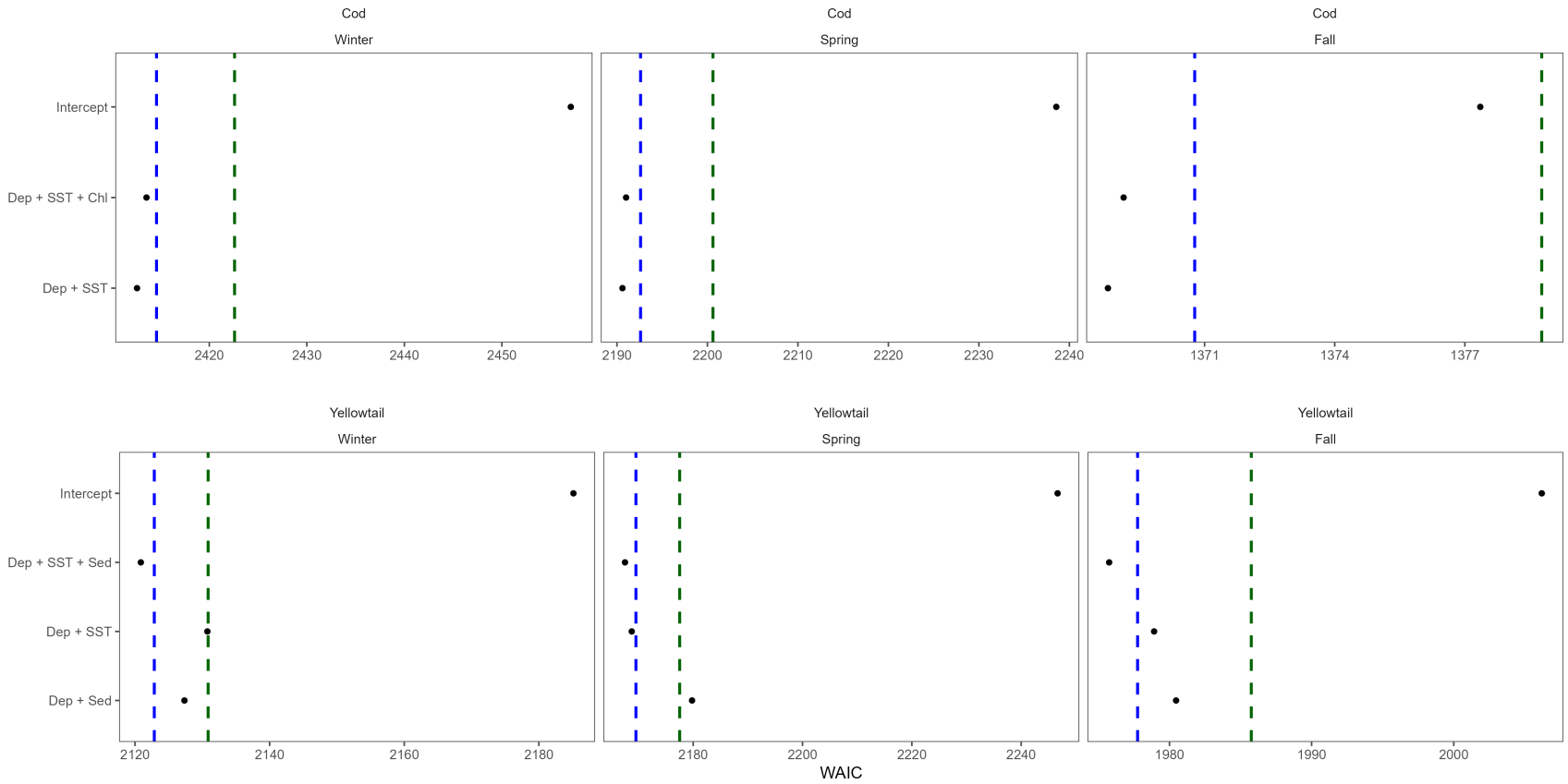

Figure 9. Stage 3 of covariate model selection which includes models with up to 3 covariate terms based on models selected at stage 2. Blue dashed line represents 2 WAIC units larger than the lowest WAIC model, the green dashed line is 10 WAIC units larger than the lowest model WAIC.

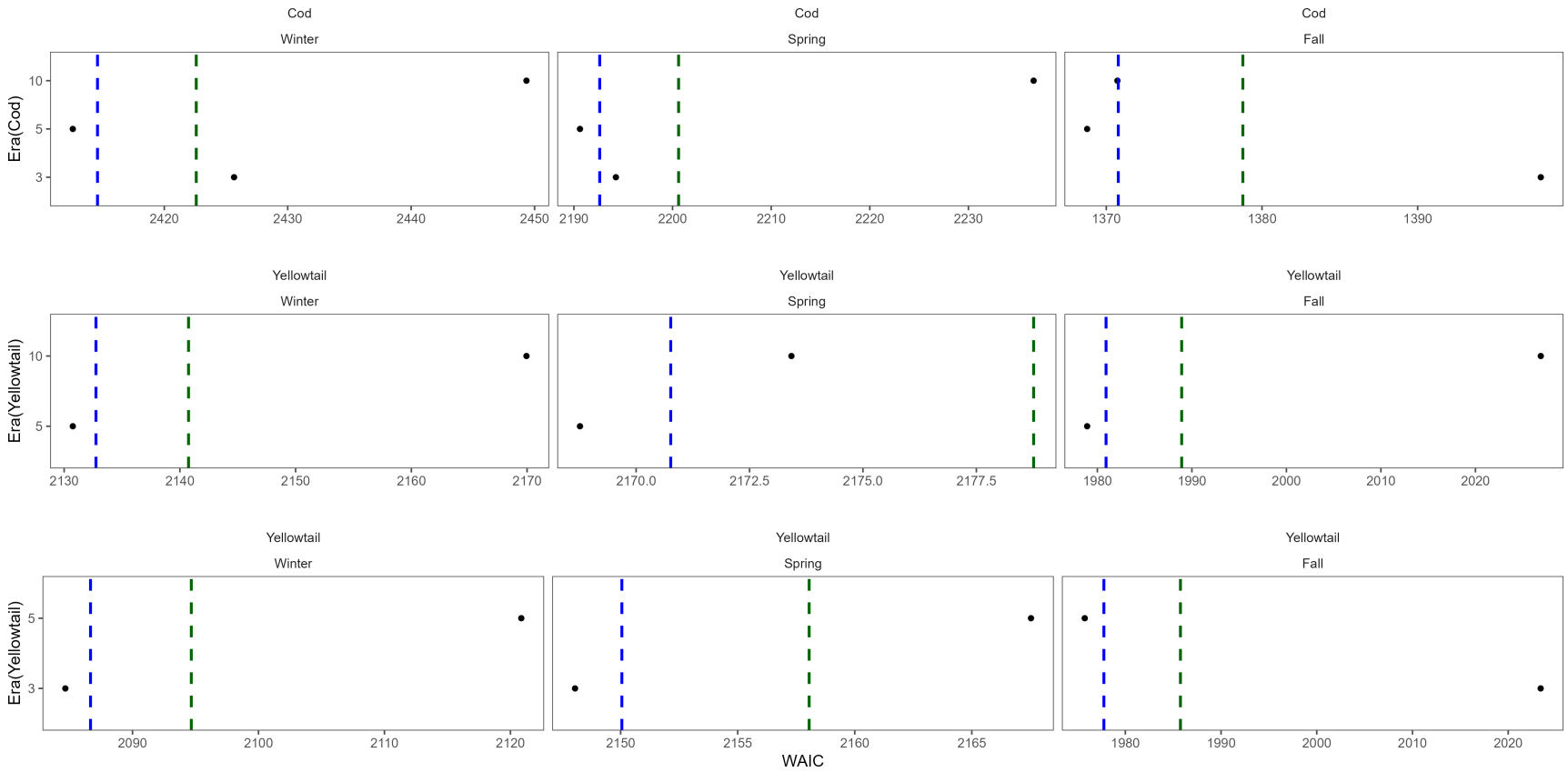

Figure 10. Model selection comparing the random fields models. For Atlantic Cod the model used is Depth (Dep) + Sea Surface Temperature (SST) for all of the random fields. For Yellowtail Flounder the 5 and 10 year random fields were compared using the Depth (Dep) + Sea Surface Temperature (SST) model, while the 5 and 3 year random fields were compared using the Depth (Dep) + Sea Surface Temperature (SST) + Sediment type (Sed) model. Blue dashed line represents 2 WAIC units larger than the lowest WAIC model, the green dashed line is 10 WAIC units larger than the lowest model WAIC. For Yellowtail Flounder, the 10 year random field model was not run using 3 covariates, while 3-year random field model was not run using 2 covariates in all 3 seasons; therefore there are no results shown for these model combinations.

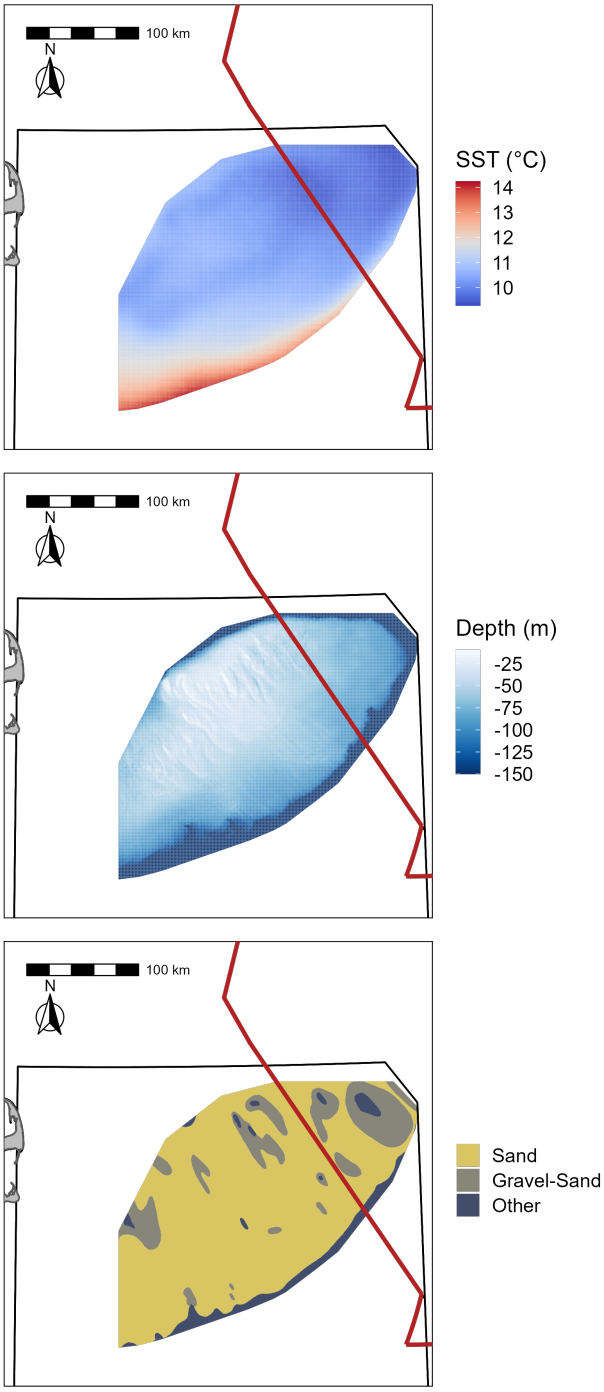

Figure 11. Average Sea Surface Temperature on Georges Bank (GB) from 1997-2008 (SST in °C) in the top panel, GB bathymetry (depth in meters) in the center panel, and GB sediment type in the bottom panel.

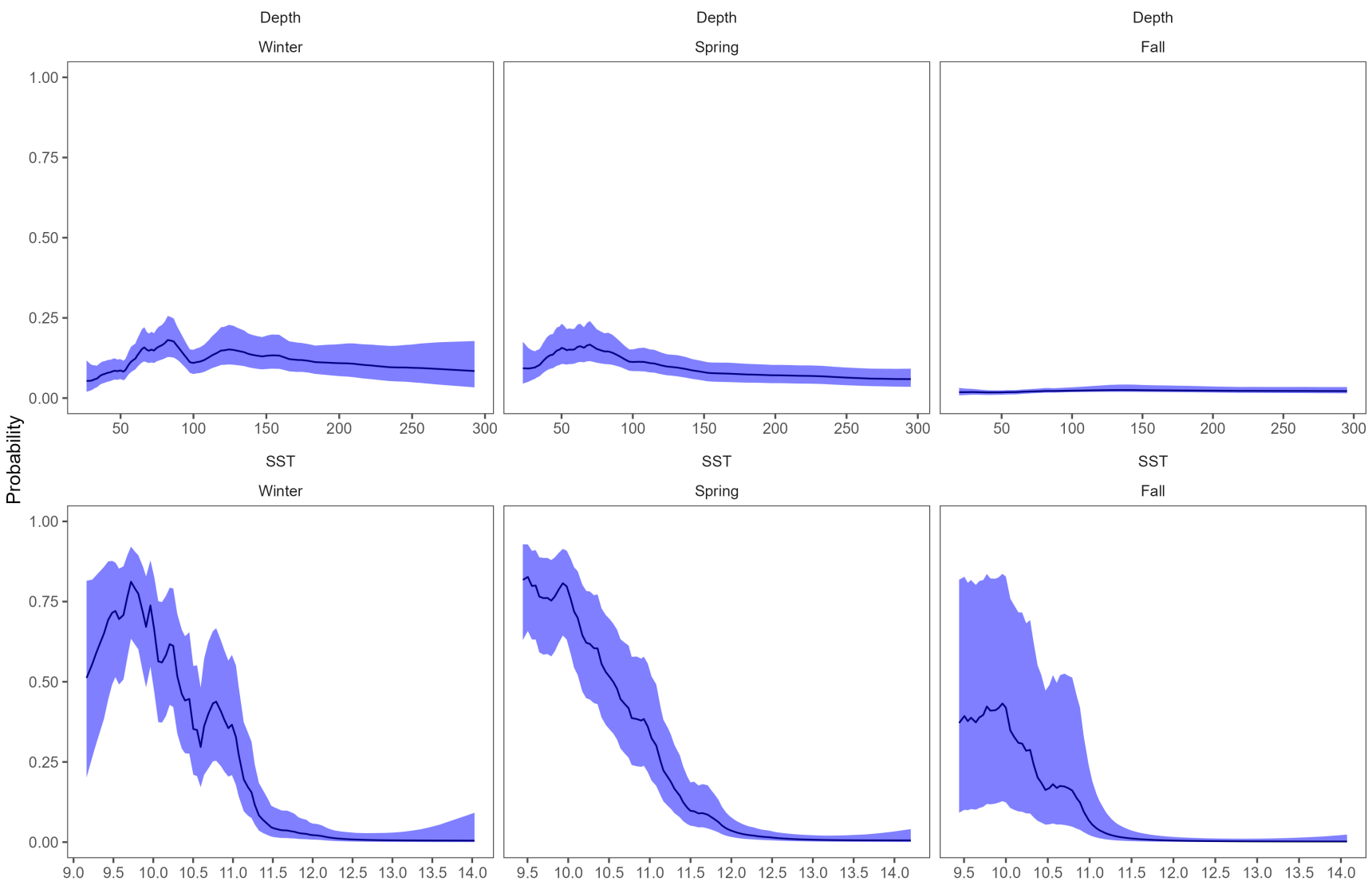

Figure 12. Environmental covariate effect of Depth (Dep, top row) and Sea Surface Temperature (SST,bottom row) for Atlantic Cod in each season. Results transformed to the probability scale and the blue shaded region represents the 95% CIs.

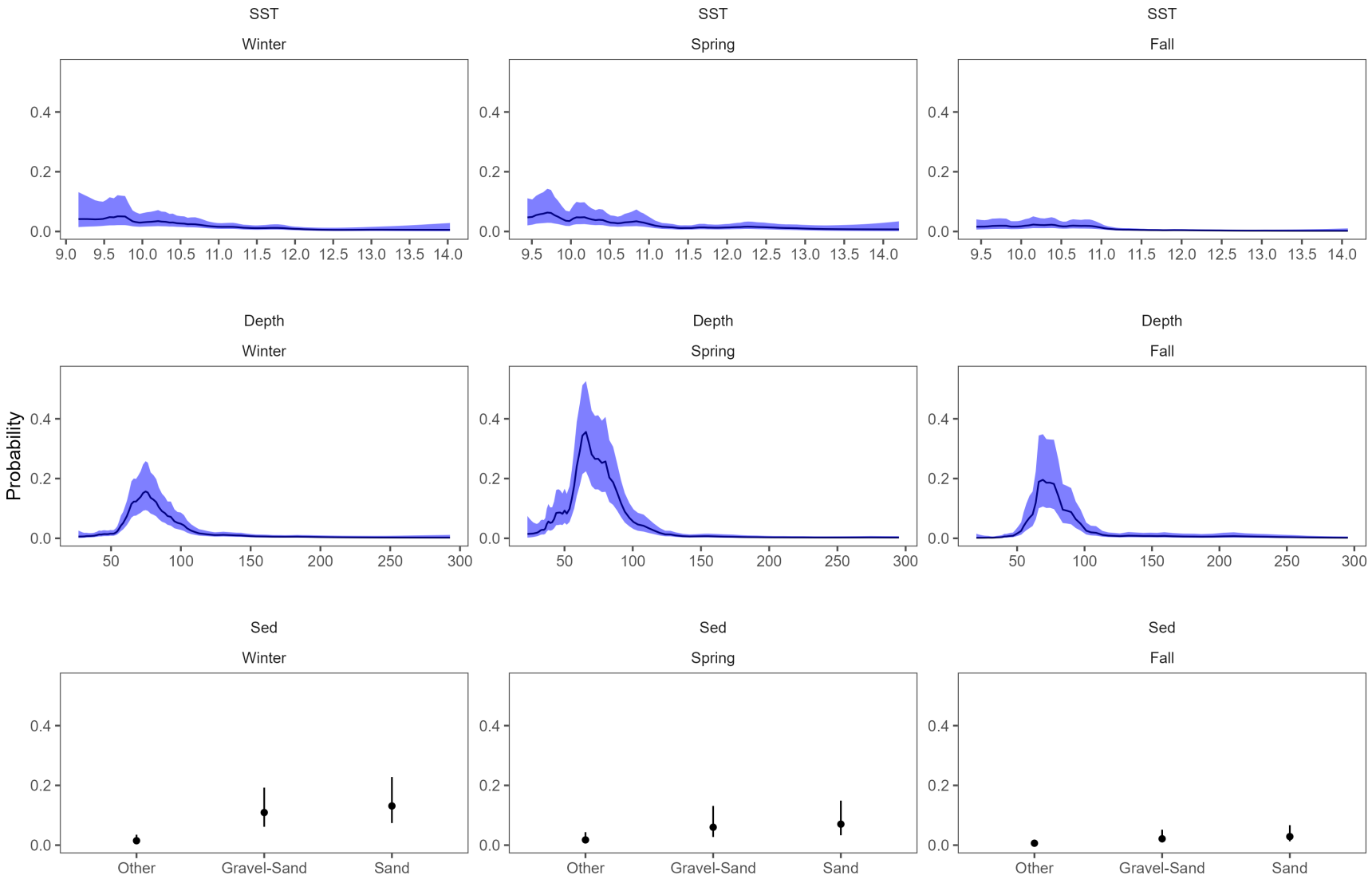

Figure 13. Environmental covariate effect of Depth (Dep, top row) and Sea Surface Temperature (SST,middle row), and Sediment type (Sed, bottom row) for Yellowtail Flounder in each season. Results transformed to the probability scale, and the blue shaded region and the error bars represent the 95% CIs.

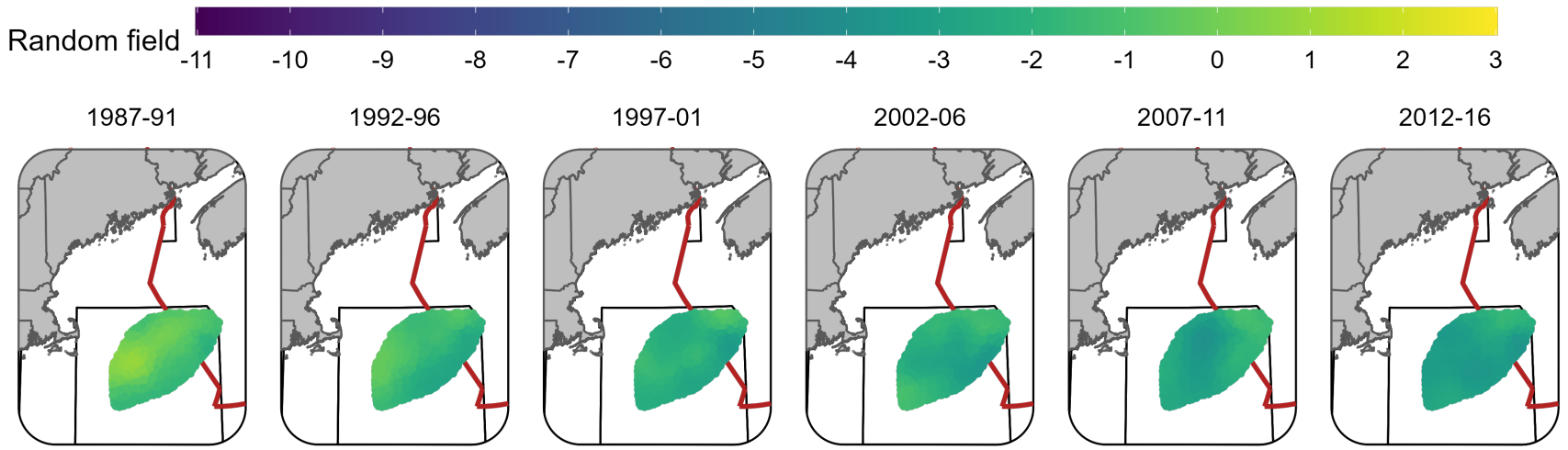

Figure 14. Random fields (logit scale) for Atlantic Cod in each era during the Winter (RV survey) using the SST + Dep model and 5 year random field.

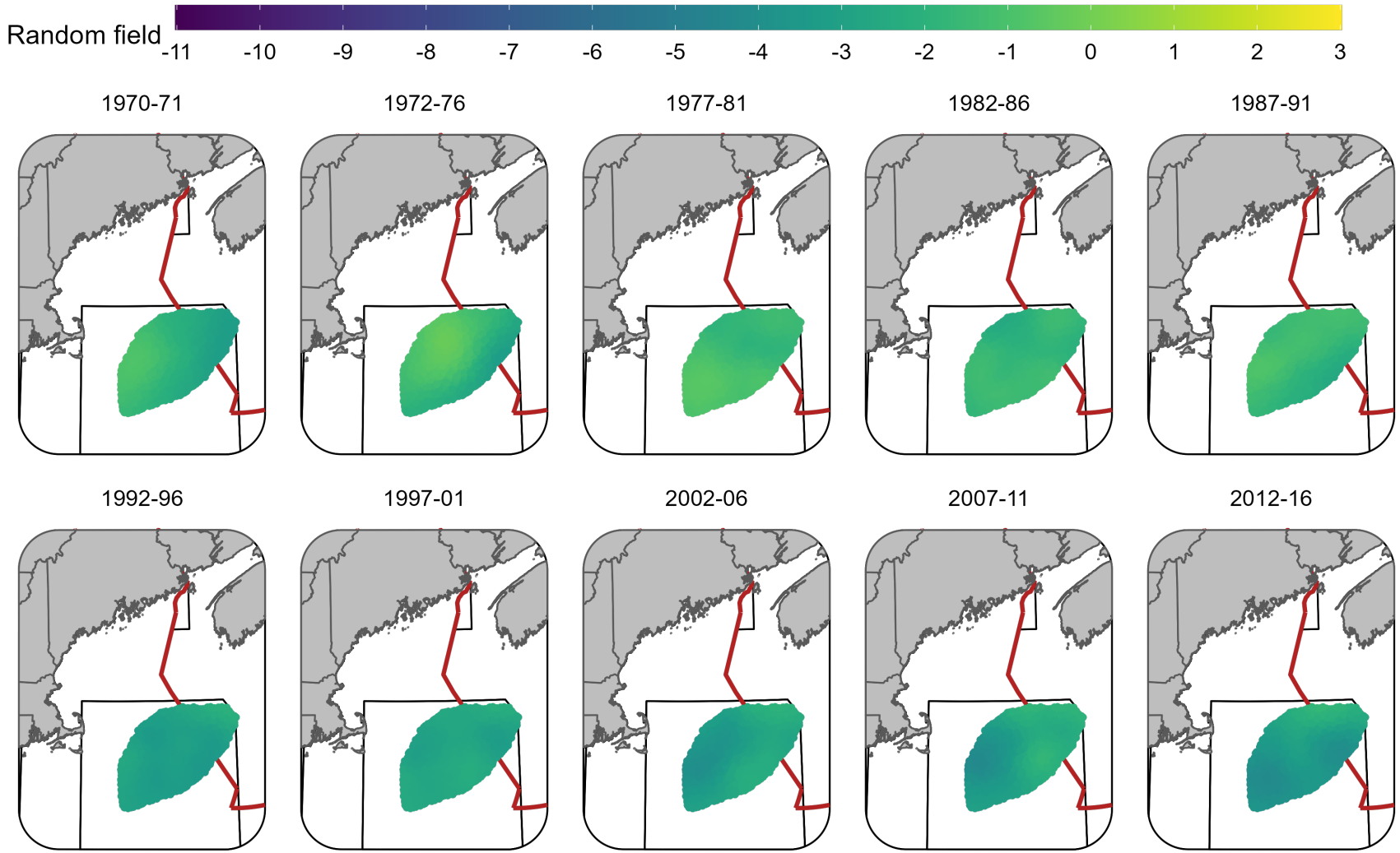

Figure 15. Random fields (logit scale) for Atlantic Cod in each era during the Spring (NMFS-spring survey) using the SST + Dep model and 5 year random field.

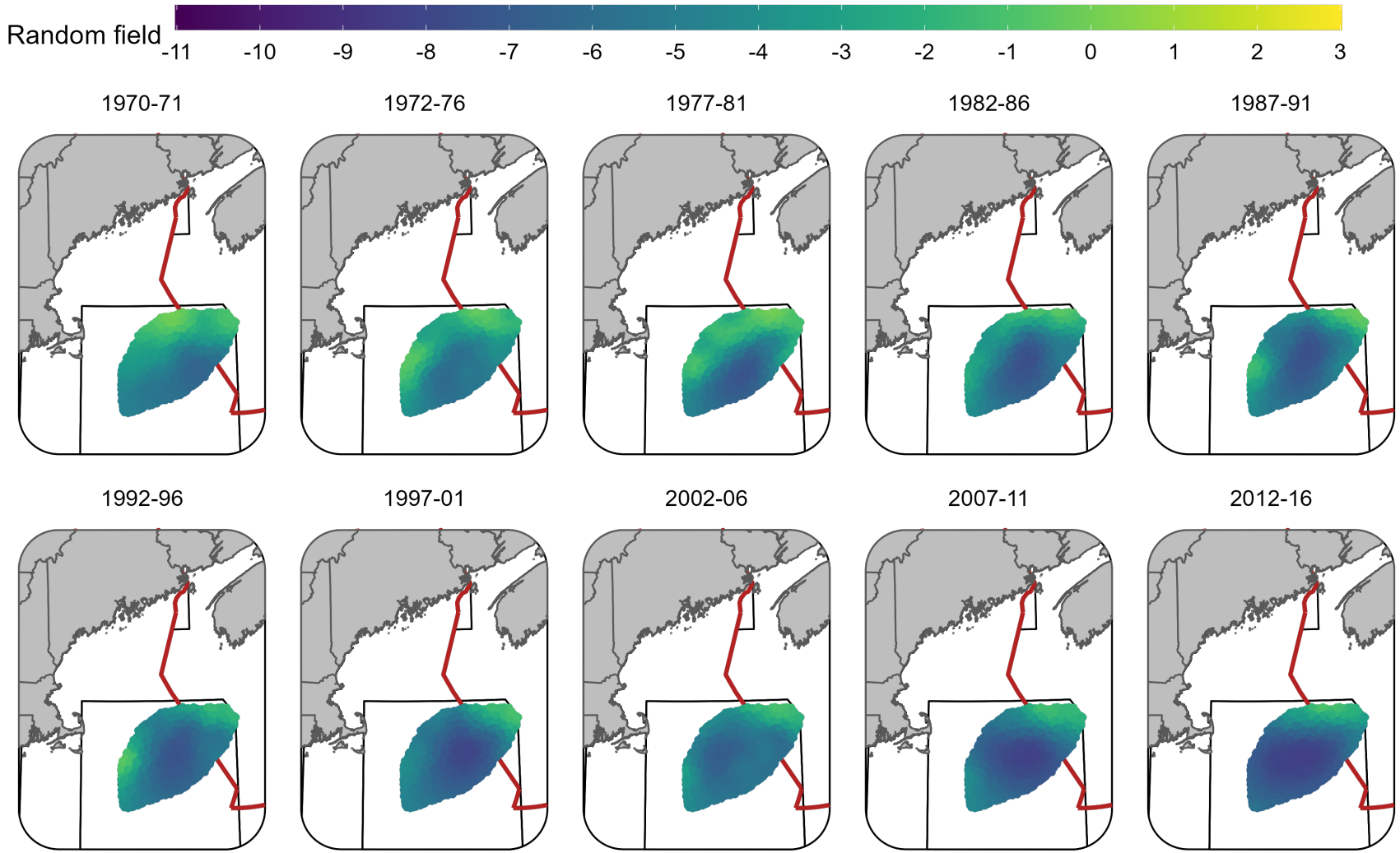

Figure 16. Random fields (logit scale) for Atlantic Cod in each era during the Fall (NMFS-fall survey) using the SST + Dep model and 5 year random field.

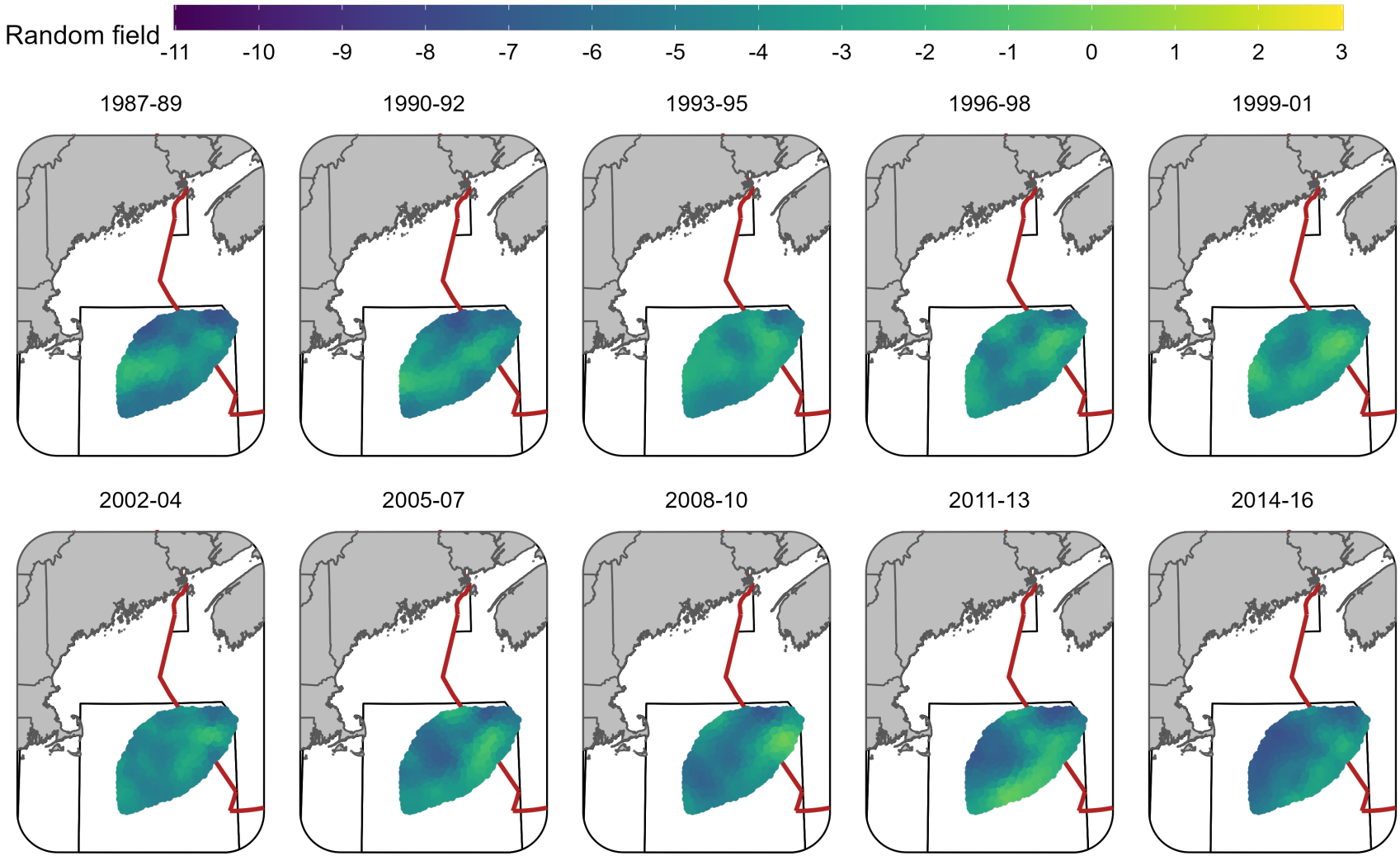

Figure 17. Random fields (logit scale) for Yellowtail Flounder in each era during the Winter (RV survey) using the SST + Dep + Sed model and 3 year random field.

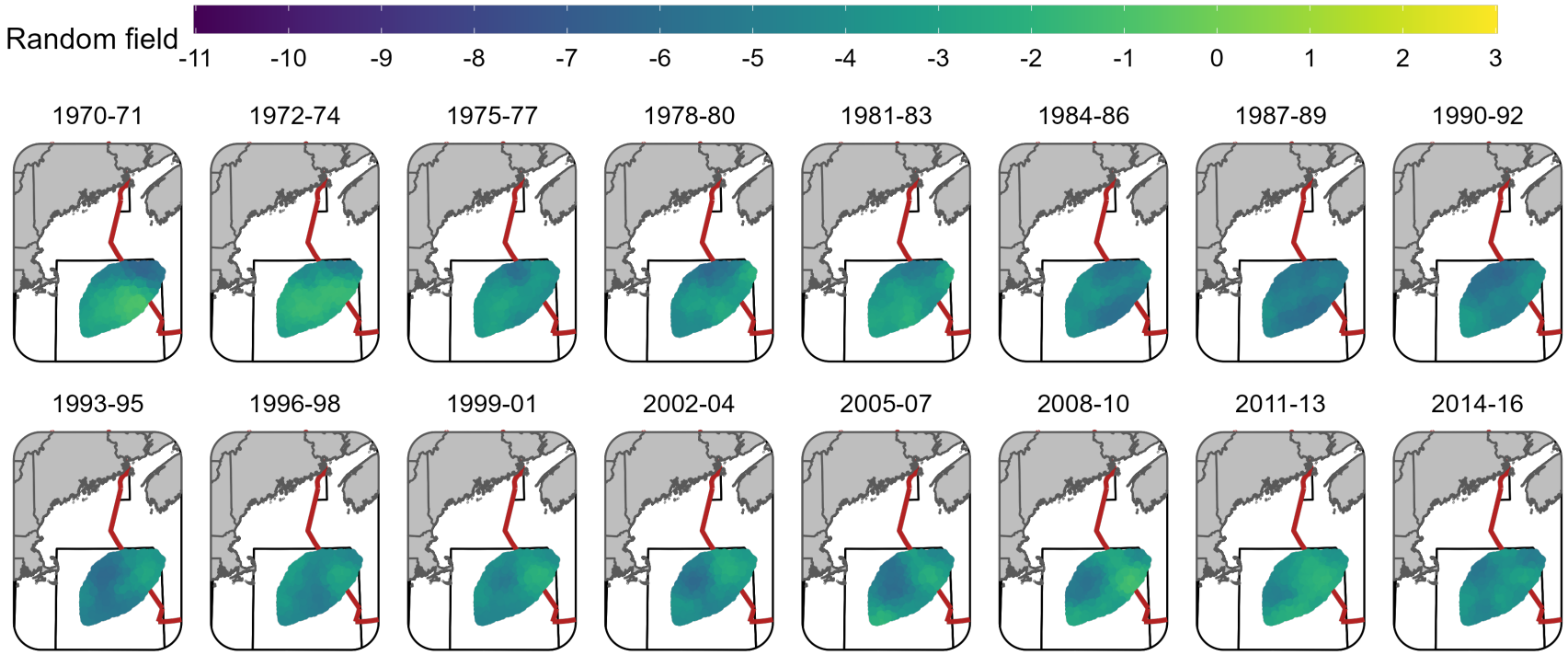

Figure 18. Random fields (logit scale) for Yellowtail Flounder in each era during the Spring (NMFS-spring survey) using the SST + Dep + Sed model and 3 year random field.

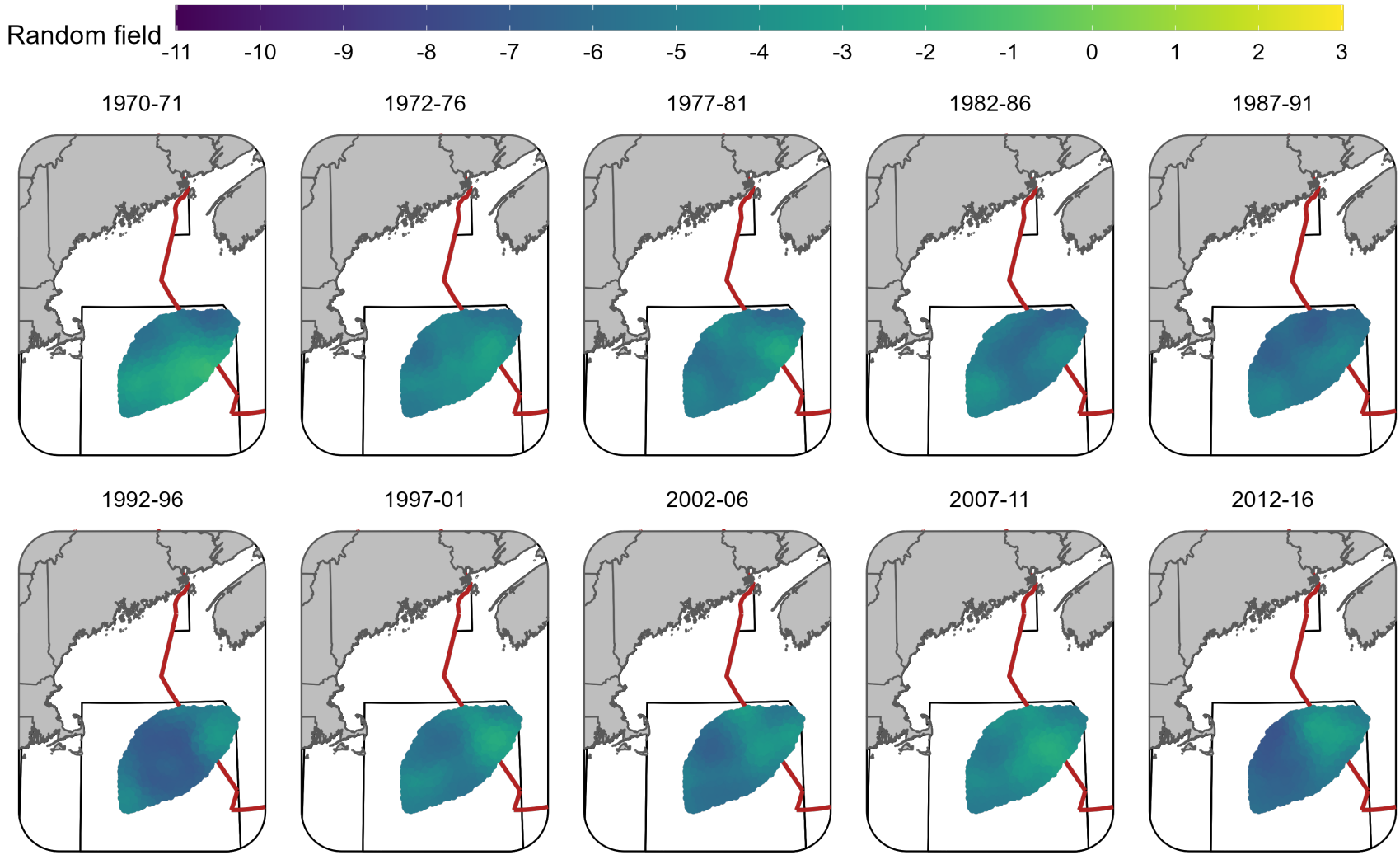

Figure 19. Random fields (logit scale) for Yellowtail Flounder in each era during the Fall (NMFS-fall survey) using the SST + Dep + Sed model and 5 year random field.

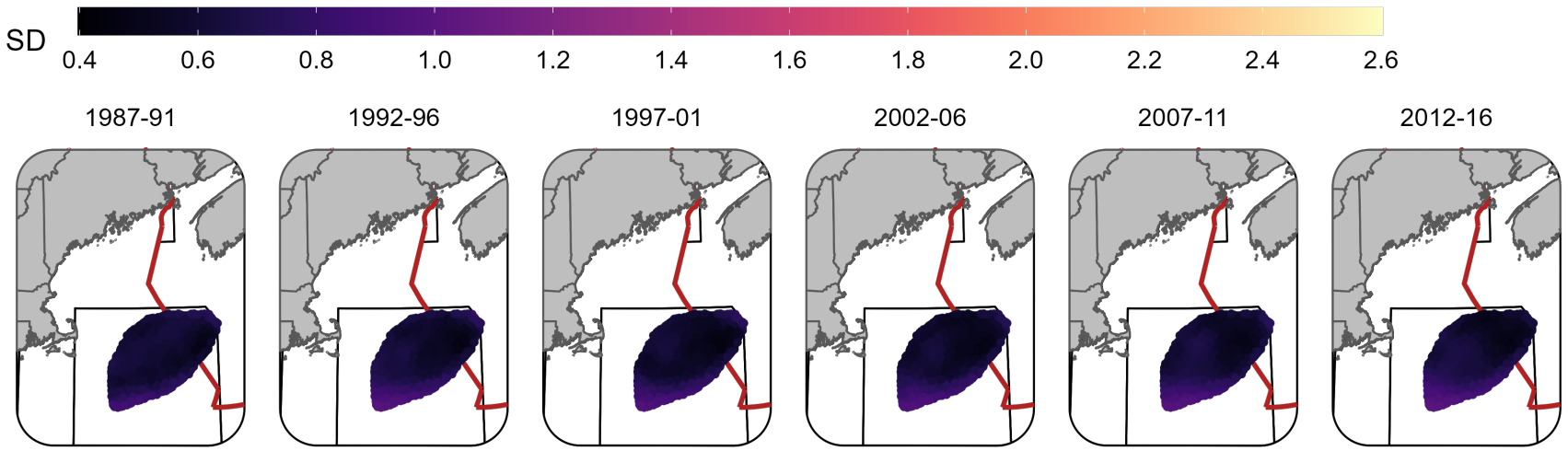

Figure 20. Standard deviation of random fields (logit scale) for Atlantic Cod in each era during the Winter (RV survey) using the SST + Dep model and 5 year random field.

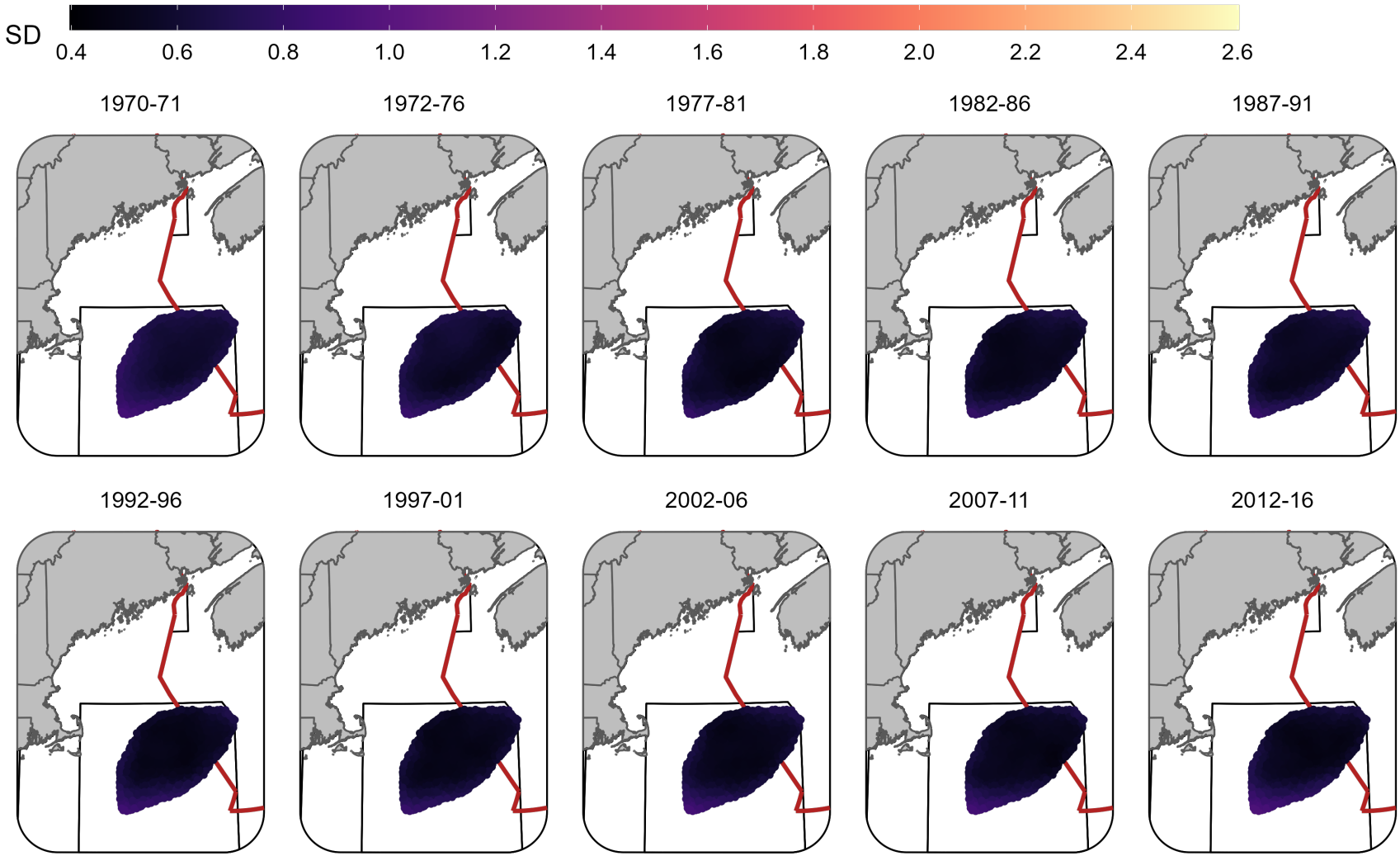

Figure 21. Standard deviation of random fields (logit scale) for Atlantic Cod in each era during the Spring (NMFS-spring survey) using the SST + Dep model and 5 year random field.

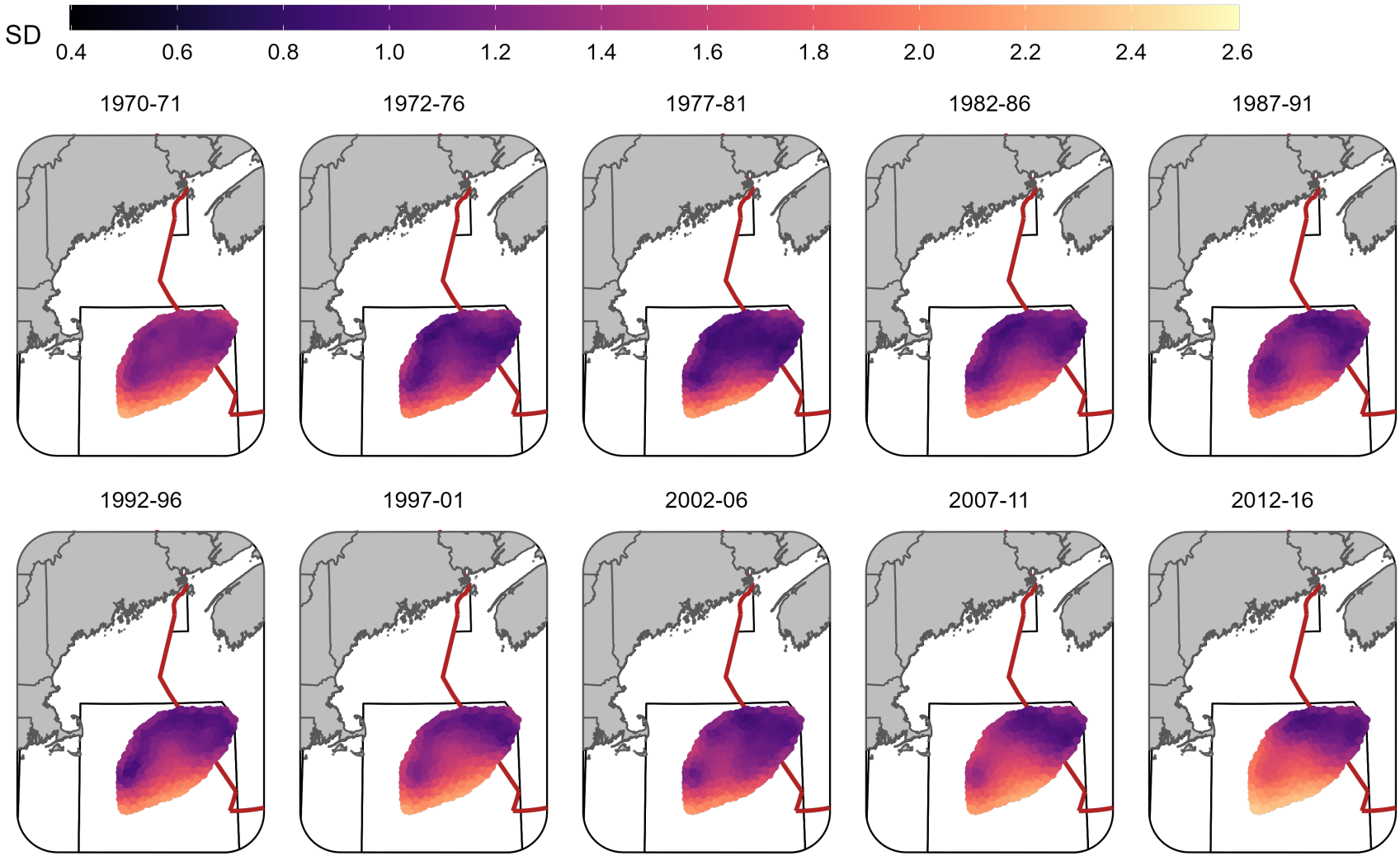

Figure 22. Standard deviation of random fields (logit scale) for Atlantic Cod in each era during the Fall (NMFS-fall survey) using the SST + Dep model and 5 year random field.

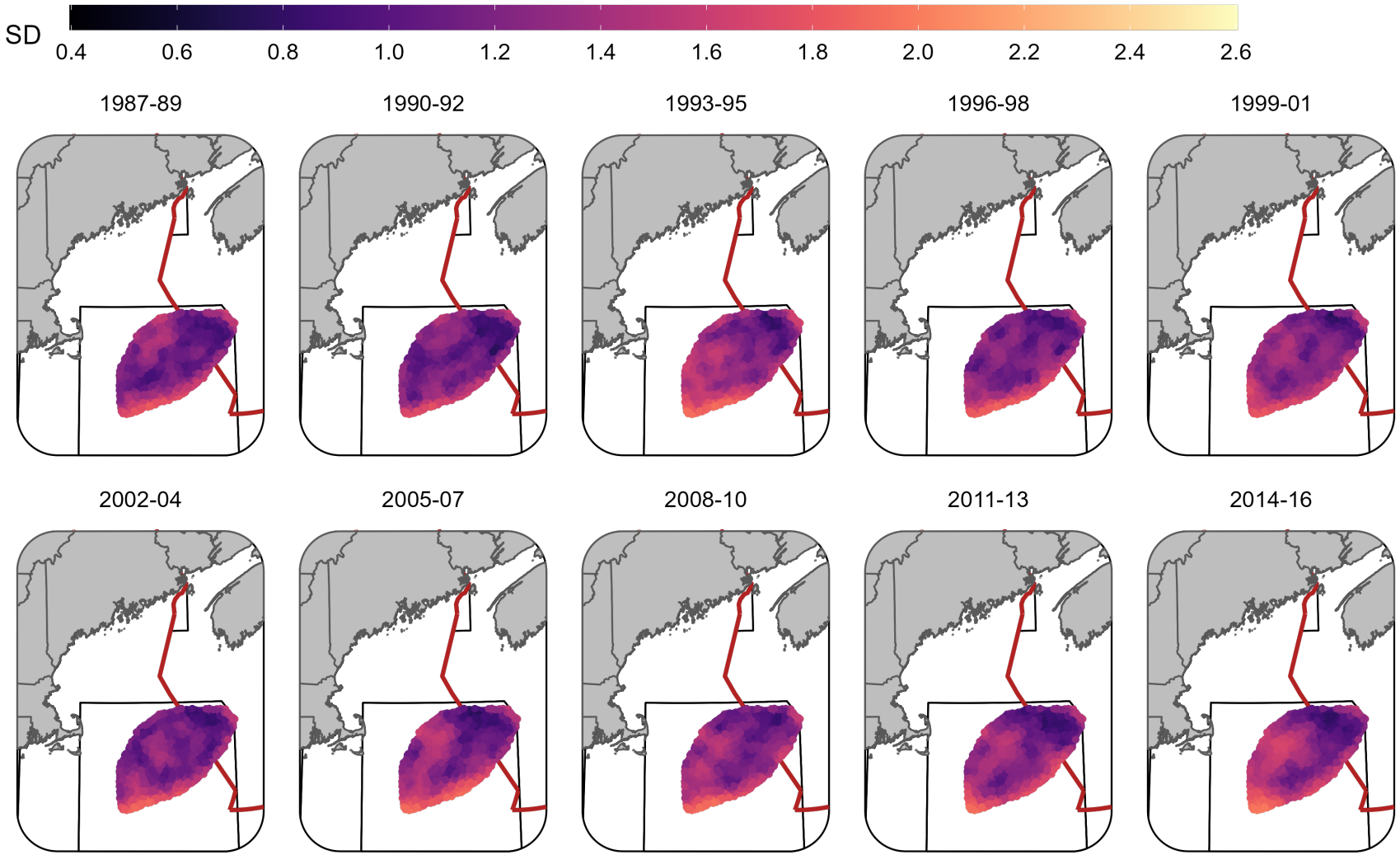

Figure 23. Standard deviation of random fields (logit scale) for Yellowtail Flounder in each era during the Winter (RV survey) using the SST + Dep + Sed model and 3 year random field.

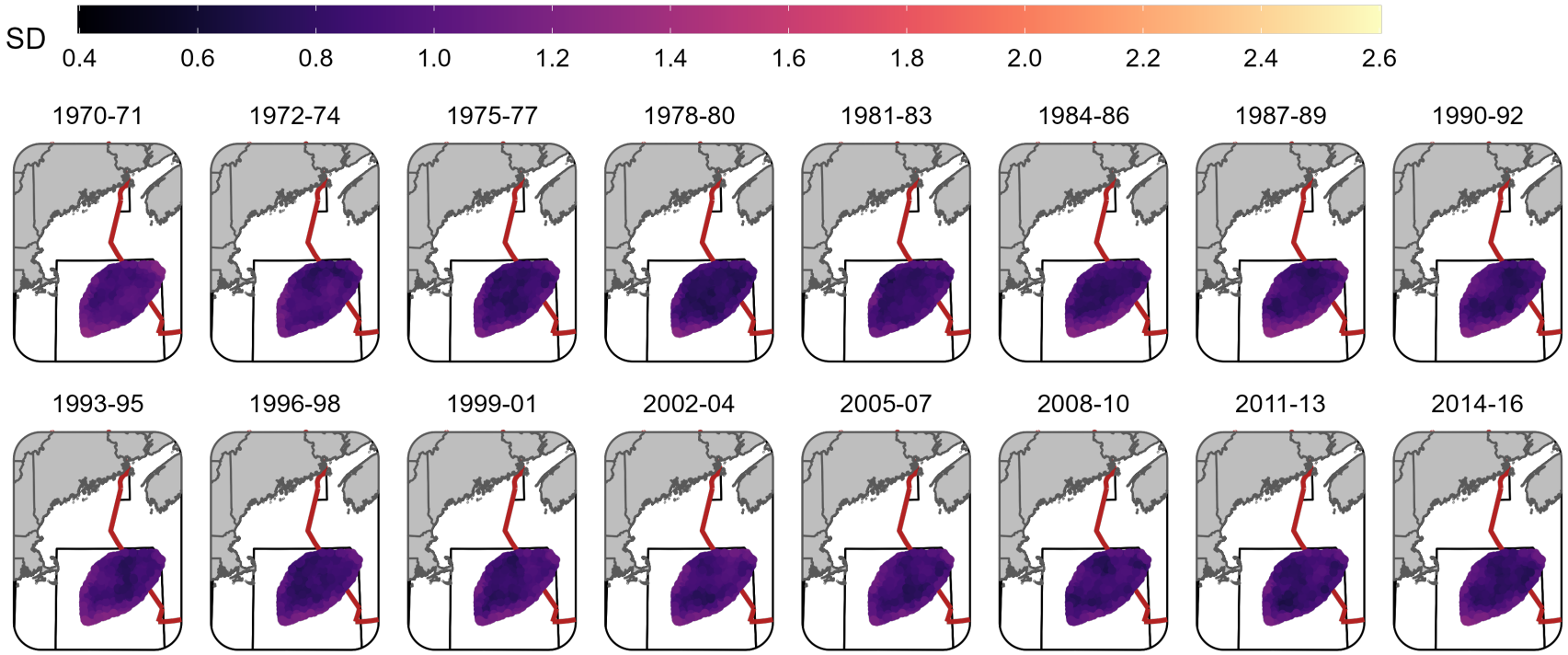

Figure 24. Standard deviation of random fields (logit scale) for Yellowtail Flounder in each era during the Spring (NMFS-spring survey) using the SST + Dep + Sed model and 3 year random field.

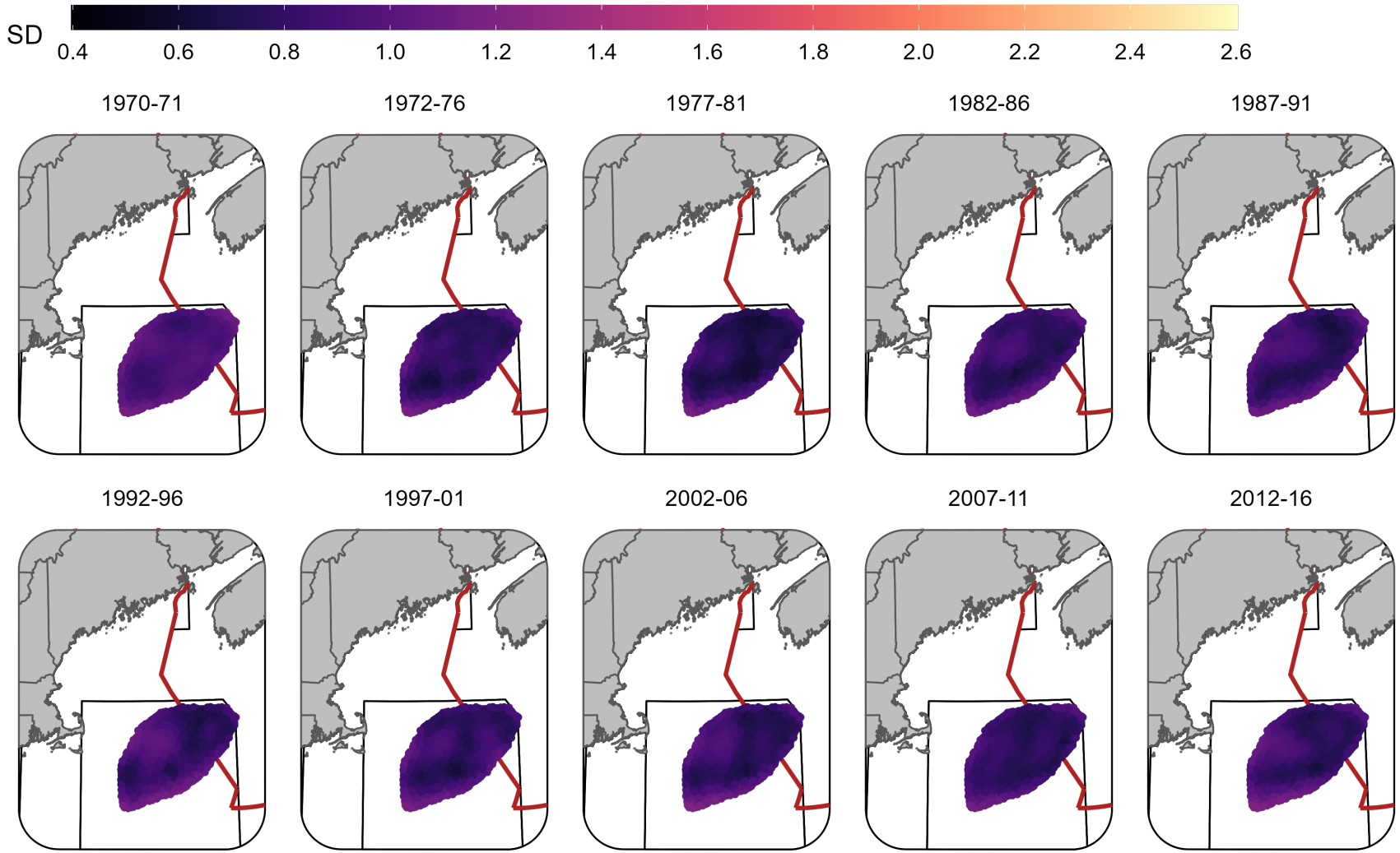

Figure 25. Standard deviation of random fields (logit scale) for Yellowtail Flounder in each era during the Fall (NMFS-fall survey) using the SST + Dep + Sed model and 5 year random field.

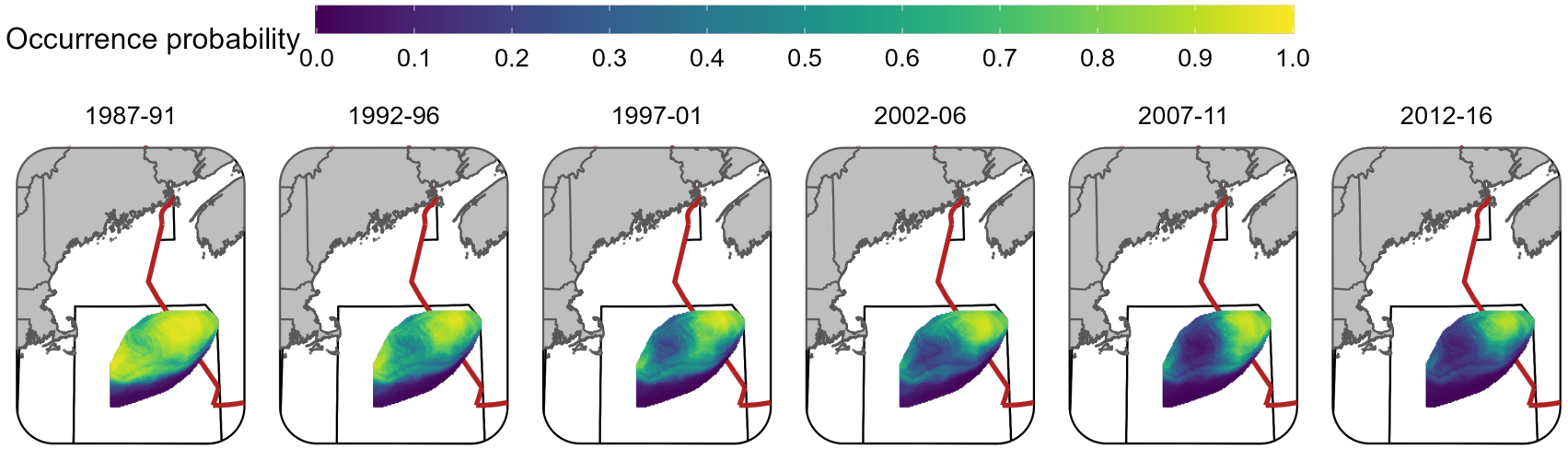

Figure 26. Predicted occurrence probability for Atlantic Cod in each era during the Winter (RV survey) using the SST + Dep model and 5 year random field.

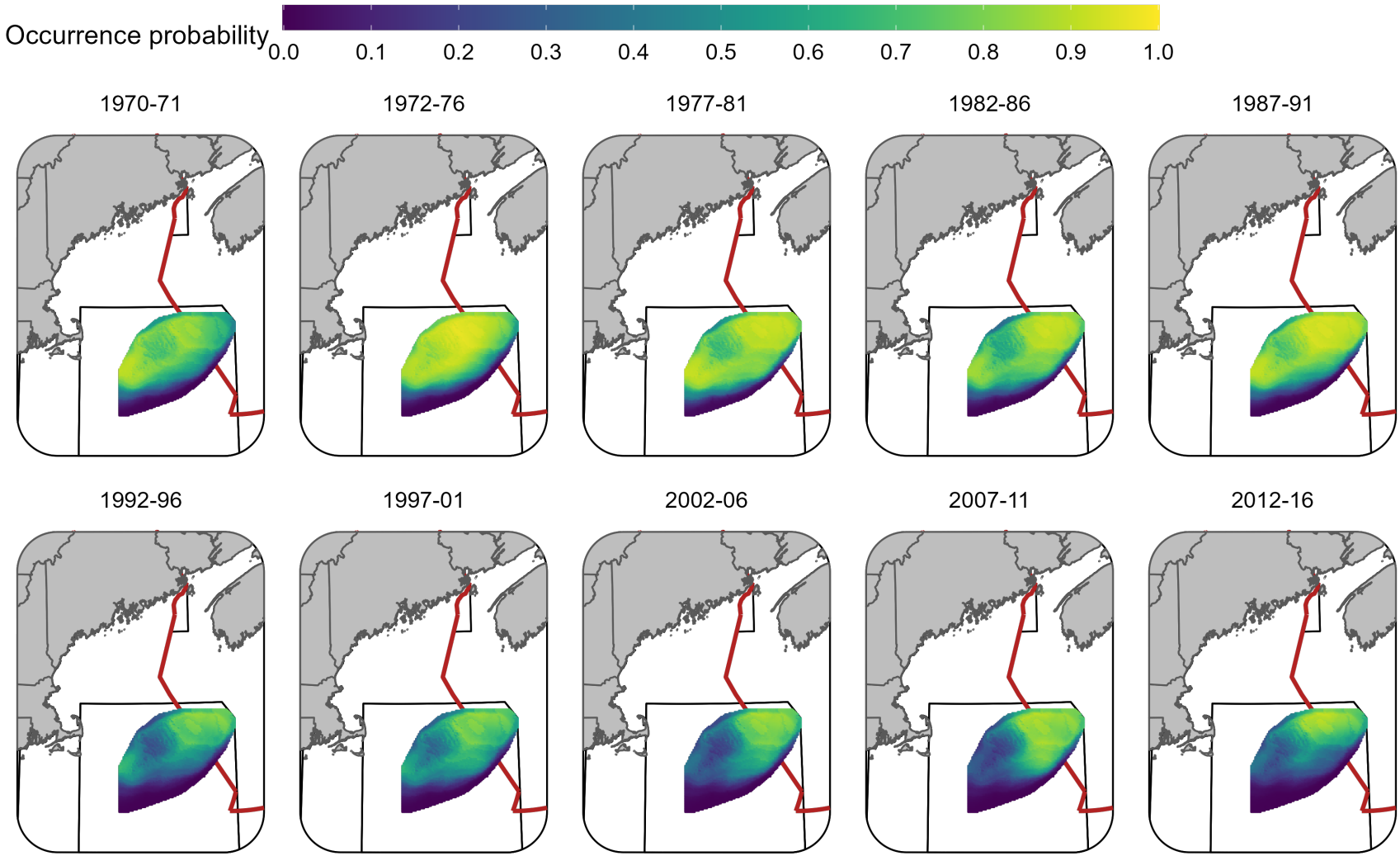

Figure 27. Predicted occurrence probability for Atlantic Cod in each era during the Spring (NMFS-spring survey) using the SST + Dep model and 5 year random field.

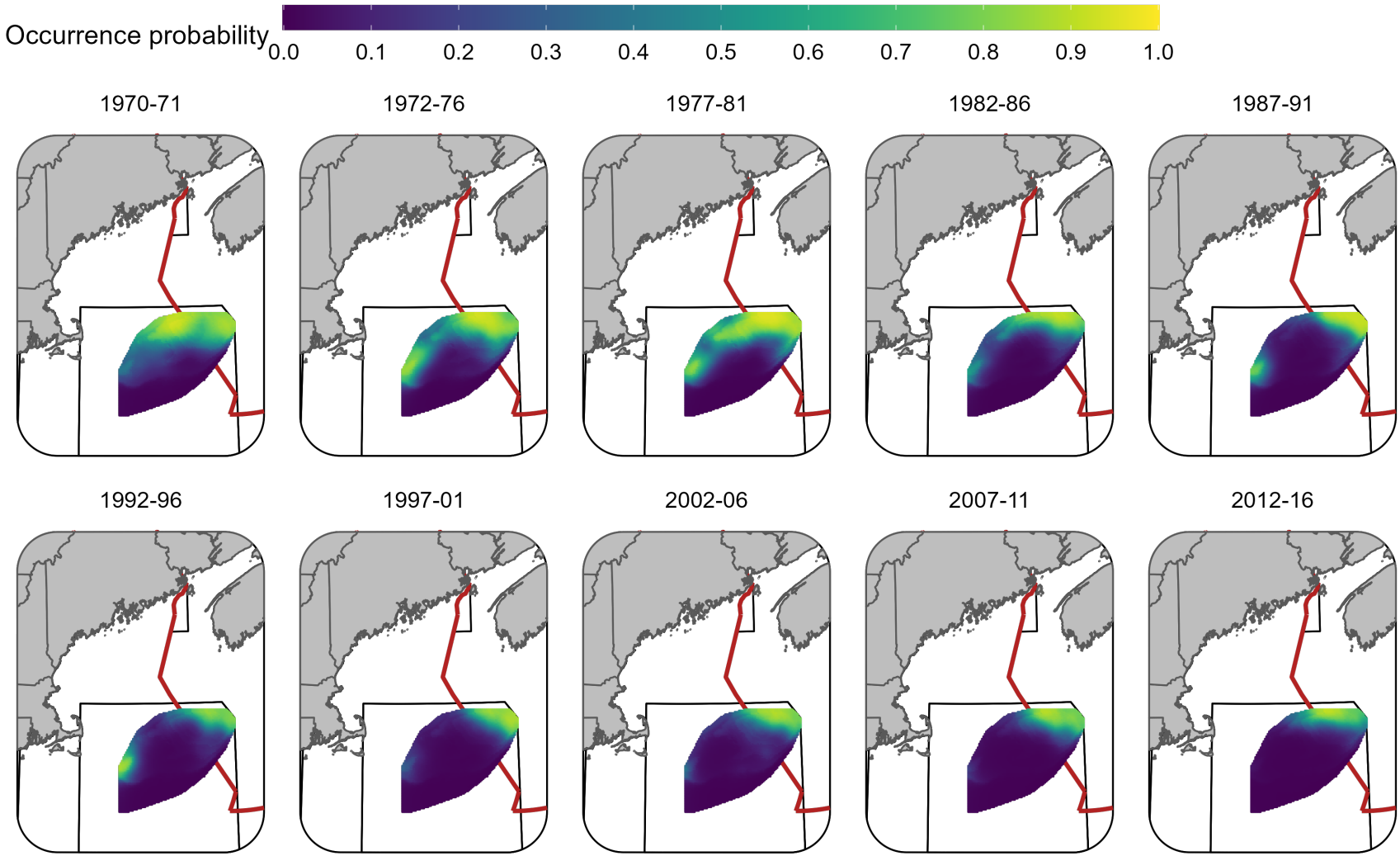

Figure 28. Predicted occurrence probability for Atlantic Cod in each era during the Fall (NMFS-fall survey) using the SST + Dep model and 5 year random field.

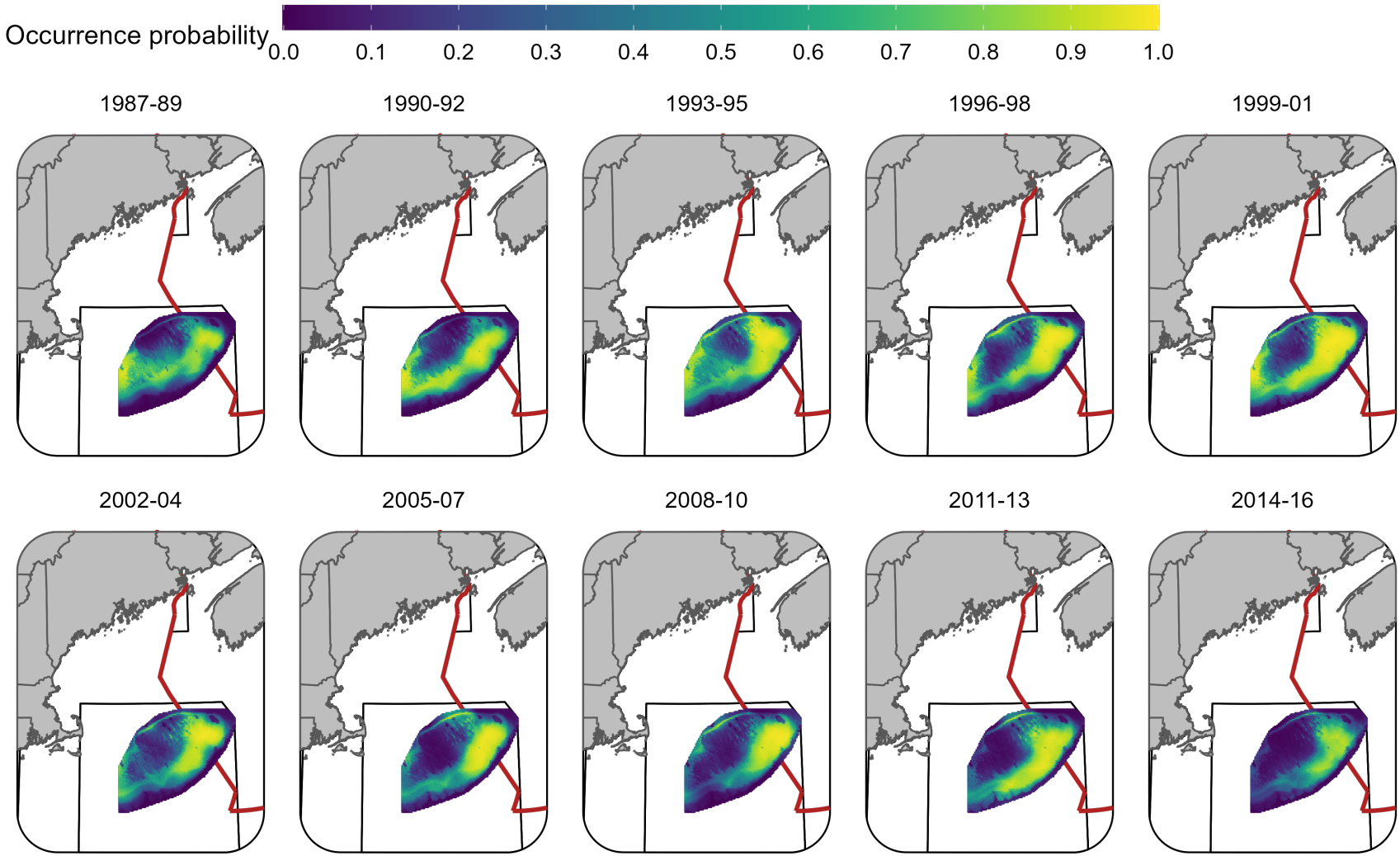

Figure 29. Predicted occurrence probability for Yellowtail Flounder in each era during the Winter (RV survey) using the SST + Dep + Sed model and 3 year random field.

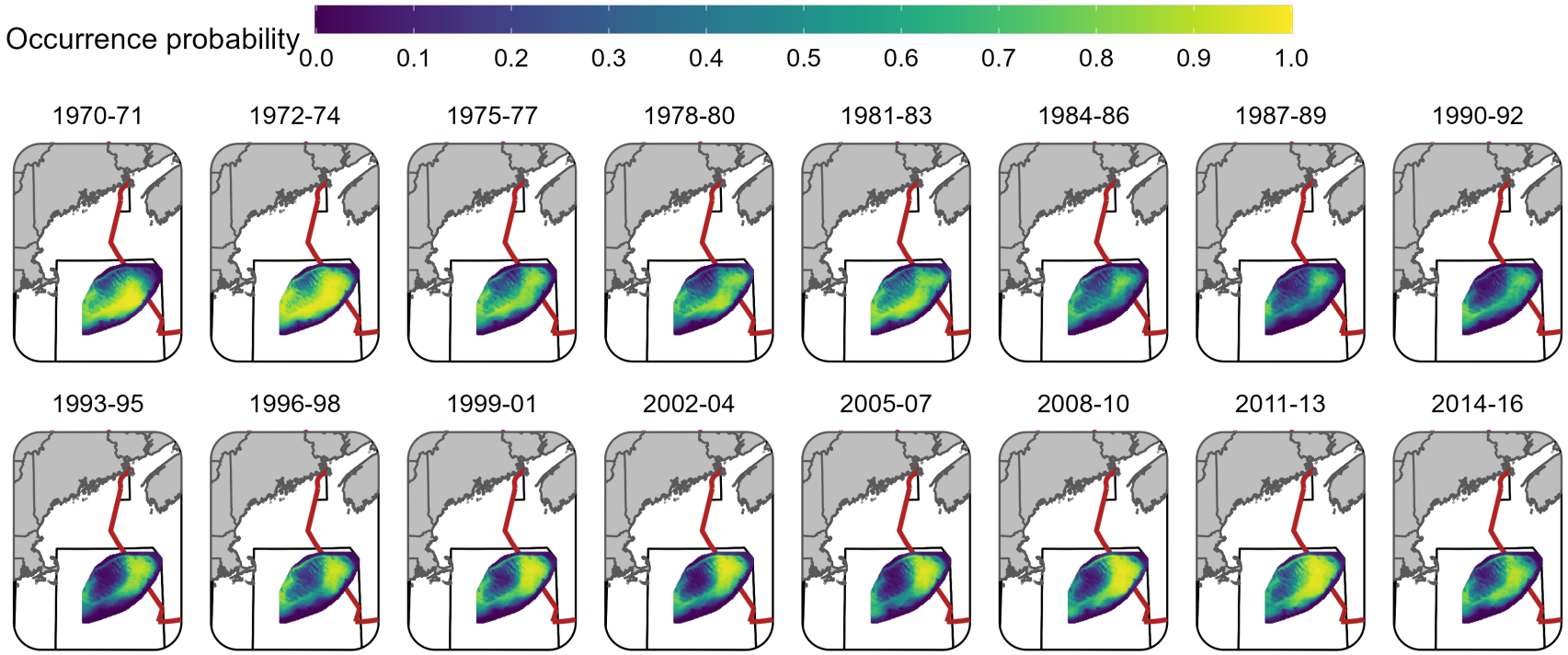

Figure 30. Predicted occurrence probability for Yellowtail Flounder in each era during the Spring (NMFS-spring survey) using the SST + Dep + Sed model and 3 year random field.

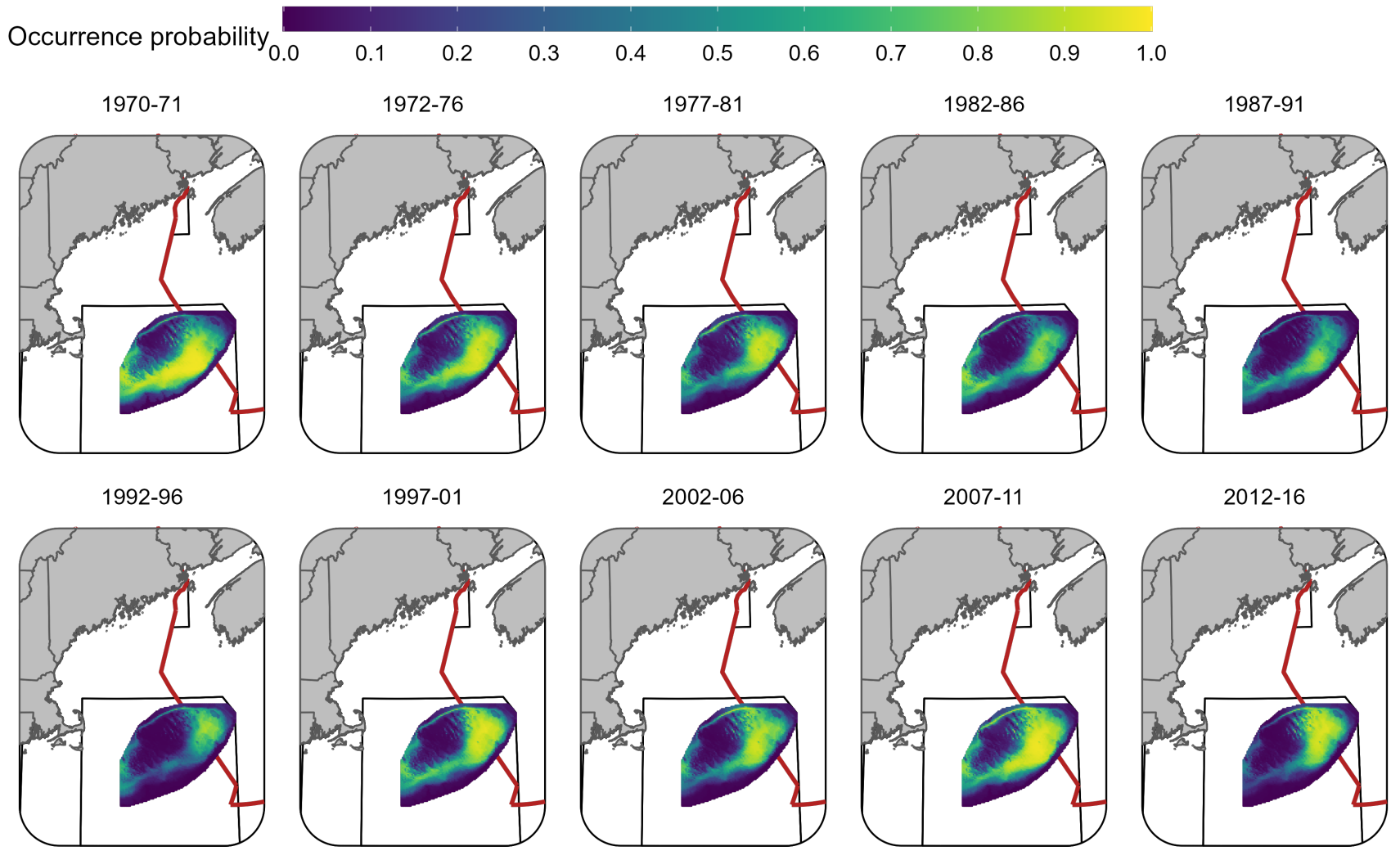

Figure 31. Predicted occurrence probability for Yellowtail Flounder in each era during the Fall (NMFS-fall survey) using the SST + Dep + Sed model and 5 year random field.

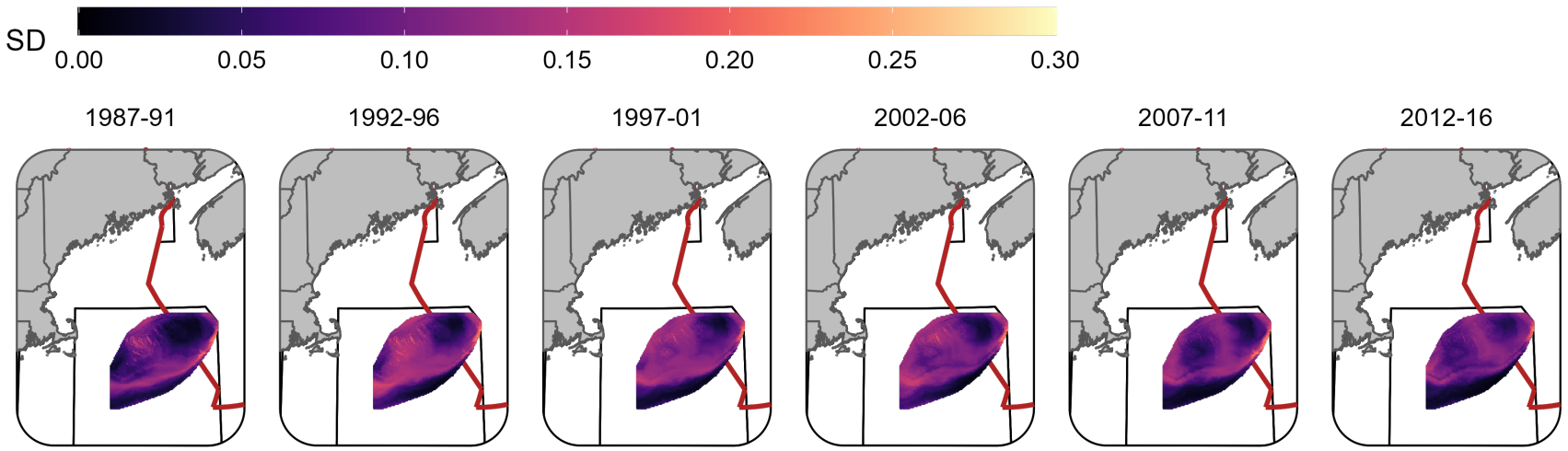

Figure 32. Standard deviation (logit scale) of predicted occurrence probability for Atlantic Cod in each era during the Winter (RV survey) using the SST + Dep model and 5 year random field.

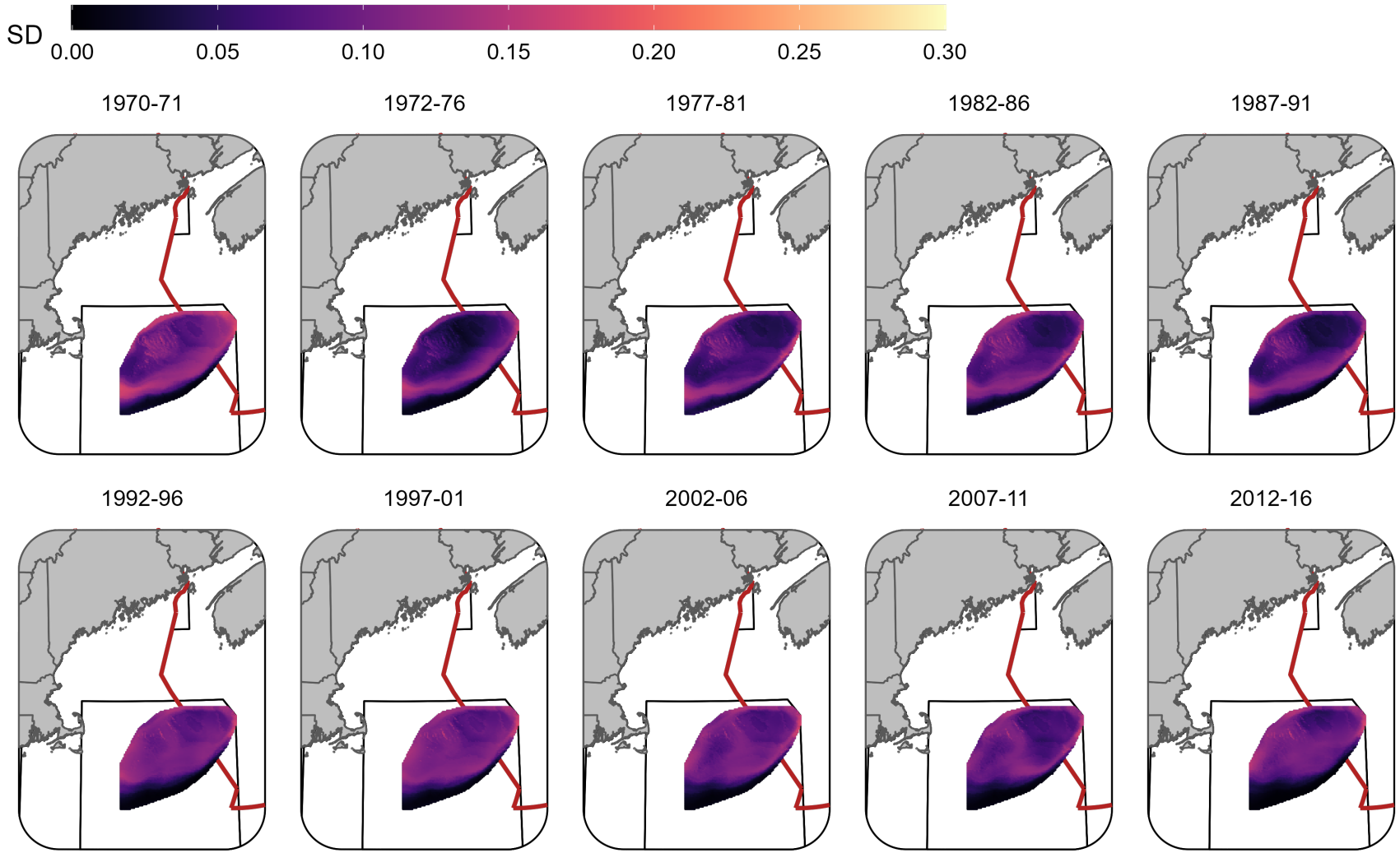

Figure 33. Standard deviation (logit scale) of predicted occurrence probability for Atlantic Cod in each era during the Spring (NMFS-spring survey) using the SST + Dep model and 5 year random field.

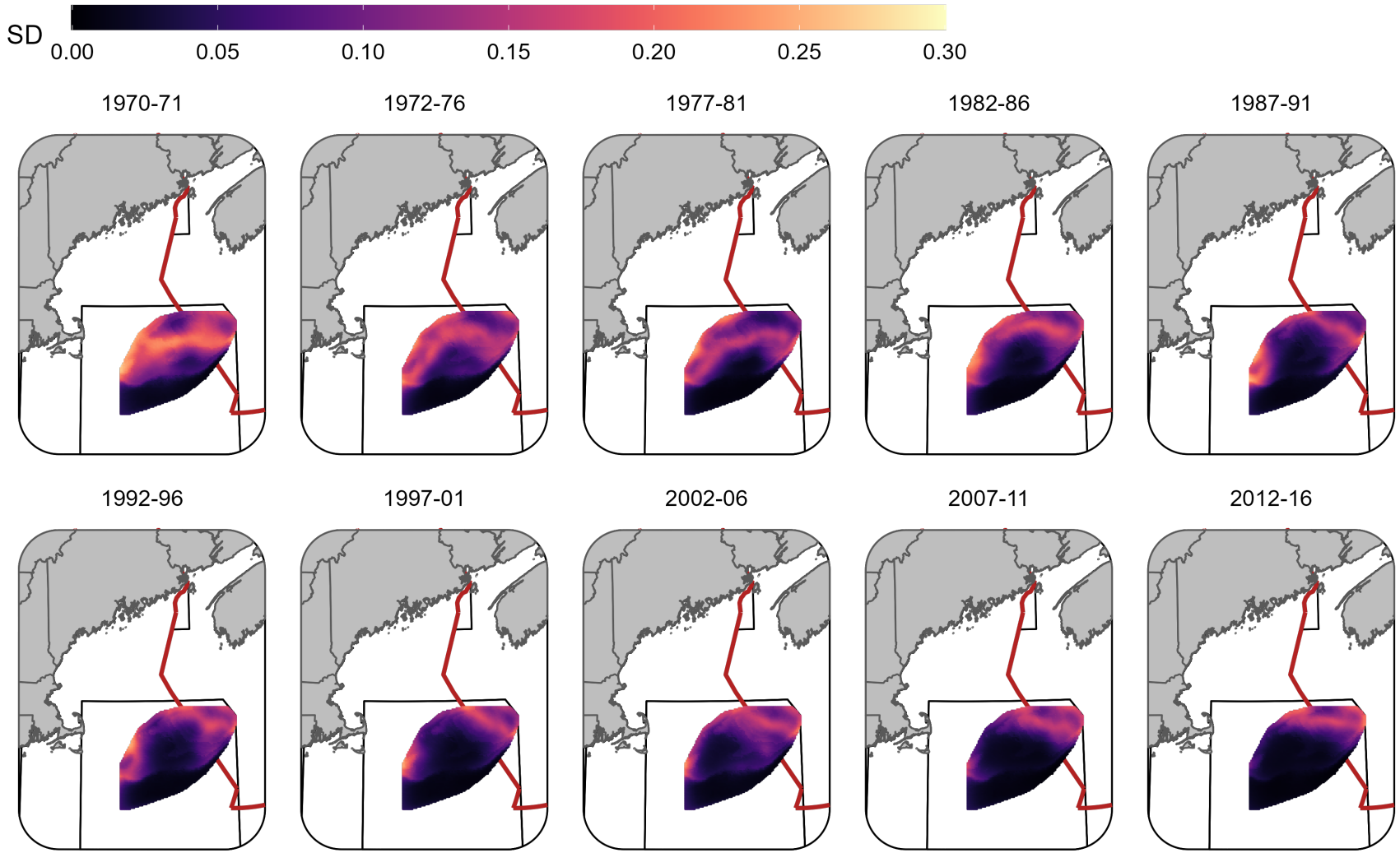

Figure 34. Standard deviation (logit scale) of predicted occurrence probability for Atlantic Cod in each era during the Fall (NMFS-fall survey) using the SST + Dep model and 5 year random field.

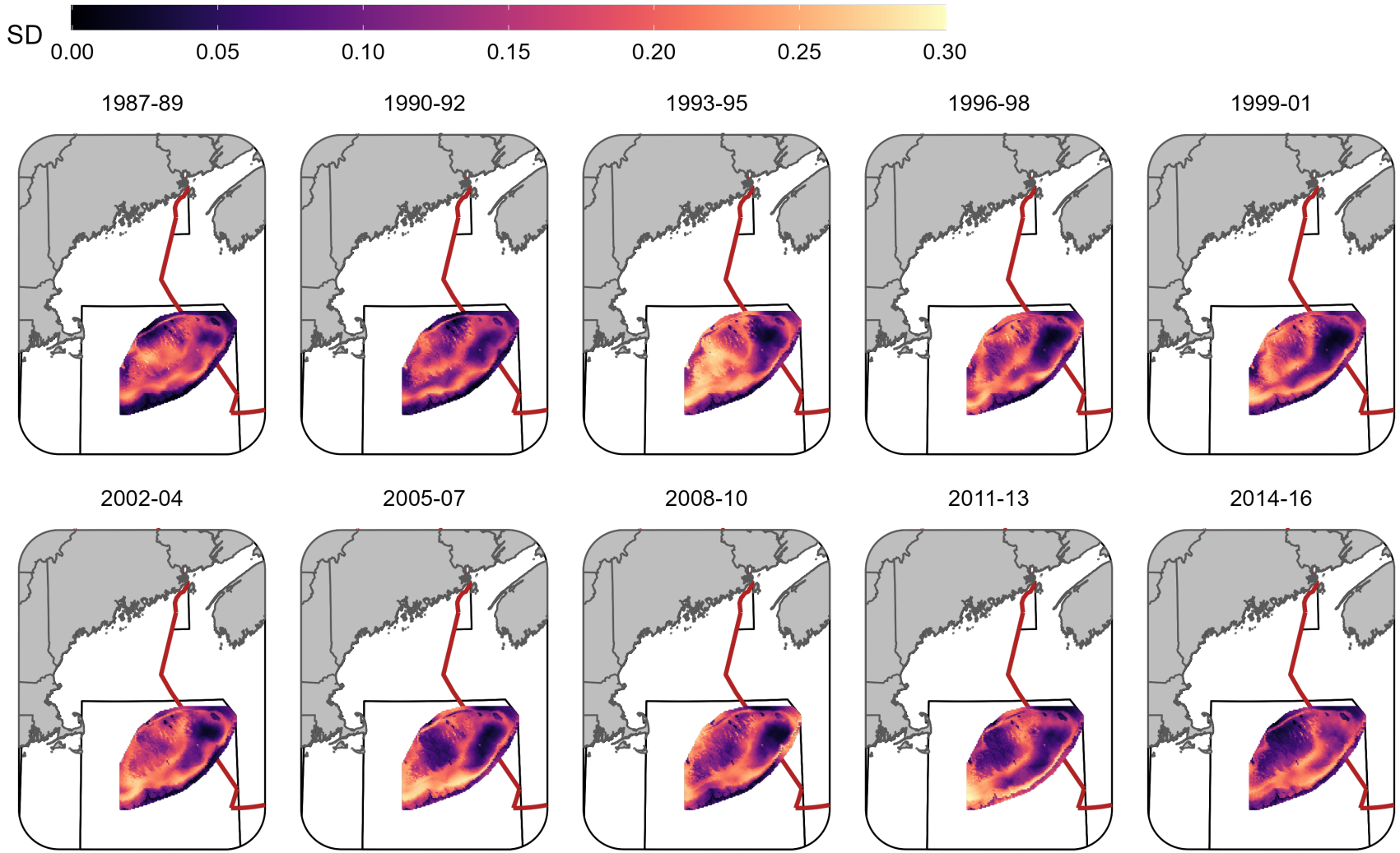

Figure 35. Standard deviation (logit scale) of predicted occurrence probability for Yellowtail Flounder in each era during the Winter (RV survey) using the SST + Dep + Sed model and 3 year random field.

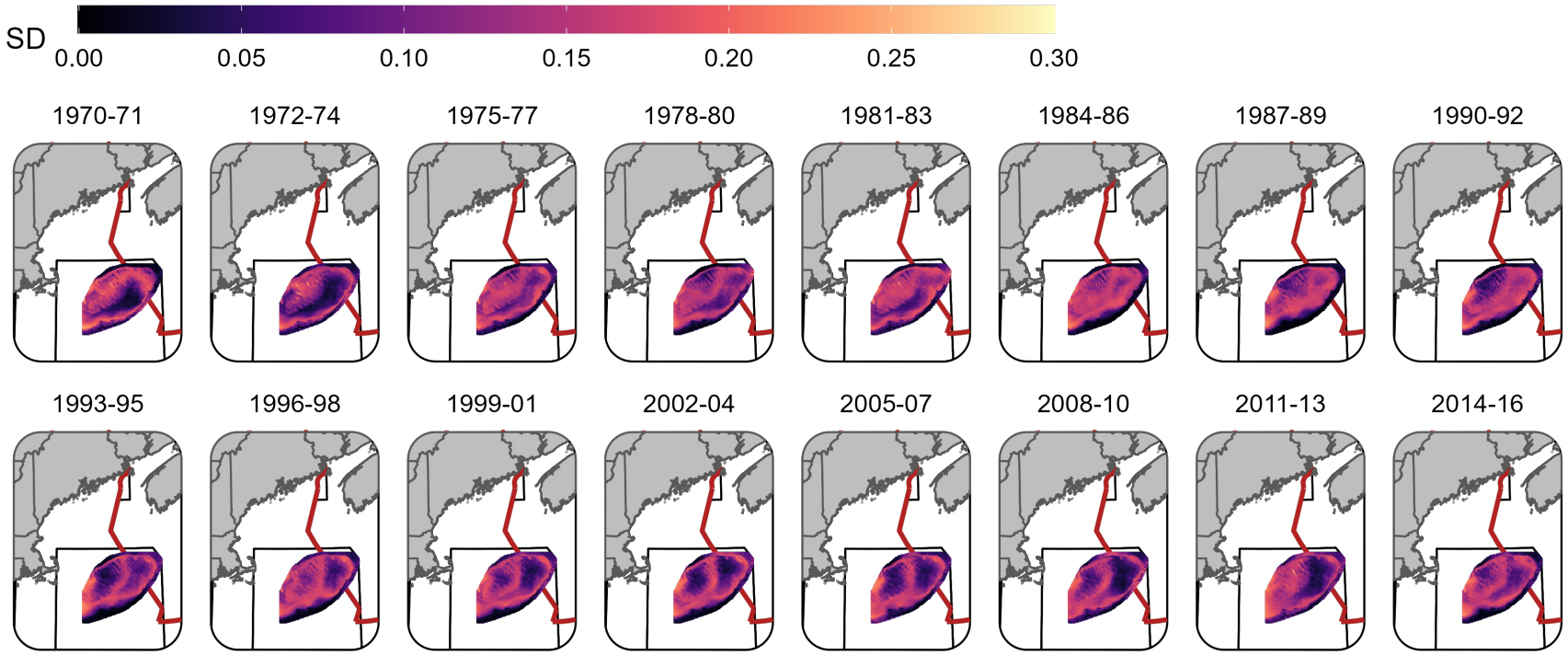

Figure 36. Standard deviation (logit scale) of predicted occurrence probability for Yellowtail Flounder in each era during the Spring (NMFS-spring survey) using the SST + Dep + Sed model and 3 year random field.

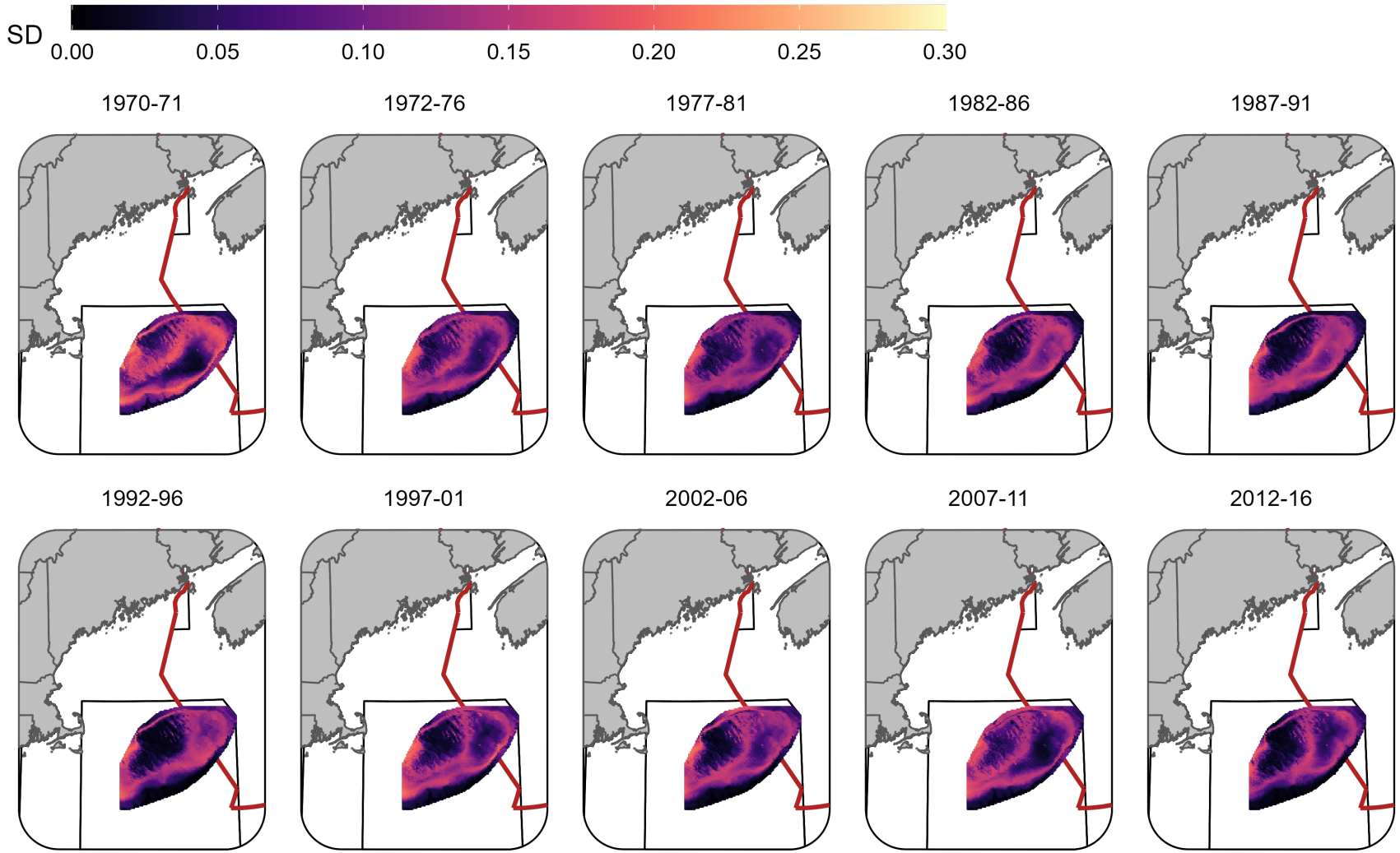

Figure 37. Standard deviation (logit scale) of predicted occurrence probability for Yellowtail Flounder in each era during the Fall (NMFS-fall survey) using the SST + Dep + Sed model and 5 year random field.

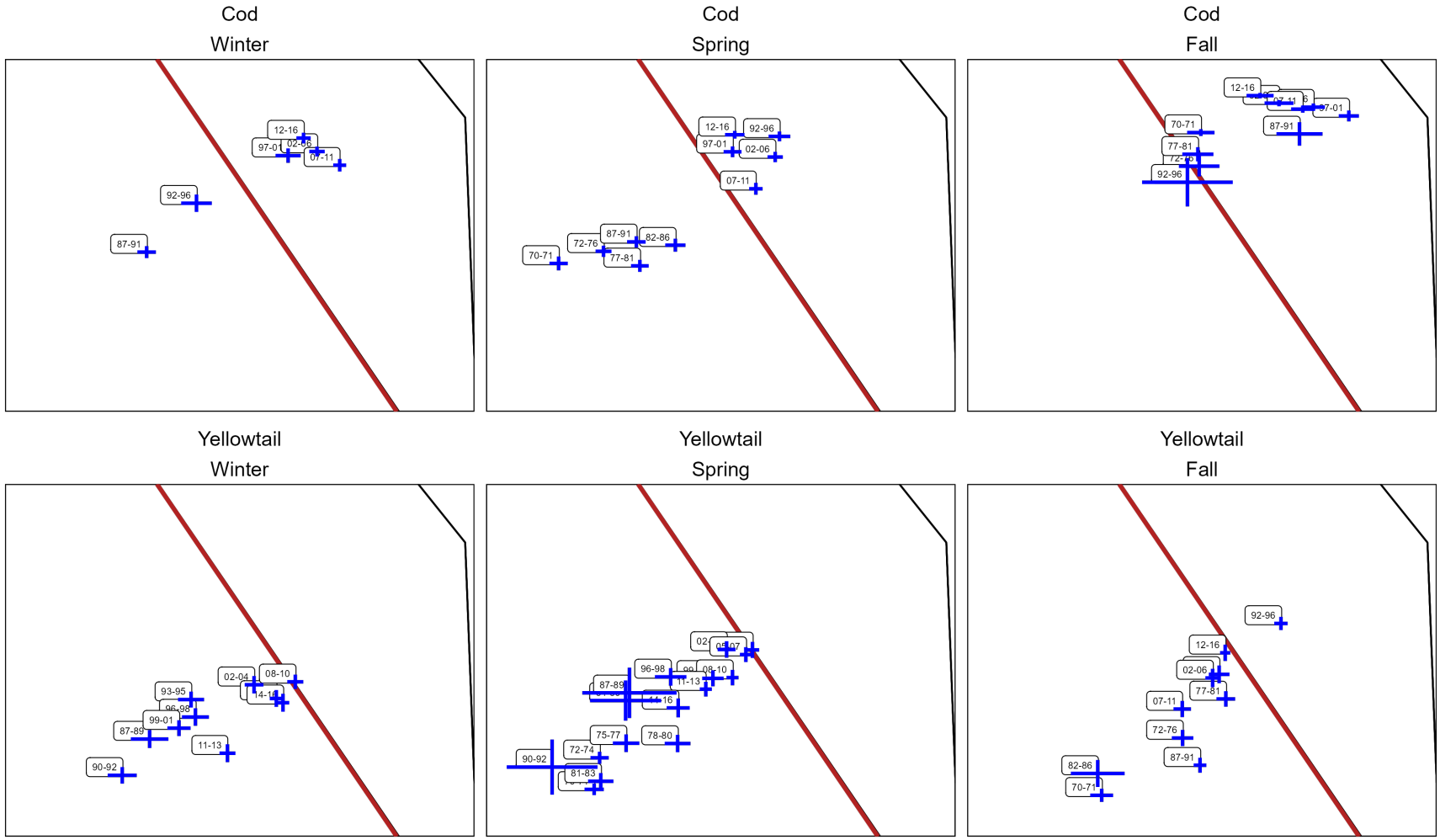

Figure 38. Center of Gravity (COG) for the core areas for Atlantic Cod (top panel) and Yellowtail Flounder (bottom panels) in the Winter (left), Spring (center), and Fall (right). Blue lines indicate ± 3 standard deviation units from the mean COG for each era using the 5 year random field models. Labels indicate the years associated with each era and the red line is border between the U.S. and Canada.

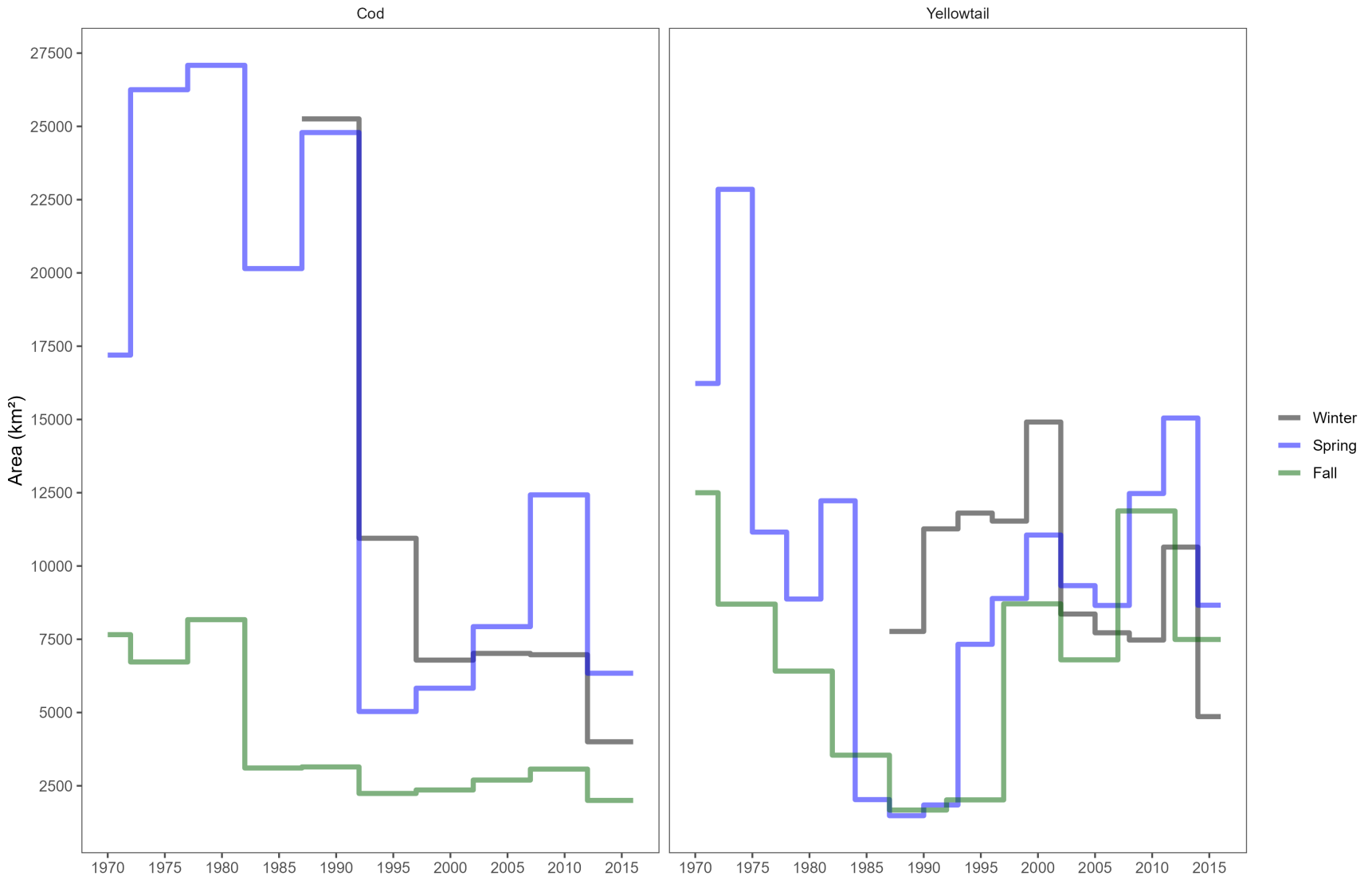

Figure 39. Time series of the total area on GB classified as core area for each of the three seasons. The Atlantic Cod time series is on the left and the Yellowtail Flounder on the right. The black line represents the Winter trend, the Blue line is the Spring trend and the green line is the Fall trend.

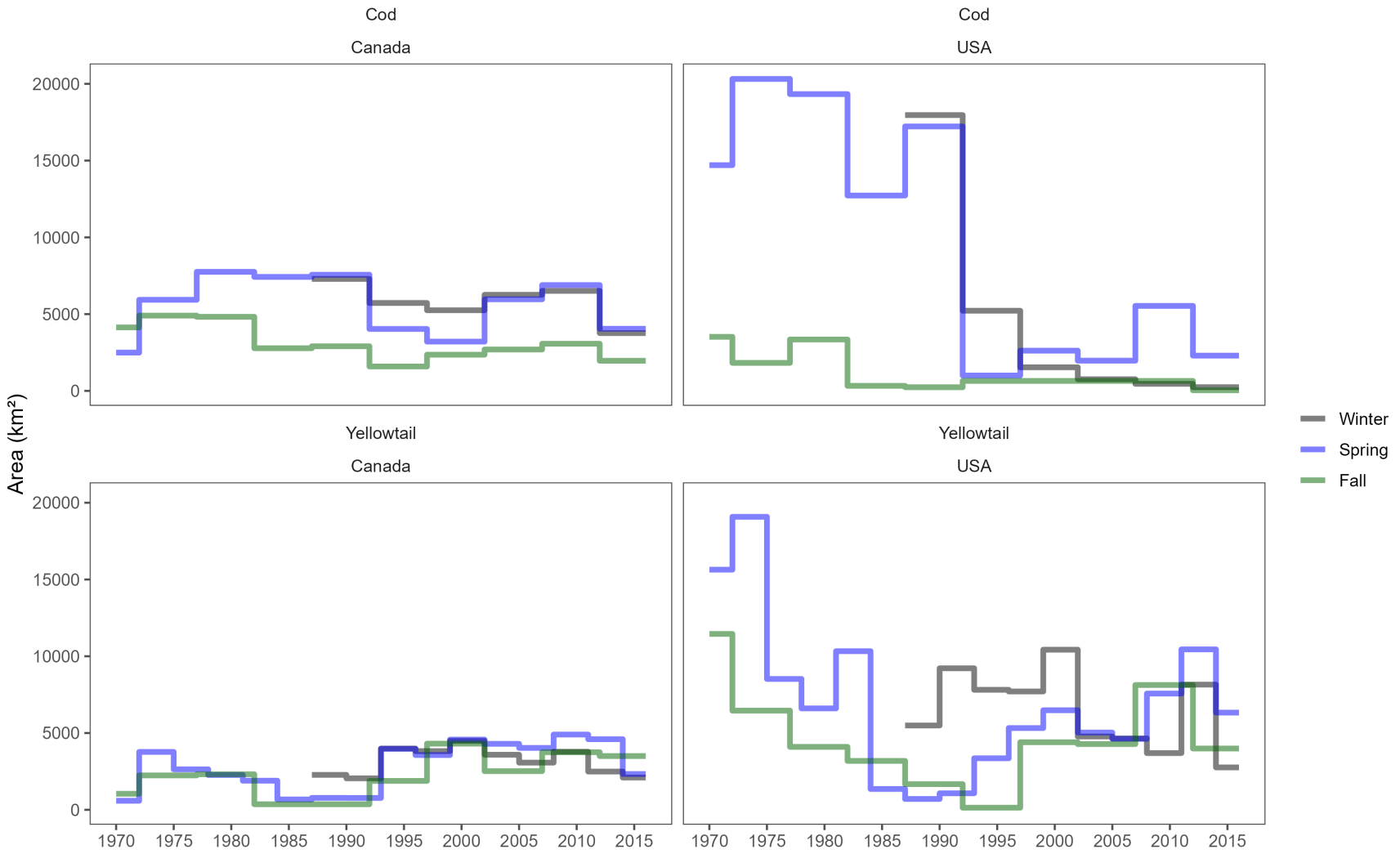

Figure 40. Time series of the total area on GB classified as core area for each of the three seasons in Canada and the U.S.. The Atlantic Cod time series is in the top row and Yellowtail Flounder in the bottom row, Canada is on the left and U.S. is on the right. The black line represents the Winter trend, the Blue line is the Spring trend and the green line is the Fall trend.

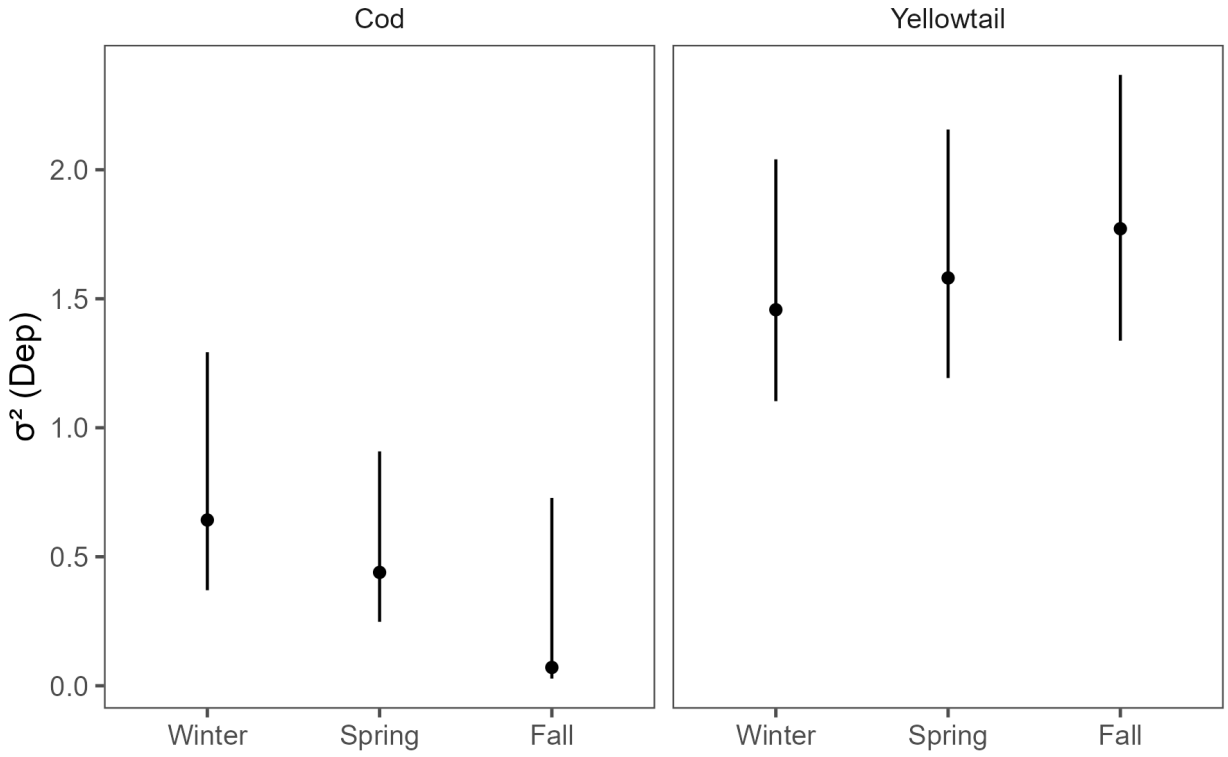

Figure 41. Dep variance hyperparameter estimate with 95% CI's for each stock in each season.

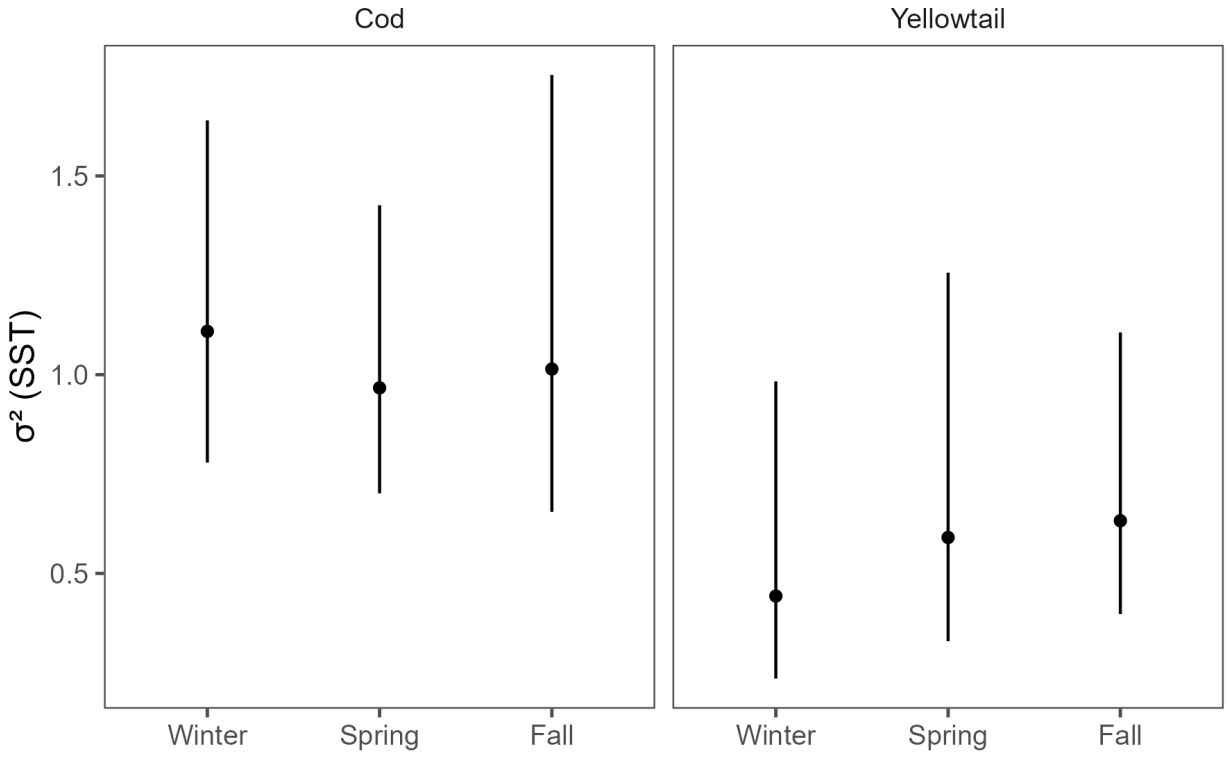

Figure 42. SST variance hyperparameter estimate with 95% CI's for each stock in each season.

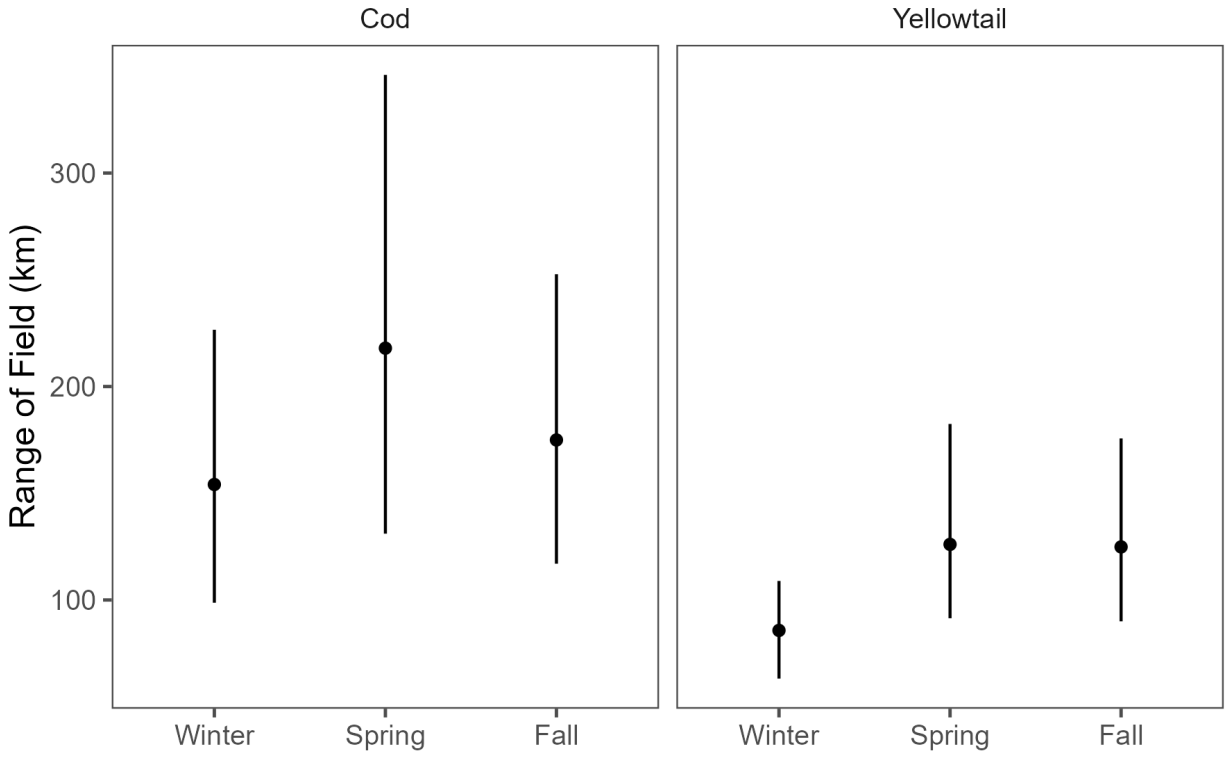

Figure 43. Decorrelation range estimate with 95% CI's for each season.

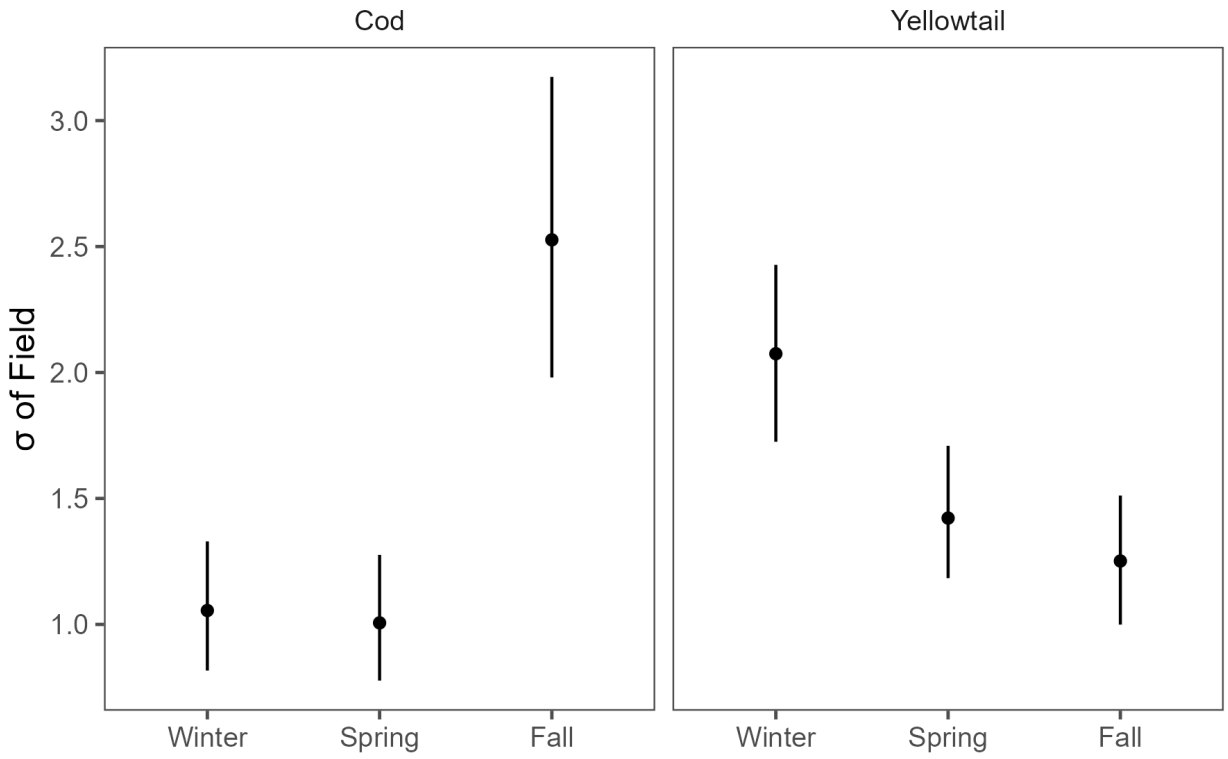

Figure 44. Standard Deviation of the field with 95% CI's for each season.

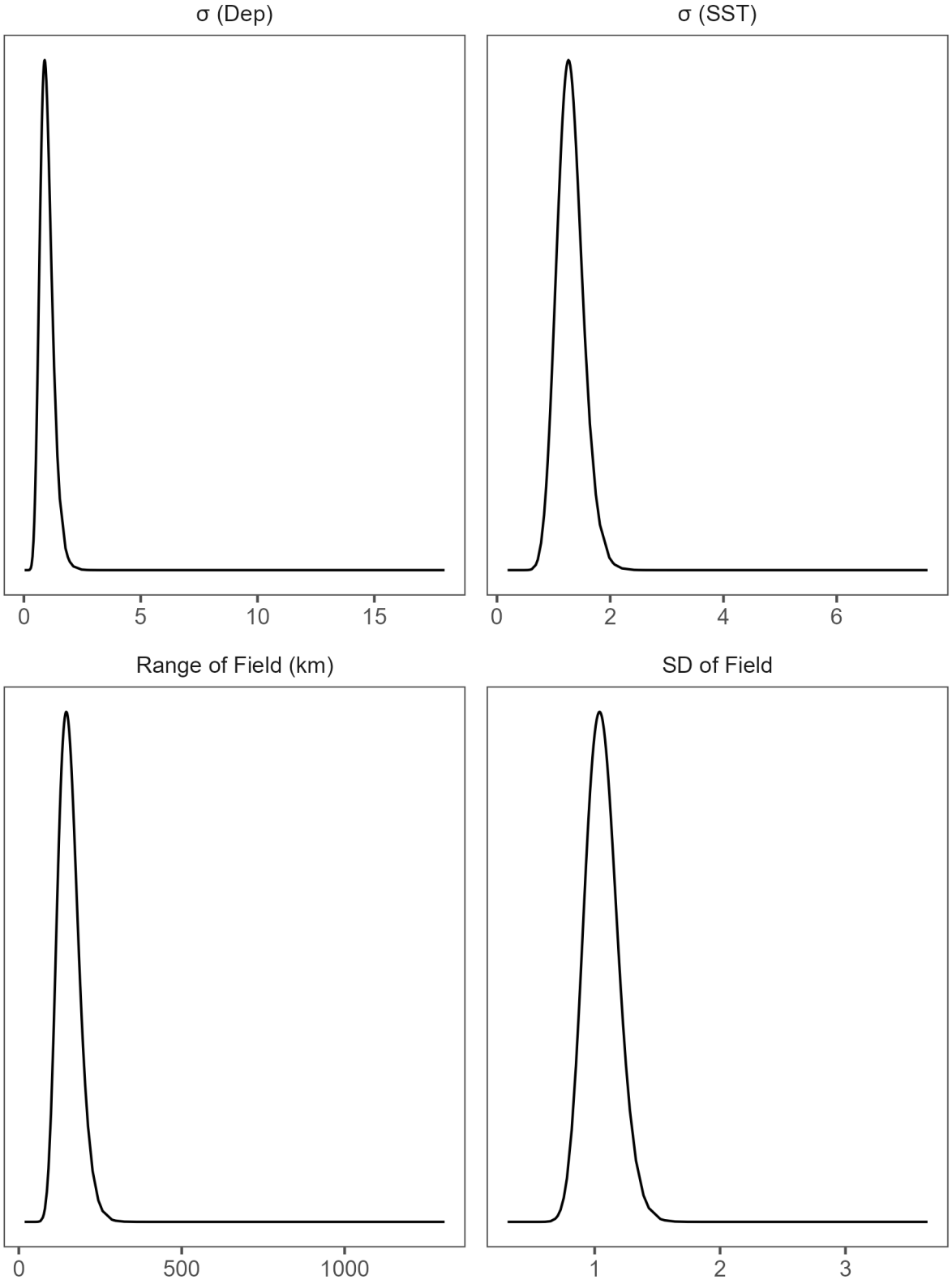

Figure 45. Posterior distributions of the four model hyperparameters for Atlantic Cod in the Winter.

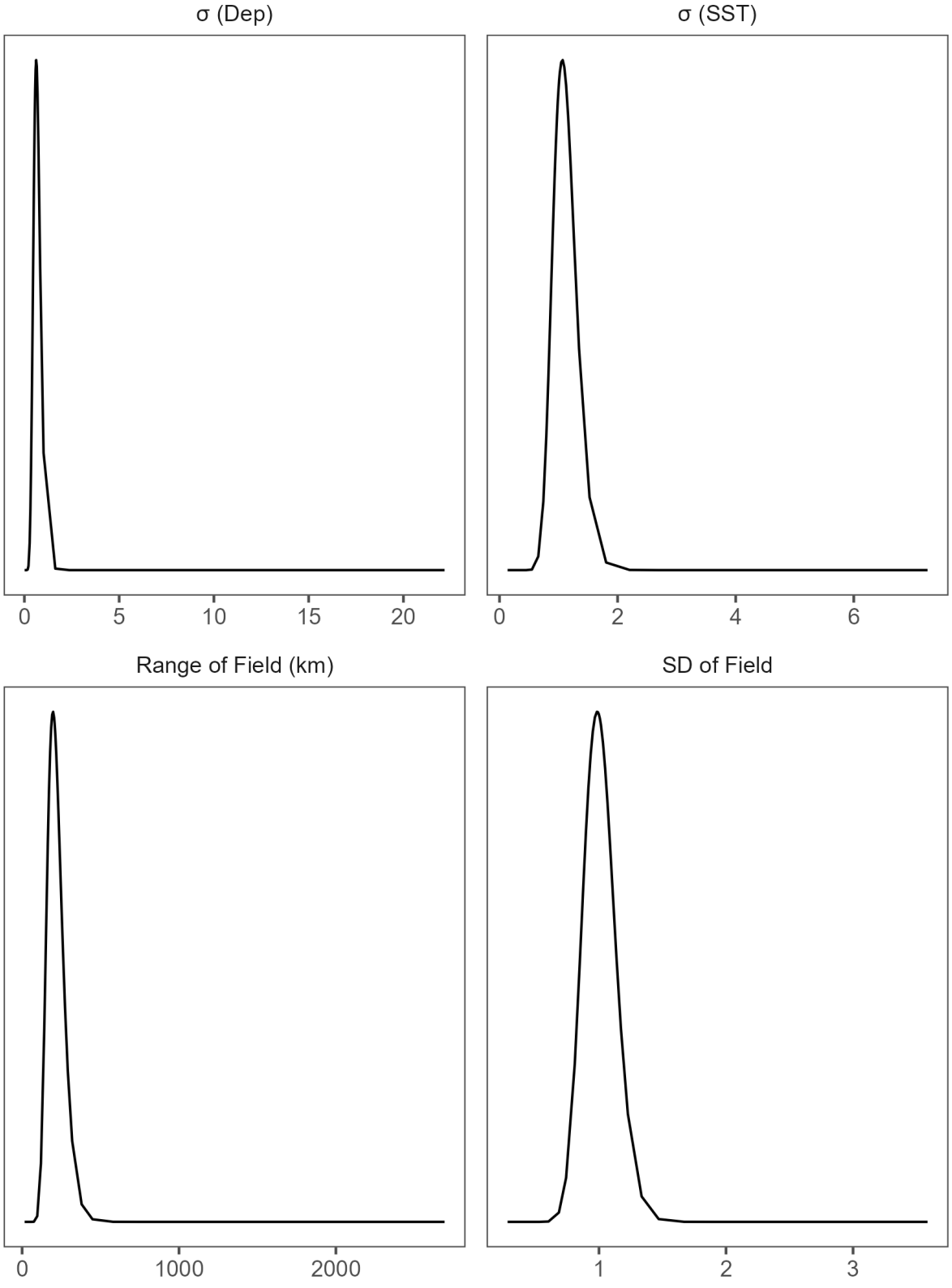

Figure 46. Posterior distributions of the four model hyperparameters for Atlantic Cod in the Spring.

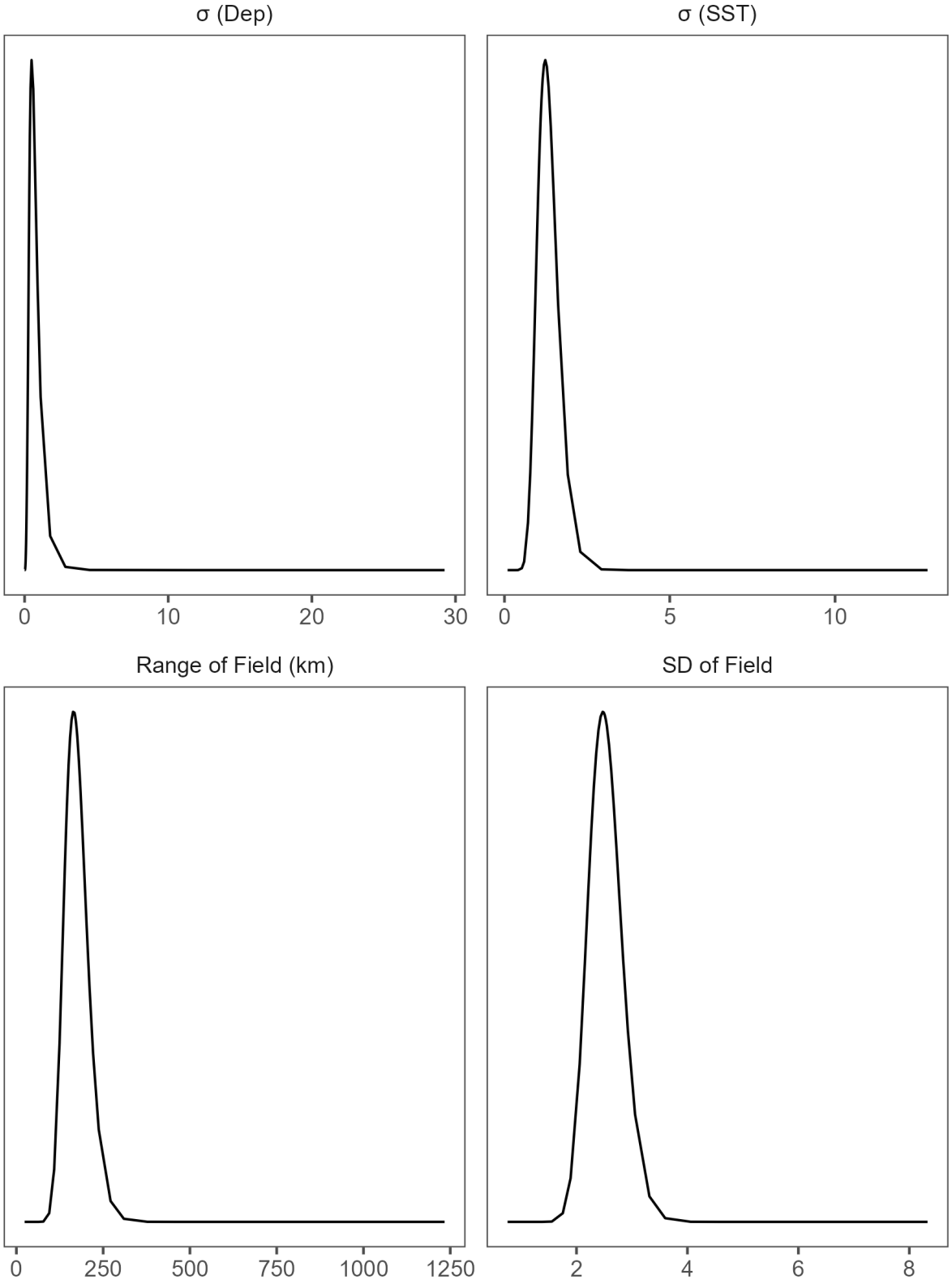

Figure 47. Posterior distributions of the four model hyperparameters for Atlantic Cod in the Fall.

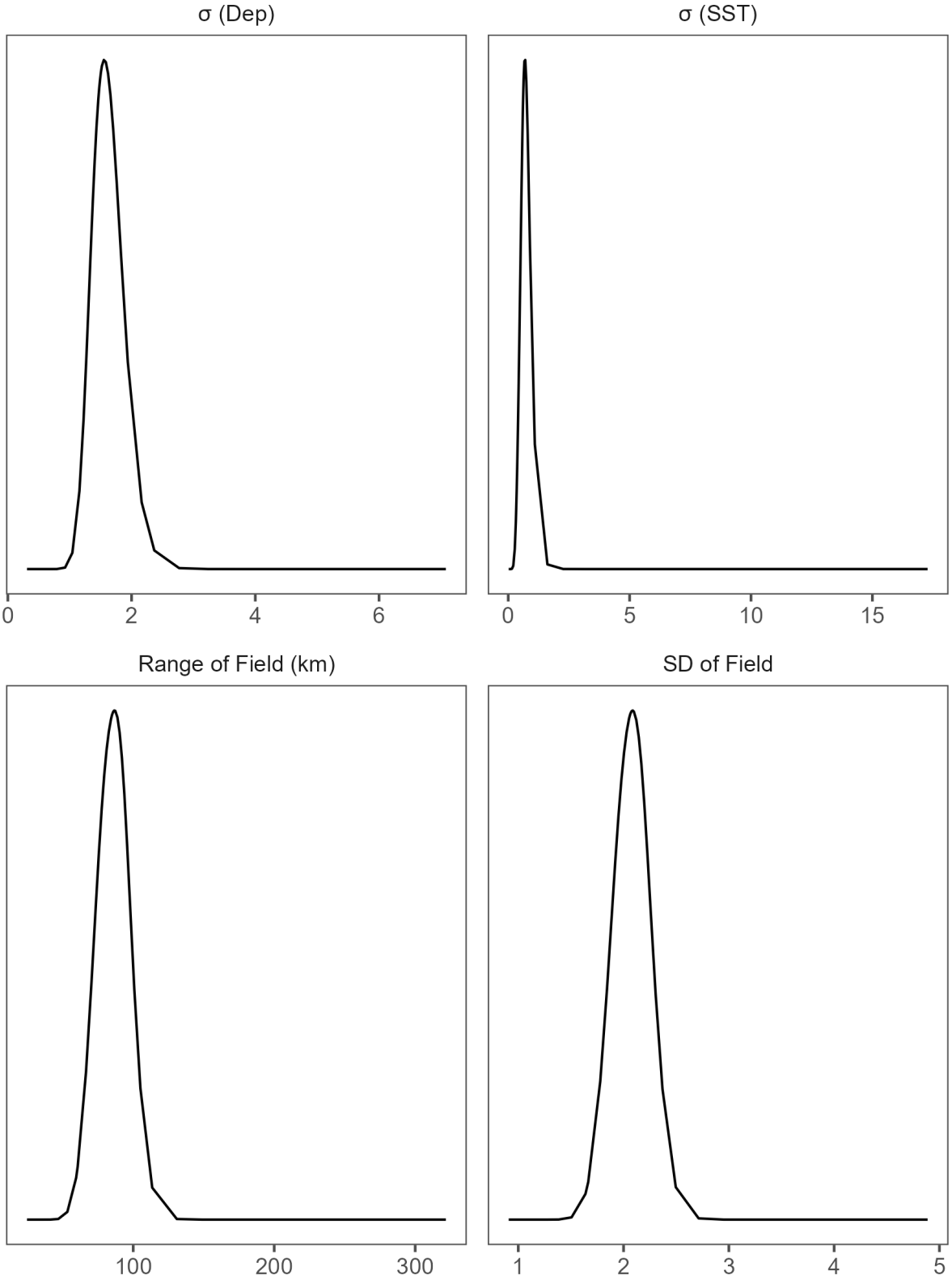

Figure 48. Posterior distributions of the four model hyperparameters for Yellowtail Flounder in the Winter.

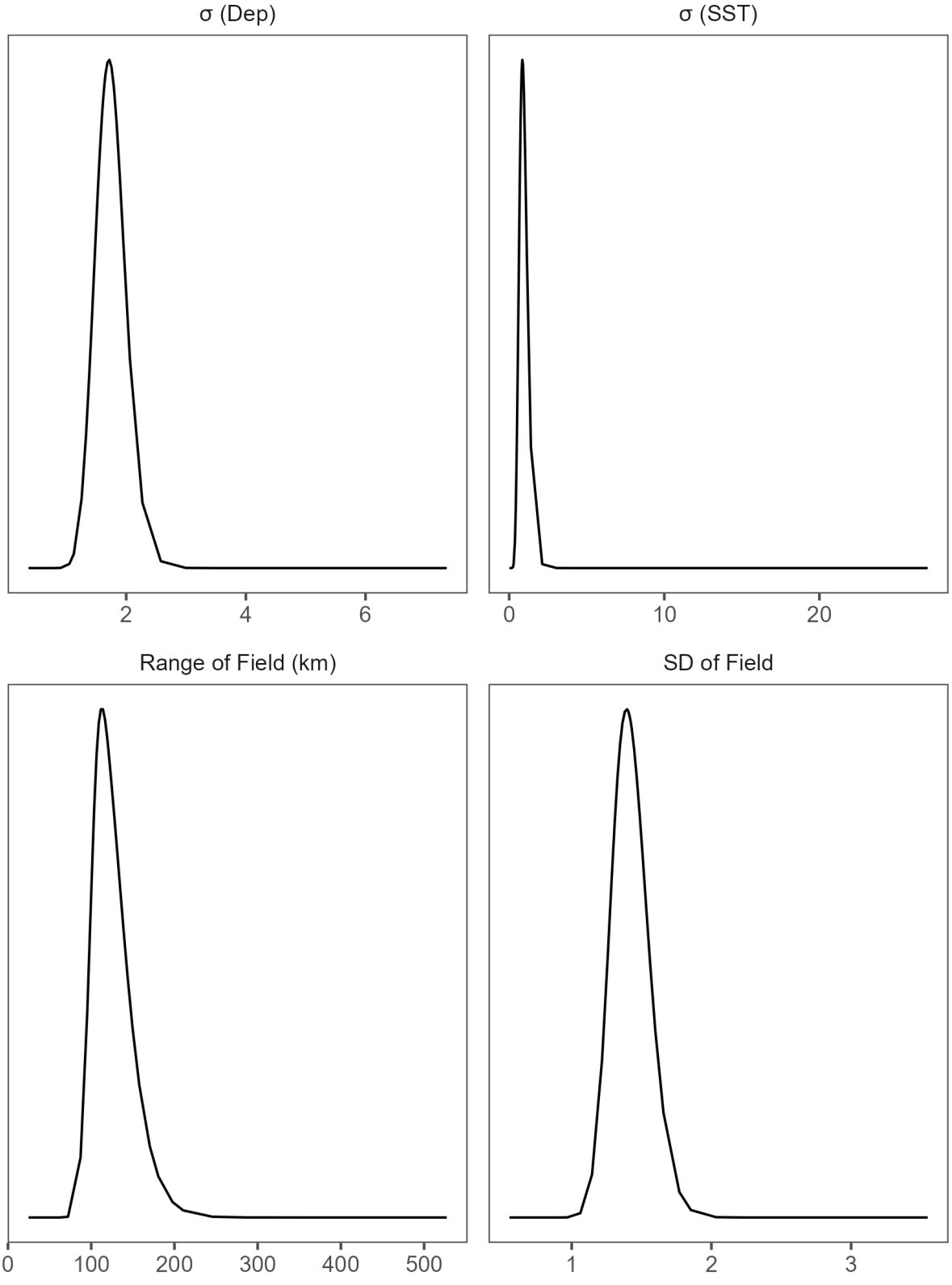

Figure 49. Posterior distributions of the four model hyperparameters for Yellowtail Flounder in the Spring.

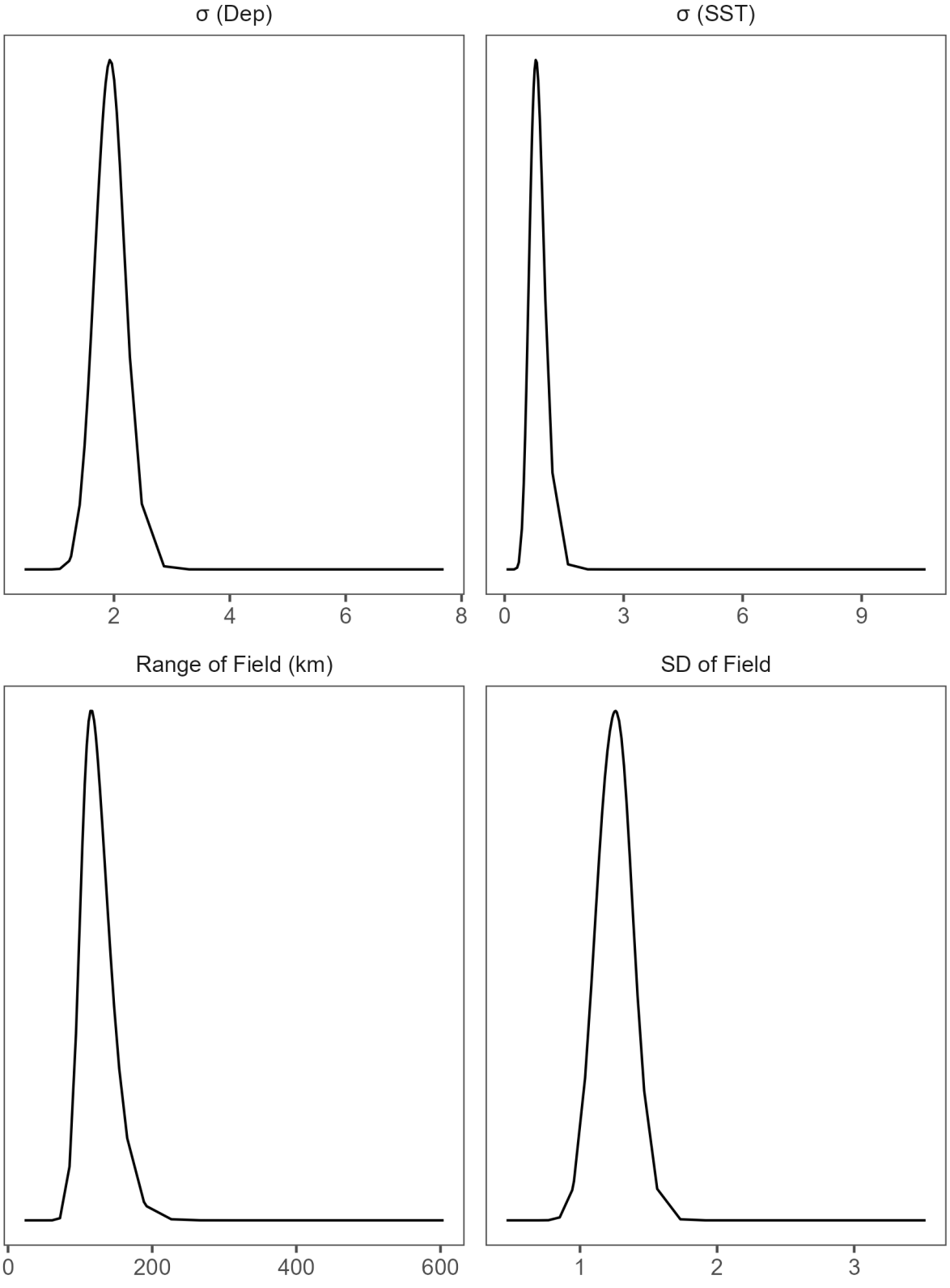

Figure 50. Posterior distributions of the four model hyperparameters for Yellowtail Flounder in the Fall.

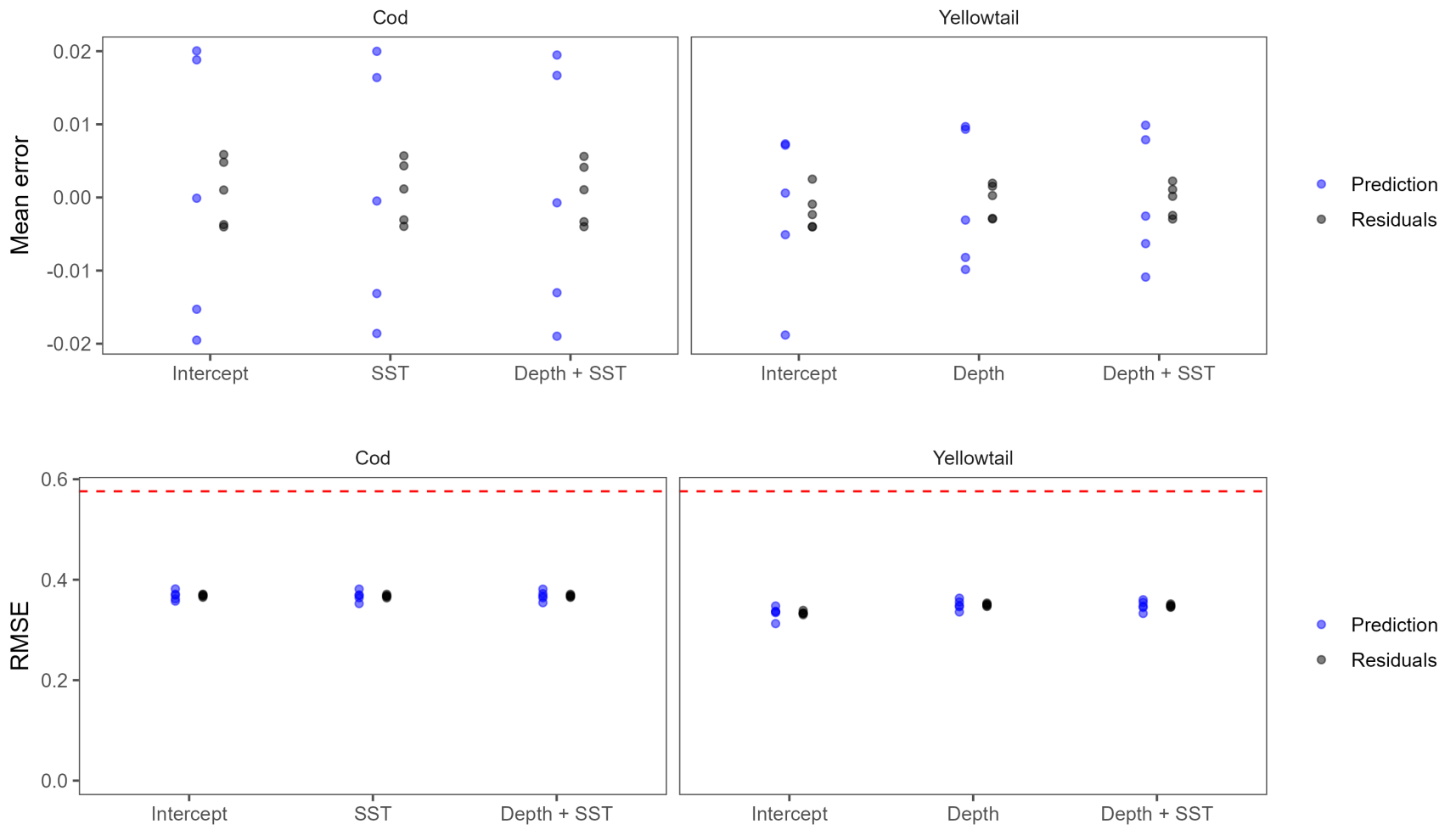

Figure 51. Results of 5 fold cross validation analyses. Top panels represent the mean error for each of the three covariate models tested for Atlantic Cod (Winter) and Yellowtail Flounder (Spring). Blue points represent the prediction error from the testing dataset, while the black points are the residuals from the training dataset. The bottom panels are the Root Mean Squared Error (RMSE) for these models. The dashed red line represents the RMSE for randomly generated data and represents the RMSE for a model with no predictive ability.

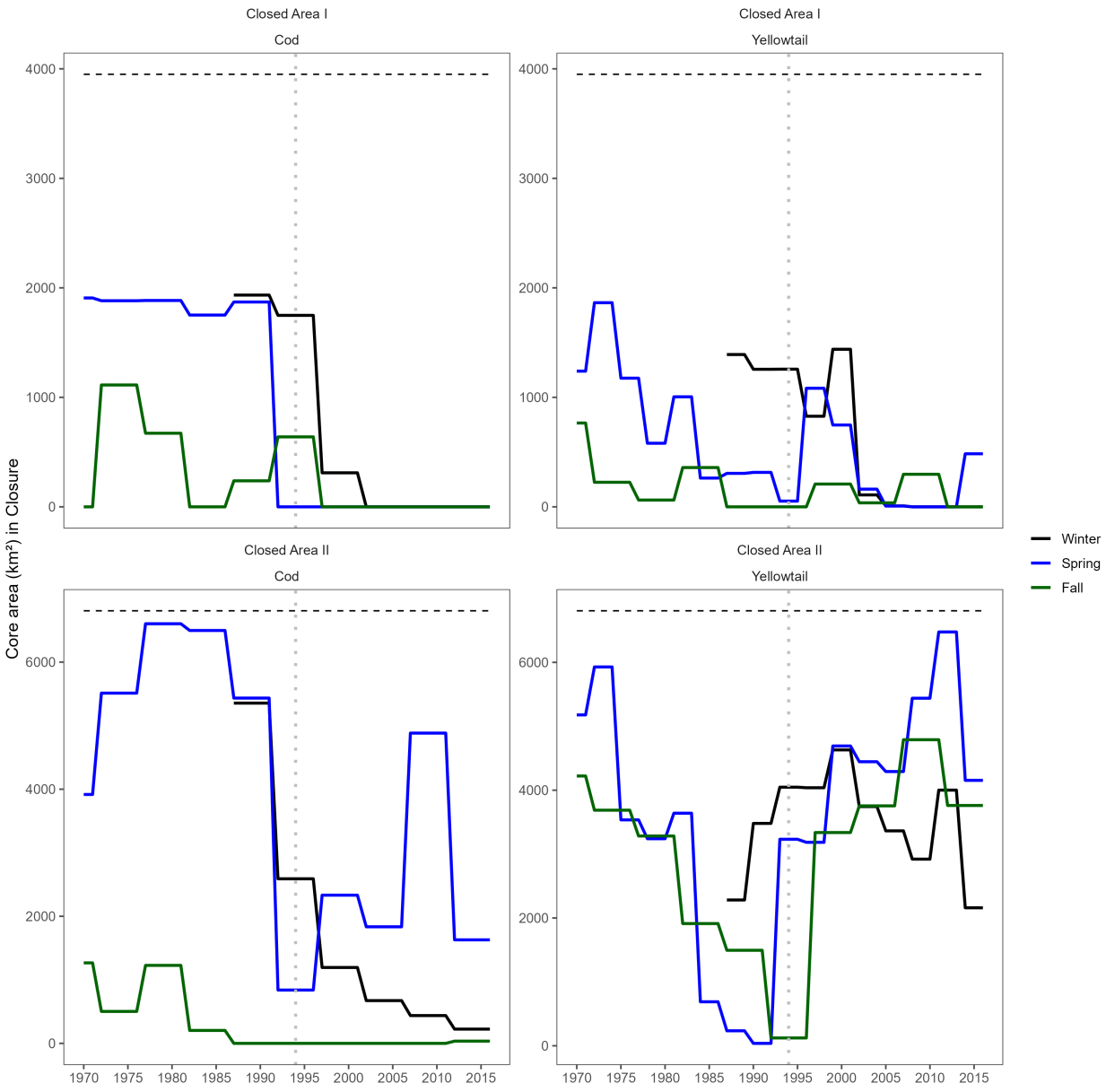

Figure 52. The total core area located within the U.S. Closed Area I (top row) and Closed Area II (bottom row) in the Winter (black), Spring (blue), and Fall (green). The panels on the left are for Atlantic Cod and the panels on the right are for Yellowtail Flounder. The horizontal black dashed line is the size of the closed area and the vertical grey line is the year the closure was implemented.

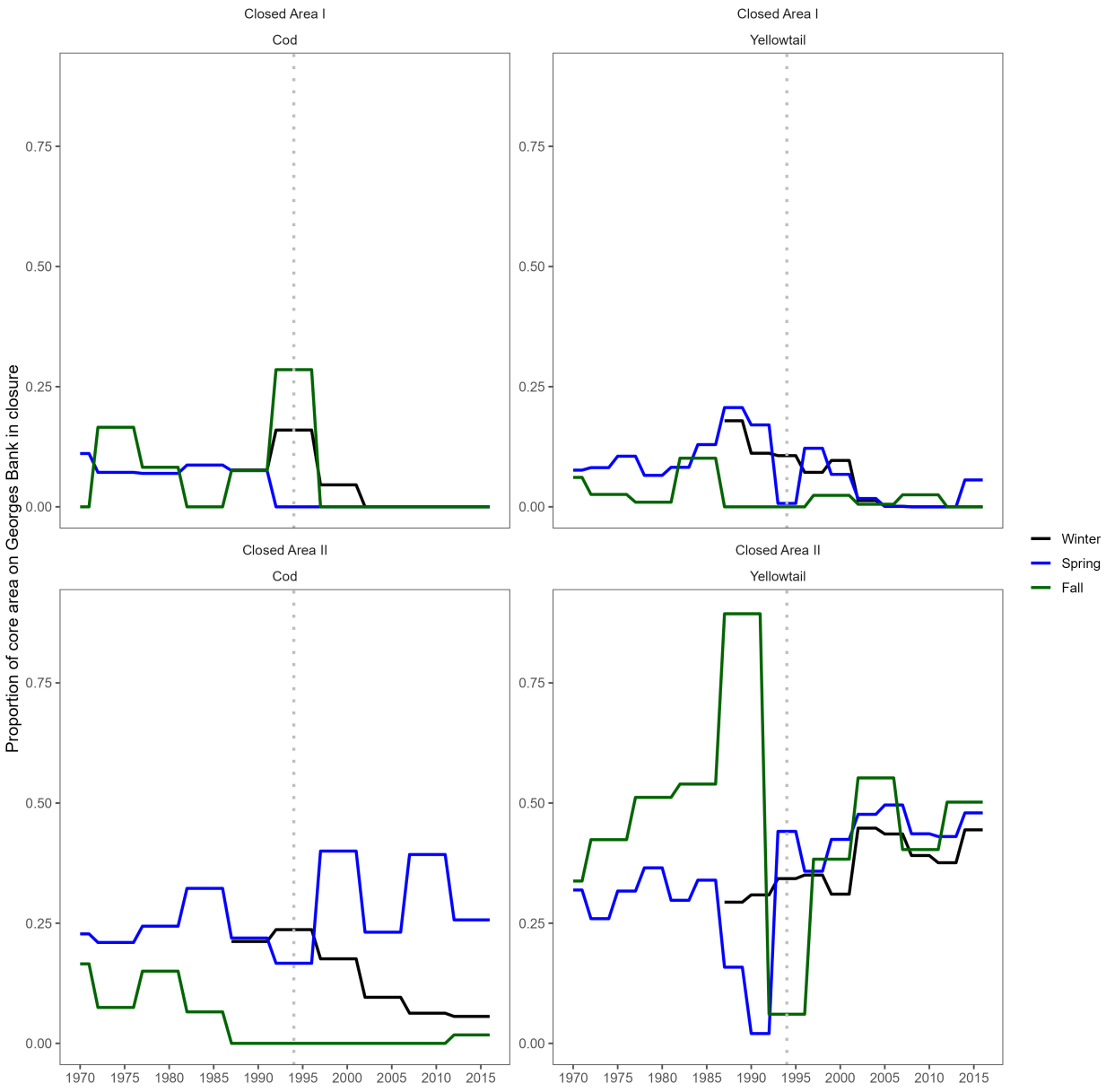

Figure 53. The proportion of core area on Georges Bank located within the U.S. Closed Area I (top row) and Closed Area II (bottom row) in the Winter (black), Spring (blue), and Fall (green). The panels on the left are for Atlantic Cod and the panels on the right are for Yellowtail Flounder. The vertical grey line is the year the closure was implemented.

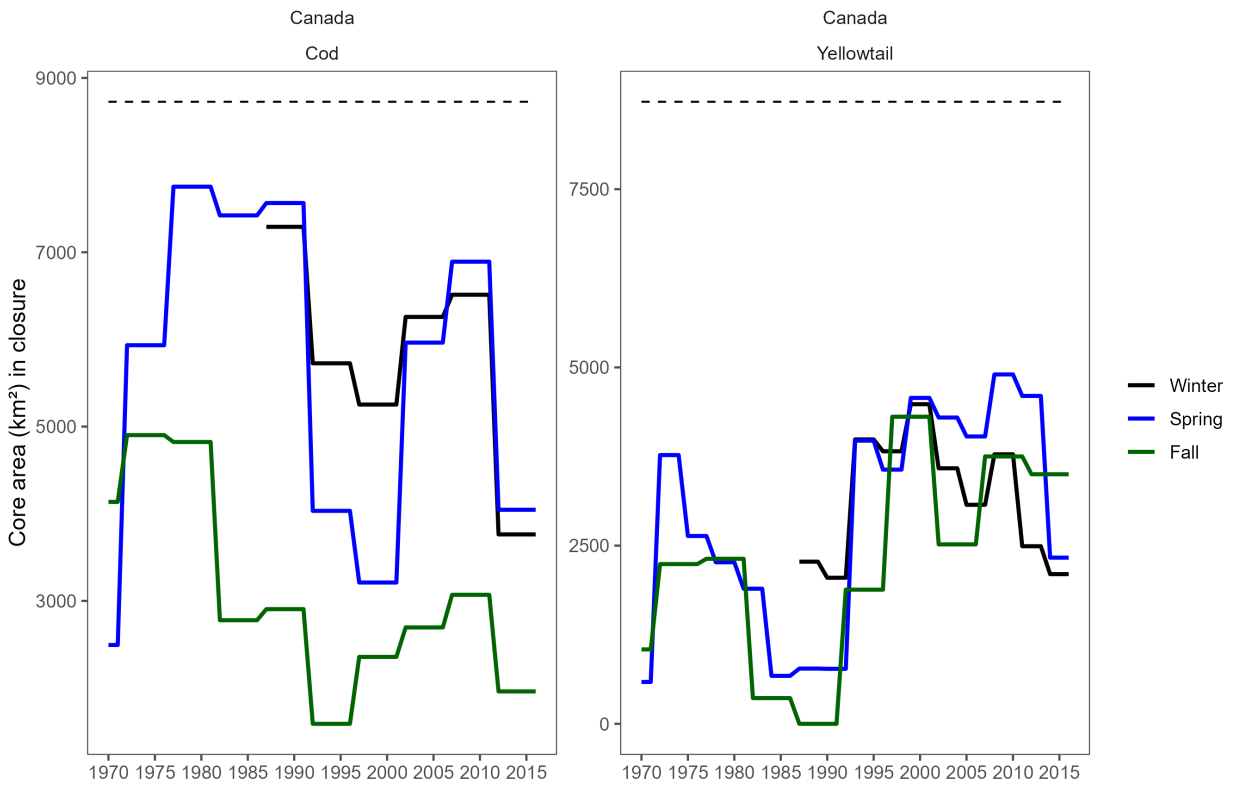

Figure 54. The core area located within Canadian waters in the Winter (black), Spring (blue), and Fall (green). The panel on the left is Atlantic Cod and the panel on the right is Yellowtail Flounder. The dashed line indicates the total area of Canadian waters on Georges Bank included in this analysis.

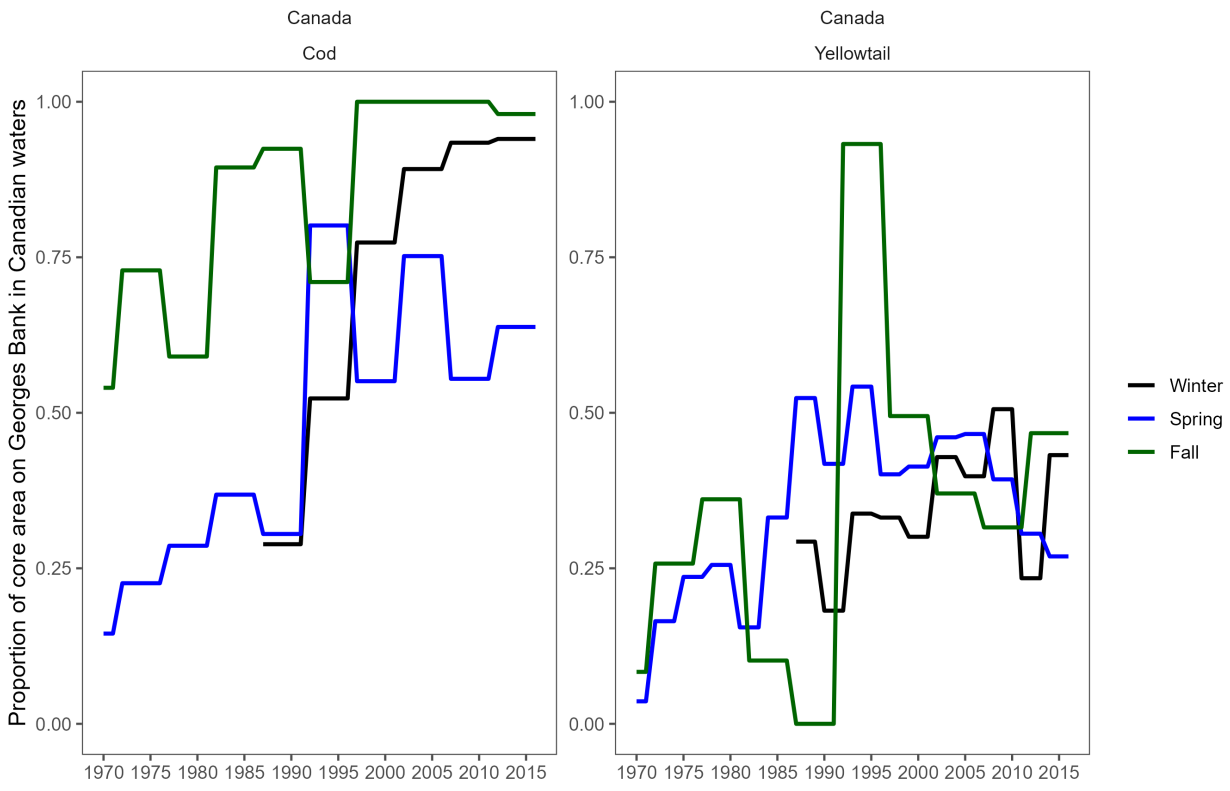

Figure 55. The proportion of core area on Georges Bank that is located in Canadian waters in the Winter (black), Spring (blue), and Fall (green). The panel on the left is Atlantic Cod and the panel on the right is Yellowtail Flounder.

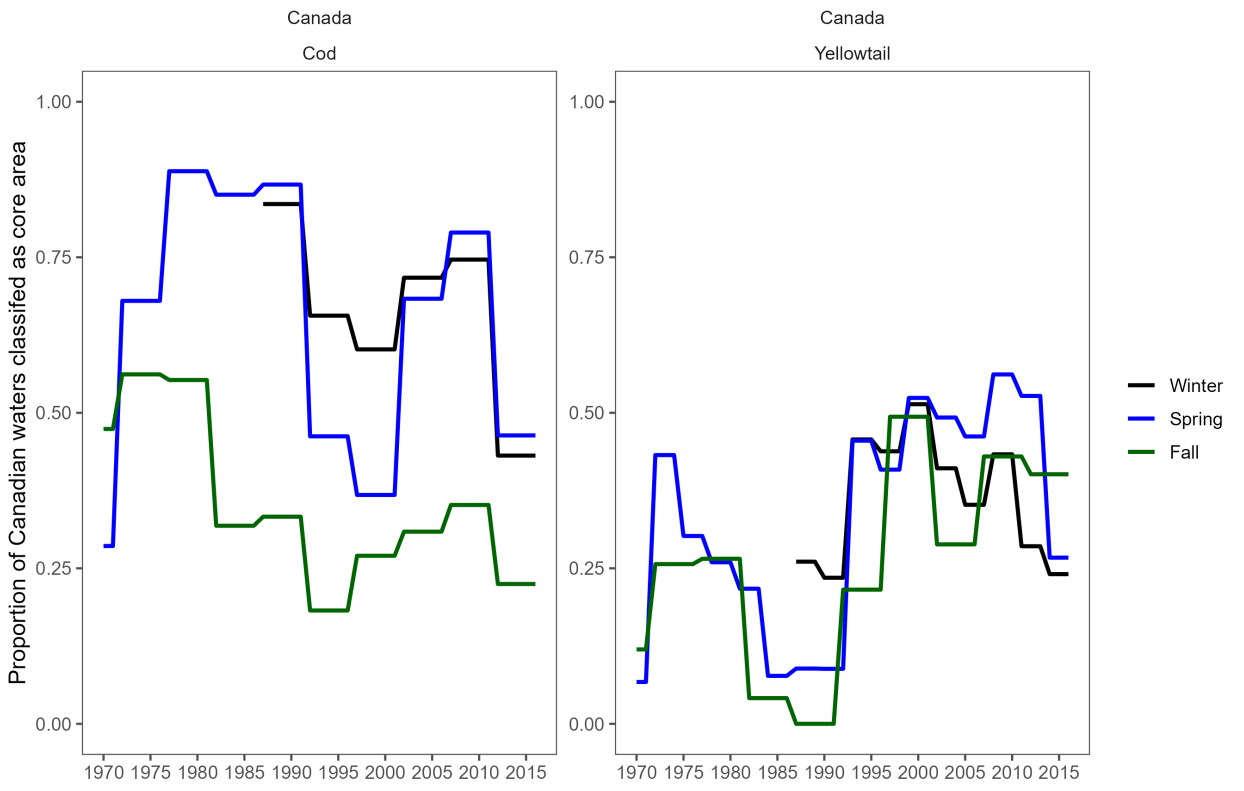

Figure 56. The proportion of the total area in Canadian waters that are classifed as core area in the Winter (black) Spring (blue), Fall (green). The panel on the left is Atlantic Cod and the panel on the right is Yellowtail Flounder.

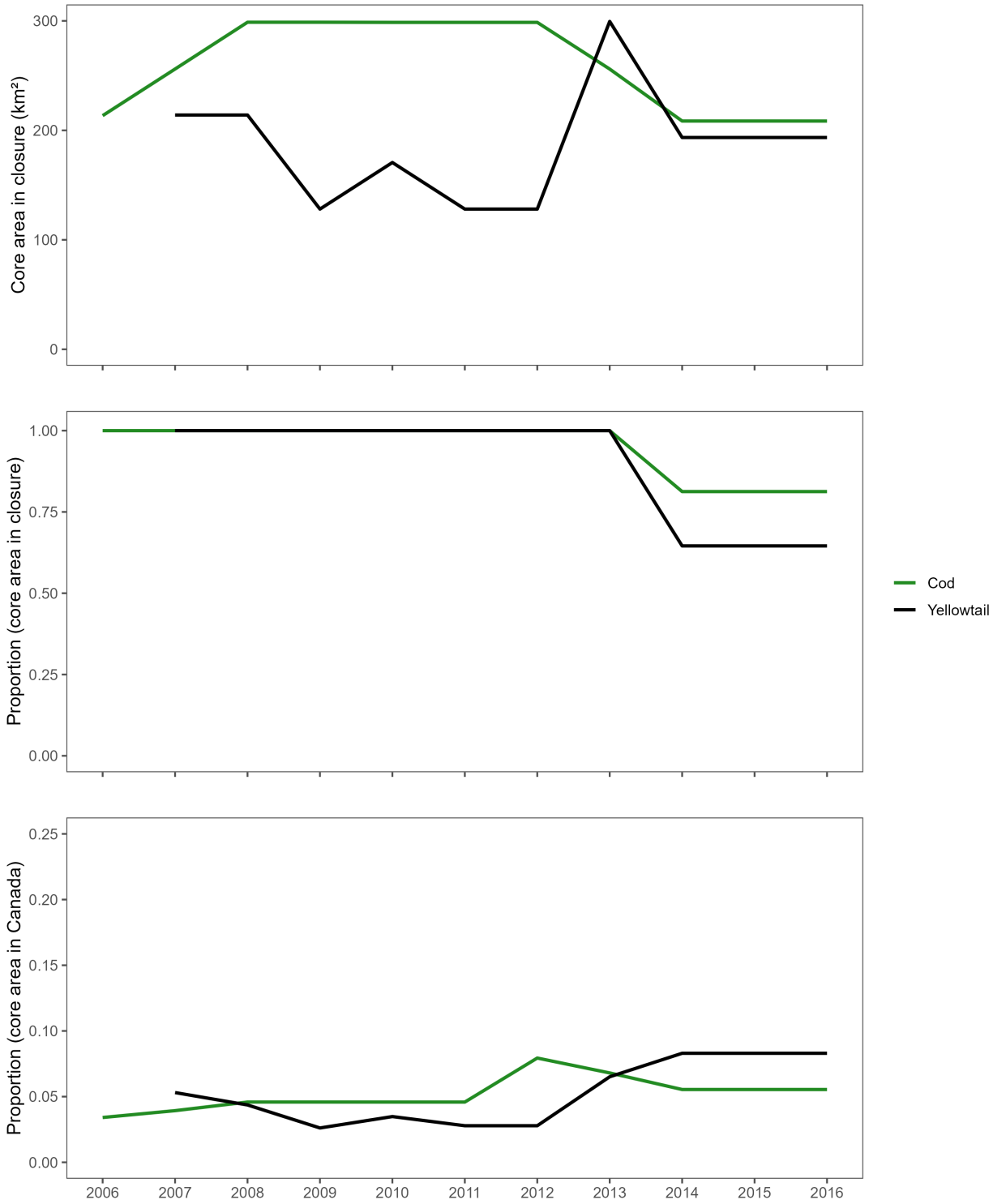

Figure 57. The core area located within the Canadian Offshore Scallop Fishery (COSF) Atlantic Cod and Yellowtail Flounder closures during spawning for each species. The panel on the top represents the total core area by year for each closure, the middle panel is the proportion of the closure with core area. The panel on the bottom is the proportion of the total core area within Canadian waters that is located within the closure. The green line represents the Atlantic Cod within the Cod closure and the black line represents Yellowtail Flounder within the Yellowtail closure.

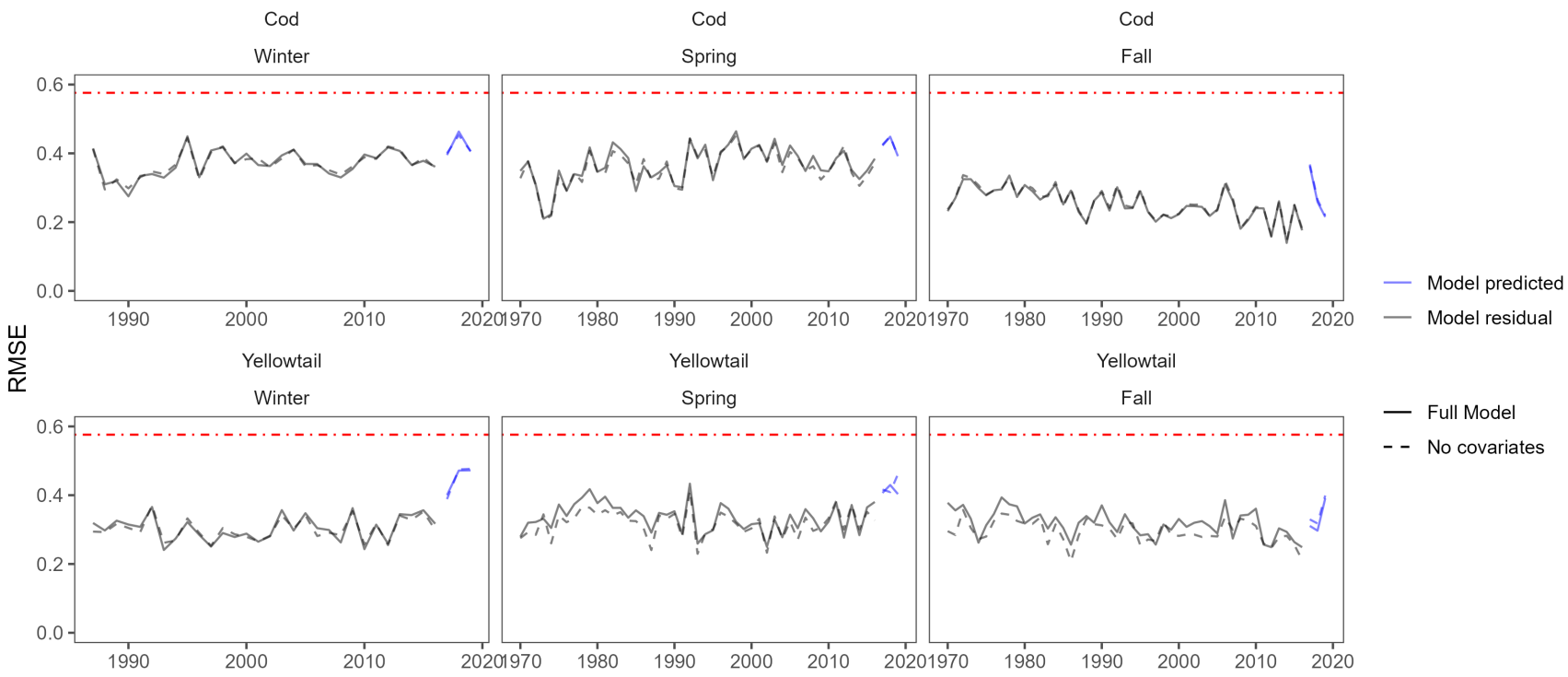

Figure 58. The residual Root Mean Squared Error (RMSE) for the model in each year in black. The blue lines represent the prediction RMSE for years 2017, 2018, and 2019. The Atlantic Cod results are in the top row and Yellowtail Flounder in the bottom row. The red dashed line represents the RMSE for randomly generated data and represents the RMSE for a model with no predictive ability.